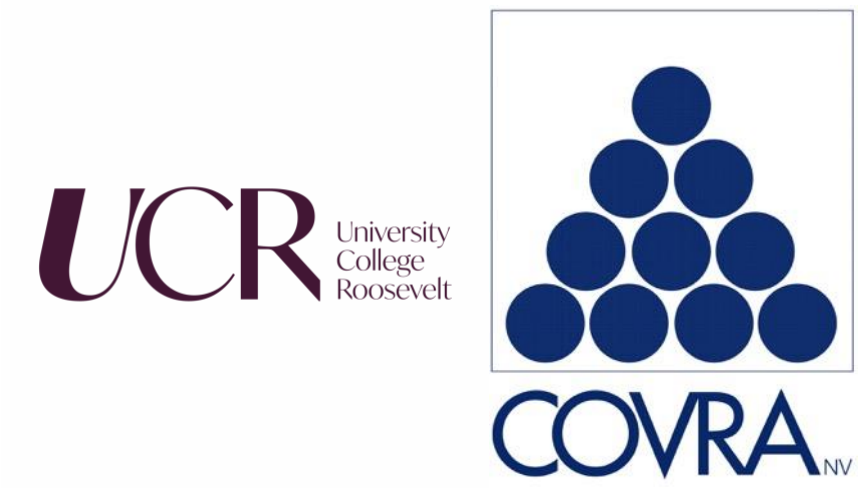


# Evaluating Solute Transport in Dutch Paleogene Clays at Borssele: Evidence for Diffusion or Advection

*Authors:*

**Christian Fernando**

**Kerly Quevedo**

*Supervisors:*

**Dr. E.A.C. (Erika) Neeft**

**Dr. Renata van der Weijden**

19th September 2025

## Abstract

The long-term safe storage of radioactive waste is currently considered a temporary solution in the Netherlands, while deep geological disposal in clay formations is being considered as a permanent solution. This study investigates solute transport mechanisms in two Paleogene clay formations obtained from a 100m core from Borssele: Boom Clay and Watervliet Clay. Determining whether chloride movement in these clays occur through diffusion or advection, is vital for assessing their suitability as hosts for radioactive waste. Chloride and sulfate concentrations were measured at ~1m intervals using Ion Chromatography along with Electric Conductivity and pH measurements to determine the dominant transport mechanism. The chloride profiles in both clay formations showed smooth gradients and isolated asymmetrical peaks which are characteristic of diffusion-dominated transport. High formation factor values with moderate variations between soil layers also supported this interpretation, as a strong ionic retardation due to capillary porosity and small grain size typical of clays, are suggested. These results demonstrate that both Boom Clay and Watervliet Clay in Borssele provide suitable conditions for the long-term containment of radionuclides. The findings provide site-specific empirical evidence to reduce uncertainties in Dutch safety assessments and support the development of predictive transport models for evaluating multibarrier systems with clay host rock as a natural barrier.


*Keywords: Radioactive waste disposal, Formation Factor, Diffusion, Boom and Watervliet Clay, Netherlands*

# Table of contents

# 1 Introduction

In the Netherlands, the storage of radioactive waste in facilities that must be continuously maintained and secured serves as a temporary isolation solution. Radioisotopes are used in medicine, industry, energy production, and research. Since the 1970s, Dutch policy has emphasized the long-term isolation of radioactive waste which has resulted in the consensus that deep geological disposal is the safest option for ultimate waste management, as it provides passive safety on a long geological time scale. Radioactive waste is removed from the immediate dynamic surface environment to a stable geological environment deep underground. A multibarrier system of engineered and natural barriers isolates the waste and contains radionuclides from the waste. Over decades of research, clay formations, especially Boom Clay, have emerged as the leading candidates to host underground disposal facilities, supported by national programs and even international programs such as those in Belgium, Switzerland and France. Clay formations are often considered for disposal of radioactive waste because of their low-permeability, strong adsorption capacities, and chemical properties such as chemical buffering, slowing down the movement of contaminants such as radionuclides. Physical properties such as self-healing and plastic behavior, although dependent on depth, may also contribute to passive safety.

However, due to their physical properties, it's hard to directly measure radionuclide movement, especially over long geological timescales. Therefore, instead of measuring the movement of contaminants directly, this study aims to measure the chloride transport in Paleogene clays, with an intermittence of sandy and peat layers, taken from Borssele to observe whether they move dominantly by diffusion or advection.

Diffusion is the movement of molecules from an area of high concentration to an area of lower concentration (Allard et al., 2009), while advection refers to the transport of a substance by

bulk motions of a fluid (Sun & Zhang, 2020). It is crucial to be aware of the dominant transport mechanism as it controls the rate and extent of contaminant transport. Clays are most often diffusion dominated, meaning ion transport is slow, while advection transports solutes at a much faster rate, affecting the safety and predictability of long-term waste isolation (Jobmann et al., 2017).

The two clays of interest are Boom Clay (formally known as Rupel clay) and Watervliet Clay. The Boom Clay in the Netherlands is regionally extensive, geologically stable and extends to several hundred meters horizontally across the region, this provides a favorable and predictable environment for long-term containment. Determining which transport mechanism method is dominant for chloride ions is key to assessing the long-term safety of nuclear waste disposal in clay formations (G.-J. Vis & J.M. Verweij, 2014).

The data analysis procedure involved obtaining clay samples at 1-meter intervals of a 100m soil core (with a diameter of 95.6 mm) from the Borssele site, drying the samples, diluting them with water, centrifuging them, and finally using Ion Chromatography (IC) to determine the chloride and sulfate concentrations in the clay. The data obtained will help explore correlations with its electrical conductivity (EC), pH, and effective diffusion coefficients to determine whether the profiles support diffusion-dominated transport.

The findings from this report will support the evaluation of whether the clay at Borssele has suitable transport properties for the long-term containment of radionuclides. By providing empirical, site-specific data with direct comparison with known benchmarks, this study will inform the Dutch safety cases, reduce uncertainty in performance assessment, and contribute to decision-making regarding the final disposal of radioactive waste in the Netherlands.

This report is divided into 8 sections including the introduction. The 2nd section provides a literature review for comparing results obtained. The 3rd section describes the methodology used: including sampling, measurement techniques, assumptions, and limitations. The 4th section presents the results obtained in graphs and describes the trends seen. In the 5th section, the results are interpreted and compared with those found in the literature review. The 6th section will summarize key findings. The 7th section is the reference list, while the 8th and final section is the Appendix.

### 1.1 Research Question

What is the dominant transport mechanism in two Dutch Paleogene clays in the Borssele site: Advection or Diffusion?

### 1.2 Sub-Questions

1) Can the proxy formation factor be derived from the EC of extracted porewater and the whole soil (pore water and solids) samples?

2) Can the concentration of chloride in these two clays and the surrounding sand formations be used to assess which transport mechanism is dominant?

3) How does pH vary over the 100 m core?

4) Does the pore water of the 100m core reflect the $Cl:SO_4^{2-}$ ratio of sea water?

5) Is it possible to use the measured data from these soils at the Borssele Site for quantitative transport modelling?

# 2 Literature Review

## 2.1 Use of natural barriers to isolate radionuclides

Investigating the long-term safety of a potential host rock for radioactive waste disposal, first requires identifying its baseline solute transport mechanism (Rumynin & Nikulenkov, 2016), (Charlet et al., 2017). This understanding is foundational as it helps answer a key question: *how fast do radionuclides move through the geological medium*, without yet layering in any site-specific attributes or complex chemical reactions which also affect radionuclide migration. Understanding the main transport pathways for radionuclides in a host rock - in this case diffusion and advection - allows predictions on the long-term solute migration rate to be made, which is necessary in order to efficiently make use of the resources which are imparted to us by these formations (Charlet et al., 2017).

Attributes which make a host rock suitable for long-term safety for a radioactive repository are determined by "depth, thickness and permeability/hydraulic conductivity." In terms of low permeability, the host rock should be "a homogeneous fine-grained sediment with a high clay content" (G.-J. Vis & J.M. Verweij, 2014). As the extent of solute transport (permeability) is one of many attributes which is necessary for long-term safety, this will be the focus in this study.

Clay rock is characterized by very low permeability despite high total porosity, compared to sand or loamy soils. This results in minimal to stagnant porewater flow, in other words a very low hydraulic conductivity (around the order of $10^{-12}$ m/s). This is due to the small size of the pores and the lack of connectivity between voids, essentially limiting fluid flow through the clay rock and acting as an aquitard. When fluid flow is mostly stagnant, the baseline transport mechanism is diffusion dominated and thus limits advective migration which is based on

significant fluid flow. (Jobmann et al., 2017). This explains the attractiveness of clay-rich (argillaceous) rocks for radioactive waste disposal, as radionuclide migration would be governed by slow rates (Charlet et al., 2017).

Gradual radionuclide migration allows further isolation alongside the buffer engineered barriers offer, as seen in Figure 1, further promoting its suitability (COPERA - CLAY, 2024). Isolation should last until the radioactivity has decayed to natural levels, according to (G.-J. Vis & J.M. Verweij, 2014), to prevent radioactive impact to accessible environments (Rumynin & Nikulenkov, 2016). Mediums that are most susceptible to the impact of radioactivity are elements of the biosphere, including soil, surface water, and groundwater (Bollermann et al., 2022).

**2.2 Introduction to Boom Clay**

Various studies including research programs coordinated by TNO, have pointed to the potential of underground Dutch rock salts and clay layers to contain radioactive waste. Both OPLA (OPLAnd, On Land, 1974-1993) and CORA (Commissie Opberging Radioactief Afval, Committee on Disposal of Radioactive Waste, 1996-2001) research programmes were involved in such discovery. The Boom Clay layer was specified as an effective option amongst other potentially appropriate clay layers such as Asse and Ieper Members, as an alternative to rock salts to dispose of radioactive waste (G.-J. Vis & J.M. Verweij, 2014). The mineralogy of Boom Clay is almost as it was at the time of deposition, which was 23 to 34 million years ago, although some differences in microbial carbonate and pyrite are expected over time. However, the clays which are candidates for radioactive waste disposal in France and Switzerland i.e. Opalinus clay, do possess diagenetic features such as cementation.

### 2.2.1 Brief Geology of Boom Clay

Rupel Clay Member, informally known as Boom Clay, is part of the Rupel Formation (Van Adrichem Boogaert and Kouwe, 1993). This subsurface clay layer is found in nearly all the onshore part of the Netherlands and in the shallow subsurface of Belgium as seen in Figure 1. It is a Paleogene marine clay layer deposited 23 to 34 million years ago and since then, has been buried by other geological processes and consolidated through compaction and diagenesis into what was once a soft marine mud into the impermeable clay we have analyzed nowadays. Paleogene clays have been deposited on the sea floor over the period 23 to 66 million years ago. Most Paleogene clays are deeper than 250 meters and although some layers are found at shallower depths, this is mainly due to erosion. The thickness of these layers is largely over 200 meters, making this an attractive host rock for radioactive waste disposal. Extensive research on this clay layer has been undertaken in Belgium, specifically near the town Mol, where an underground test facility was built to further facilitate their research.


*Figure 1: Visual representation of the extent of Boom Clay Member throughout nearly all of the onshore Netherlands as well as northern Belgium and specifically in the Campine Basin. Produced by TNO and published in a desk –study report studying the geohydrological properties of Boom Clay specifically in the Dutch subsurface, hence the borehole locations denoted as crosses (G.-J. Vis & J.M. Verweij, 2014).*

### 2.2.2 Attributes for Radioactive Waste Containment

Boom Clay offers long-term safety related characteristics including lateral homogeneity, low hydraulic conductivity (10^-7m/d), thickness (varies), high sorption capacity, high fixation capacity and high plasticity which aids in its self-sealing capacity. This limits the risk of radionuclides and other contaminants to be exposed towards the reachable environment from the repository (Gedeon et al., 2007).

Additionally, most Boom Clay layers have a thickness that is sufficient to offer the capacity of isolation and are deep enough to avoid future disturbances from geological progressions including glaciations, groundwater flow etc. However, all Paleogene clay formations are soft which makes them more susceptible to erosion by wind and water. Therefore, in an example of future ice ages, where it is projected that glaciers may expand up to several hundred meters, it is integral that the Paleogene clay layer where high level waste disposal would be contained should be deep enough as a result of a thick layer of other rock formations above it, to maintain isolation (G.-J. Vis & J.M. Verweij, 2014).

### 2.3 Introduction to Watervliet Clay

The Watervliet Member is a lithostratigraphic unit of the Zelzate formation which is a part of the Tongeren Group of the late Eocene to early Oligocene (Paleogene). It is characterized by intercalations of fat dark grey-green clay and sandy/silty soil with abundant glauconite and periodic pyrite concretions. As argillaceous rocks are candidates for radioactive waste disposal and 95,12 to 100,23 meters of the soil core (KB105) contains Watervliet Clay, its origin and potential for radioactive waste disposal is relevant (Hoving et al., 2024, Jacobs & De Coninck, 1992).

#### 2.3.1 Brief Geology of Watervliet

In the early Oligocene, sea levels were particularly high in the southern North Sea Basin and gave way for the deposition of the top layers of the Bassevelde Sand Member and the Watervliet Clay Member. The Watervliet Clay Memeber is found in the north part of East-Flanders and Antwerp province as well as in south of the Netherlands in areas including, Zeeuws-Vlaanderen and Noord-Brabant and Noord-Limburg and Winterswijk. The depth of the

Watervliet Member varies along the South of the Netherlands and North Belgium as seen in Figure 2.

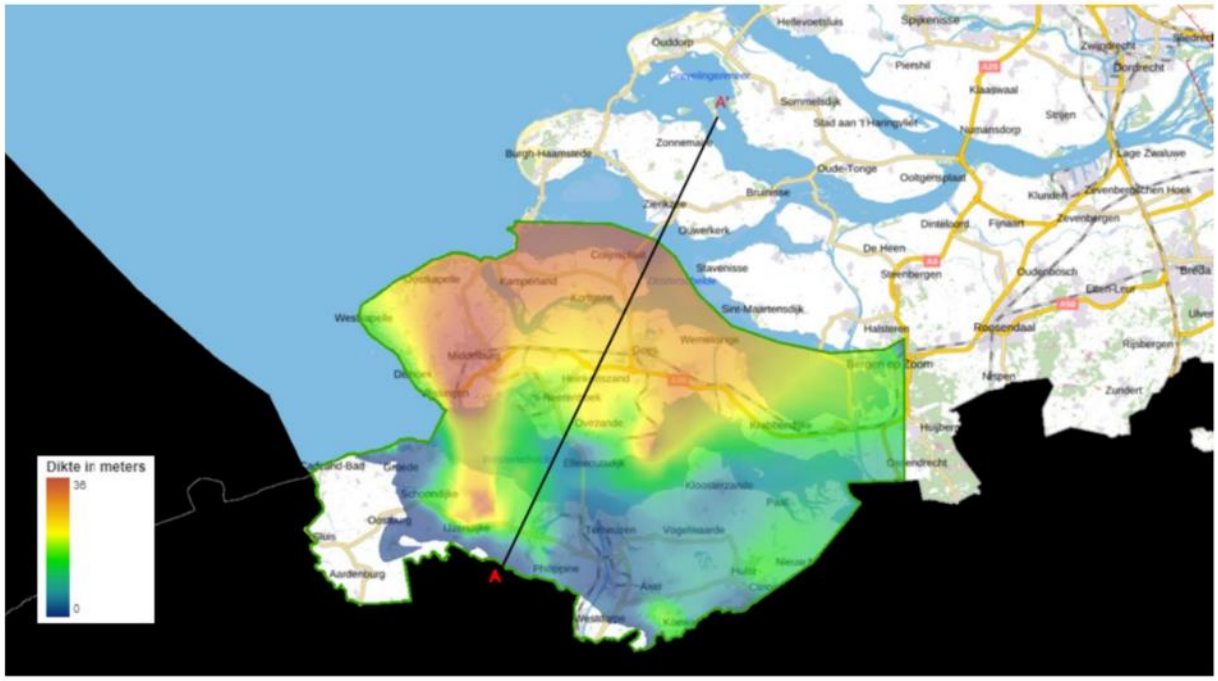


*Figure 2: The depth of the Watervliet Clay Member in the indicated area inputted into the REGIS II model v2.2.2 model (www.dinoloket.nl) by COVRA (Hoving et al., 2024)*

### 2.3.2 Attributes for Radioactive Waste Containment

The suitability for Watervliet Clay Member as a barrier for eventual radionuclide exposure from radioactive waste has been far less studied, compared to the suitability of Boom Clay. However, a technical report published by TNO with their practical projects coordinated by COVRA in late 2024 has undergone extensive research on the geochemical properties of the Watervliet Member. They focused on the concentration of natural analogue elements such as Uranium (U), Thorium (Th), Cesium (Cs), Selenium (Se) and Rare Earth Elements (REE) in the clay minerals of Borehole KB-101 also from the Borssele Site in Zeeland, Netherlands. The top layer was comprised of a combination of sandy/silty and clayey layers rich in carbonates in the

first 25 meters followed by non-calcareous in the next 15 meters. Calcite, feldspar, and quartz dominated the mineralogy of this clay.

It was found that this Watervliet Clay had high retention of such radionuclides as these were found to be concentrated or correlated within the clay minerals. Specifically, Uranium and Selenium showed a correlation with pyrite, suggesting that these elements are related to sulfide phases. However, the presence of clay minerals has a natural ability for binding and immobilizing radioactive elements which consequently retards their migration. This is similar to the functionality of Boom Clay; however, it is to be noted that the concentration of radionuclides was slightly lower in the Watervliet Clays. Meaning the ability for conservation and immobilization of these radioactive elements was slightly less than Boom Clay. This was attributed to the heterogeneity of the Member as alterations between sand or silt and clayey layers make up this unit. Specifically, having less clay overall in this lithological unit decreases the attractive properties such as binding and reacting with radioactive elements to mitigate and immobilize their exposure. As Watervliet Clay has more sand than Boom Clay, the degree of quartz minerals increases and with it, therefore, clay and its characteristics as a reactive barrier are subject to an overall dilution (Hoving et al., 2024)

**2.4 Radioactive waste barriers**

There are several options for radioactive disposal facilities, each designed in terms of varying degrees of waste. Including high-level (HLW), intermediate-level (ILW), and low-level (LLW) waste. Each has a different extent of isolation and containment related to the type of radioactive waste that is received. According to IAEA (2011), a geological disposal facility "constructed in tunnels, vaults or silos in a particular geological formation" is where HLW could be contained. This facility must be at least a couple hundred meters underground. As mentioned,

according to the degree and classification of radioactive waste, different disposal facilities such as near surface disposal for LLW and caverns, vaults or silos at least a couple tens to hundreds of meters underground for ILW (IAEA, 2011).

Multibarrier systems have been the base of geological disposal internationally established for the past 45 years. Essentially, this system encompasses both the natural and engineered barrier to isolate and contain radionuclides in the waste as seen in Figure 1 (COPERA, 2024).

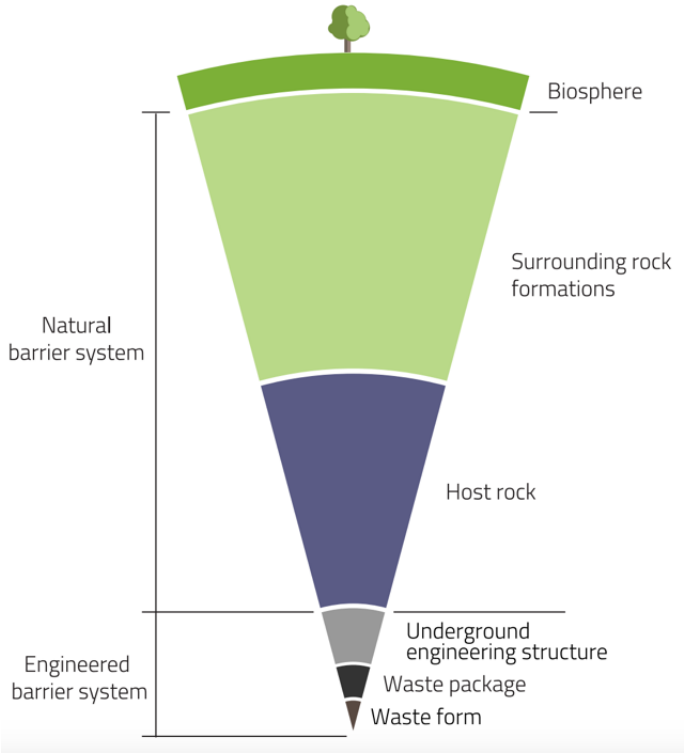


*Figure 3: Visualization of the host rock location in a radioactive waste disposal system (COPERA, 2024)*

**2.5 Expected chloride profiles**

Transport of solutes like chloride in clay-rich formations is governed primarily by two mechanisms: diffusion and advection. Each has distinct and diagnostic shapes to concentration profiles over time, which is how they can be differentiated. Diffusion is typically slow in low-

permeability clays, whereas advection can transport solutes more rapidly, having asymmetry and curvature in its profiles.

The chloride profiles obtained in the present study can be compared with those compiled by the CLAYTRAC Project (NEA), which includes European clay-rich formations such as Opalinus Clay (Mont Terri, Switzerland) and Boom Clay (Mol, Belgium). These settings are hydrogeologically similar to Borssele as they have marine origin, low-permeability clay boundaries, and histories of meteoric flushing, making them suitable benchmarks for interpreting observed profiles and assessing transport mechanisms.

It was found that the shape of diffusion-controlled profiles depends primarily on clay layer thickness, diffusivity, and duration since the boundary conditions change. For example, the relatively flat chloride profile in the Boom Clay in Mol supports nearly complete out-diffusion of marine chloride and demonstrates how profile shapes reflect past hydrogeological processes (NEA, 2019). When advection is significant, profiles deviate from these patterns and show asymmetry and curvature, especially at higher velocities or when flow directions vary.

Few reports have studied the expected chloride profile and transport mechanism of Watervliet Clay. A report by Hoving et al. (2024) found valuable insights. Their geochemical tracer data showed direct evidence for diffusion-controlled chloride transport certain locations: two samples from the Tongeren aquifer show distinctly negative δ37 Cl values (−1,63‰ and −2,08‰). The authors interpret these signatures as resulting from diffusive exchange with surrounding clays or diffusion within stagnant groundwater. However, groundwater chemistry indicates clear advective influences in some areas. Shallow screens and multi-level wells reveal evidence of seawater infiltration and freshening, reflected in elevated chloride concentrations and

electrical conductivity within the upper ~50 m. This demonstrates that advection and mixing dominate the shallow, more connected domains.

Therefore, for Watervliet Clay, diffusion may dominate long-term solute exchange in the deeper, low-permeability Watervliet Clay, while advection and mixing are locally important in shallower, more connected zones, reflecting the heterogeneous sand–clay structure of the site.

# 3 Methodology

## 3.1 Location and extraction

The 100m core sample was extracted from the Borssele 2 Power Plant (KCB2) Site near Middelburg, the Netherlands, by drilling boreholes in the ground. The site is located along the Rijn-Maas-Schelde delta. This was originally done to conduct a geological investigation to assess the suitability and safety of the site for nuclear technology. The study aimed to investigate the site's subsurface conditions, establish engineering properties of the soils, and evaluate ground risks. Four 100 m borings titled KB-102, KB-103, KB-104, and KB-105 were extracted using two sampling methods: SPT sampling coupled with side-discharge wash boring in accordance with the depths 0-30 m, and the SMET® push sampling method for the remaining depth. The core being analyzed in this experiment is KB-105 (Coordinates**:** N 384,398.32 m; E 38,812.79 m; Rijksdriehoekscoördinaten, Amersfoort datum, RD New projection).

The SMET® push sampler coring system was used because it provides a high yield in challenging soil conditions, allowing the geologic profile to be better understood for up to a 200m depth. After drilling to the termination depth, the coring head removed soil around the sample tube using mud circulation and rotation, the inner tube with the soil sample was then brought to the surface, and the PVC tube with the core was taken out. The PVC tube was cut open downwards with a powered cutting wheel, leaving the tube and sample split into two

halves. The tube was divided further into multiple intervals, with each interval containing ~1m of soil. The divided halves were then put back together with three wraps of PVC adhesive tape and placed inside of another PVC storage tube with sealed endcaps (Paul C. Rizzo Associates, Inc., 2013).

### 3.2 Storage and sample collection

The samples were sealed in the PVC pipes and stored in the VOG 1 (Verarmd uranium Opslaggebouw) at the COVRA NV site. VOG 1 is the same structure which stores depleted uranium at COVRA, providing ideal conditions to ensure the samples are not subjected to high temperatures.

The collection procedure of samples from the KB-105 pipes are as follows: the pipes had to be unwrapped and split open at the seam, 100g were weighed from each sample twice using a digital mass balance, the 2 measurements were divided into labelled plastic containers ".1" and ".2" to distinguish between replicates (Figure 4). Stainless steel spoons and an aluminum soil borer were used to remove soil from the pipes (Figure 5). After the soil was collected and the resistivity was measured (see Section 3.3.3), the halves of the pipes were then put together and resealed with duct tape. The samples were then transported back to the Anne lab at University College Roosevelt (UCR) for testing.

*Figure 4: Sample 2 split open. The soil borer and plastic containers can be seen placed above the sample.*

*Figure 5: Soil was taken from sample 58 using the soil borer.*

The two halves could only be removed for sandier samples; they could not be removed from their outer PVC tube for samples with high clay content. The loss in underground compaction pressure allowed swelling of the core sample by which the two halves could not be removed (see Section 3.4).

### 3.2 Preparation

From each plastic container, 40g of each sample was placed in a beaker and placed in an oven to be dried for 24 hours at 100$^{o}$ C in order to remove all moisture from the samples (Figure

6). The samples were then weighed after drying to find the true mass of the clay without moisture.

*Figure 6: All the weighed samples in the oven before drying*

From the dried samples, 5g of each sample was placed in centrifuge tubes and leached with 50ml of distilled water. The samples were then transported to the Joint Research Center in Zeeland (JRCZ) and were placed in a shaker at 2,25 Mot 1/min (movements per minute) for 2 days. This process helps to extract ions from the clay by mixing it thoroughly with the water and

facilitates the movement of salts from the solid to liquid phase (Figure 7).

*Figure 7: Samples placed in shaker prior to centrifugation*

After the shaking, the samples were placed in a centrifuge at 4500RPM for 10 minutes. Then, the resulting supernatant in each sample was filtered with a 0,45µm filter and placed into labeled IC vials. This process ensures that any remaining solid particles are removed from the sample, allowing only a clear liquid to enter the IC.

Two sets of 20mL standards for chloride and sulfate were prepared for the IC to generate calibration curves which were necessary to derive the concentration of the unknown samples. For chloride, a 1000ppm chloride stock solution was made by dissolving 1,650g of sodium chloride (NaCl) in 1L of distilled water. Using this stock, lower concentrations of 125ppm, 250ppm, 500ppm, and 750ppm were made by diluting the stock in distilled water (Table 1). The sulfate stock solution was made by dissolving 0,123g of sodium sulfate ($Na_2SO_4$) in 1L of distilled water. The standards of 3,125ppm, 6,25ppm, 12,5ppm, and 25ppm were then made through serial dilution with distilled water (Table 2).

**Table 1: Dilution series for chloride standards**

| Concentration (ppm) | Volume of Stock (mL) | Distilled water (mL) |
|---|---|---|
| 125 | 2,50 | 17,50 |
| 250 | 5,00 | 15,00 |
| 500 | 10,00 | 10,00 |
| 750 | 15,00 | 5,00 |
| 1000 | 20,00 | 0,00 |

**Table 2: Dilution series for sulfate standards**

| Concentration (ppm) | Volume of Stock (mL) | Distilled water (mL) |
|---|---|---|
| 3,125 | 2,50 | 17,50 |
| 6,25 | 5,00 | 15,00 |
| 12,5 | 10,00 | 10,00 |
| 25 | 20,00 | 5,00 |

## 3.3 Testing

### 3.3.1 Ion Chromatography (IC)

The IC vials were placed in the Ion Chromatographer along with blanks (distilled water) and the standard solutions of NaCl and sulfate (Figure 8). The results provided the area under the curve, height, and concentration (see Ion Chromatography results in Appendix). However, the concentration provided by the IC is not the actual concentration in the sample, but rather the concentration in the supernatant. To find the actual concentration in the sample, a calibration curve was first created using the standard solutions of known chloride concentrations. The relationship between peak area and concentration is assumed to be linear:

$$C = \text{Area} - b \,/a \qquad (1)$$

The result in ppm (mg/L) was then multiplied by the extraction volume (0,05 L) to calculate the total chloride mass in mg for each sample. Finally, this value was divided by 0,005 to find the

chloride concentration per kg of dry clay (mg/kg). The porewater content of the sample was determined by multiplying the dry mass of the clay, and then dividing the mass of water lost during drying (See Table B3 in Appendix).

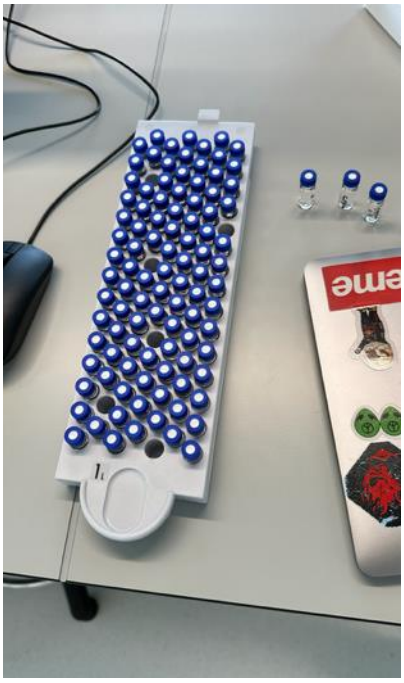

*Figure 8: IC vials in chromatographer tray before running the chromatogram.*

### 3.3.2 Electrical Conductivity (EC)

With the extracted porewater that remained after filtration and IC measurements, the electrical conductivity (EC) was measured. This was done using an EC probe and meter with a set up that included a retort stand and clamp to hold the probe for ease of measuring the 1:10 solid to liquid ion extraction (5 grams dried clay with 50 mL distilled water). The probe was fully submerged into the extracted porewater, and measurements were taken after the number on the meter settled. EC and temperature were each measured three times, and the average measurement for each was used for further calculations. After each submersion the probe was rinsed using distilled water to start at 0 μS/cm for each sample.

However, as both EC measurements proved to be uncharacteristically dominated by sulfate, most likely because of sulfide oxidation after the exposure of oxygen during coring processes, new EC values were calculated using Geochemist Workbench for all 73 samples. These were calculated solely using chloride concentrations as EC depends on ionic concentrations, making these values comparable across depths and samples. Sodium was made equal to chloride for ion balancing, and pH values were inputted as well, as seen in Figure 7. The proxy formation factor was then calculated using Equation 2.

| | | 1 | 2 | 3 | 4 | 5 | 6 | 7 |
|---|---|---|---|---|---|---|---|---|
| Sample ID | | 1 | | | | | | |
| $Ca^{++}$ | mmol/l | | | | | | | |
| $Mg^{++}$ | mmol/l | | | | | | | |
| $Na^{+}$ | mmol/l | 609.8 | 501.8 | 579.8 | 460.1 | 460.5 | 596 | 393.9 |
| $K^{+}$ | mmol/l | | | | | | | |
| $HCO_3^{-}$ | mmol/l | | | | | | | |
| $SO_4^{--}$ | mmol/l | | | | | | | |
| $Cl^{-}$ | mmol/l | 609.8 | 501.8 | 579.8 | 460.1 | 460.5 | 596 | 393.9 |
| pH | | 7.36 | 7.34 | 6.6 | 7.2 | 8.21 | 7.75 | 7.56 |
| Electrical conductivity | uS/cm | 54800.1 | 45888.6 | 52339.8 | 42403.3 | 42437.2 | 53669.8 | 36809.0 |

*Figure 7: Snapshot of the new estimated EC values calculated using pH, chloride concentrations in mg/L (ppm) of the extracted porewater of all samples, and the same value of chloride for sodium for an electrically neutral system. All the EC values and pH values can be seen in Table B3 in the Appendix.*

### 3.3.3 Resistivity

The bulk electrical resistivity was measured for 42 out 73 samples using a makeshift resistivity cell at COVRA premises. This cell was made up of two electrodes where the thicker (around 1cm) steel circular plate acted as the base electrode. Its thickness was useful for holding up the rest of the cell, ensuring stability. These circular stainless-steel plates acted as a conductive contact surface for electric current to pass through the sample evenly. A cloth saturated with de-mineralized water was placed between the base plate and a thinner (around 0,5cm) circular steel plate acting as a conductive bridge between plates. This was followed by a

short PVC tube where the soil was placed. The same arrangement as the lower electrode was placed on top of the PVC tube and on top of that a heavy object (filled spray bottle) was placed as well to compress the cell and avoid any gaps where air may interrupt the current flow as it can act as an insulator. This setup can be seen in Figure 9. The base plate was connected to a resistivity meter where measurements were displayed and recorded in k Ω cm.


*Figure 9: Make-shift resistivity cell at COVRA premises. (Image by author)*

Each soil sample was taken from the PVC pipes with a soil sampler or spoon and placed into the tubular compartment of the cell. This short tube helped keep the soil sample intact as it was made up of PVC, which is a non-conductive material. From the bulk resistivity it is possible to calculate the proxy formation factor for each sample, however, due to time constraints and the

unavailability of the resistivity cell on the first day of soil sampling, only 42 out of 73 samples had their resistivity measured.

In this respect, the formation resistivity factor indicates the degree of connectivity in the pore matrix through calculating the ratio between the soil's bulk resistivity (Ro) and extract resistivity (Rw) as seen in Equation (2). It should be noted that as the porewater resistivity is the inverse of the conductivity of the porewater, which is not what was measured but rather the extracted leachate (1:10 soil to water ratio), it is not the true porewater resistivity. The calculation of extracted porewater is illustrated in Equation (3), where ρ is resistivity and σ is conductivity.

Therefore, the formation factors are a proxy to the true values which would be calculated with original porewater resistivity. The formation factor is dimensionless and always greater than one. Calculating the proxy formation factor aids the evaluation of the solute transport mechanism in the two Dutch Paleogene clays. However, as bulk resistivity measurements could not be made for Watervliet clay, proxy formation factors were only calculated for Boom clay although values were assumed to be similar or greater due to its deeper location in the core (~15m) resulting in a greater compaction affecting pore channels and size.

$$F* = \frac{Ro}{Rw} \qquad (2)$$

$$\rho = \frac{1}{\sigma} \qquad (3)$$

A greater formation factor tends to indicate a more tortuous pore matrix which may inhibit or limit the flow of ionic species such as NaCl, thus an electric current is limited as well. Similarly, if the proxy formation factor is lower, then it can be concluded that the pore matrix is well-connected or has wider pores. As mentioned, impermeable layers are characteristic of diffusion-dominated systems as advection is negligible in low permeability environments. Therefore, if both Paleogene clays have a large formation factor, it can be concluded that diffusion is the dominant transport mechanism (Gimmi & Churakov, 2019).

### 3.3.4 pH

The pH of each sample was measured in the Anne lab using a pH probe. Before measurements, the probe was calibrated with a buffer solution of pH 7. The probe was fully submerged for about 5 minutes in the centrifuge tubes containing the distilled water leachate. As some samples had replicated, a few of the samples have a pH as an average between the replicates instead of a measurement directly read from the pH meter as seen in the Appendix in Table B3. This gives greater reliability to measurements. Similarly, the probe was rinsed with distilled water with every submersion to remove the porewater from the previous sample which may have had a different pH, ensuring accurate readings.

### 3.3.5 Effective Diffusion Coefficients

The effective diffusion coefficient ($D_{eff}$) indicates the rate of solute transport in porous mediums, correcting the molecular diffusion coefficient for pore structure effects, mainly tortuosity using resistivity derived formation factors. In this manner, determining the rate of solute transport is an effective tool for understanding the type of solute mechanism apparent

within these sandy to clayey layers. To calculate the $D_{eff}$, the molecular diffusion coefficient ($D_0$) for chloride in free water, at 25 degrees ($2.0 \times 10^{-9}$ $m^2/s$ ) was divided by the proxy formation factors as seen in equation 6 (Boudreau, 1997). The use of the formation factor indirectly corresponds to tortuosity and porosity for these layers, which are essential and most common elements for calculating the $D_{eff}$ , as seen in equation 4 (Meeussen et al., 2017; Busch et al., 2018)

$$D_{eff} = \eta D_{pore} = \eta \frac{\delta}{\theta^2} D_0 \qquad (4)$$

where:

$D_{pore}$ - pore water coefficient (or bulk diffusion coefficient) accounting for the effects of tortuosity ($m^2$ /s)

$D_0$ - molecular diffusion coefficient in free water ($m^2$ /s),

$\theta^2$ - tortuosity factor (-) and equal to $(L_a/L)^2$ where $L_a$ represents the longer path through the solid grains the molecules can flow through and L is the distance in a straight line.

$\delta$ - constrictivity factor (-),

$\eta$ - total porosity (-)

In many cases it is difficult to distinguish the $\theta^2$ from the $\delta$, therefore they are often combined into a geometrical factor.

$$\frac{\delta}{\theta^2} = \frac{1}{G} \qquad (5)$$

$$D_{eff} = \frac{D0}{F} \qquad (6)$$

$D_{eff}$ coefficient values could only be calculated for samples 11 to 41 for the Breda Formation, samples 59 to 68 for the Ruisbroek Sand layer and samples 69 and 70 of the Watervliet Clay layer due to the lack of bulk resistivity measurements for the remainder of the samples. Therefore, a conservative literature-based formation factor (143) was used to estimate $D_{eff}$ coefficients in Boom clay and the remaining Watervliet Clay samples of which were also compared with published $D_{eff}$ coefficients for such marine clays. Hence, these values should not be interpreted as direct measurements but rather approximations. $D_{eff}$ coefficient values for all layers can be found in Table B4 in the appendix, and a snapshot of it is also found in the results section. A deeper overview of the differences in $D_{eff}$ coefficient values between layers is found in the discussion.

Two Watervliet Clay samples (69 and 70) had their bulk resistivity measurements; these were the only samples that had direct $D_{eff}$ coefficient calculations made. Therefore, taking into account the formation factor range (143 to 181) for Mont Terri Opalinus Clay samples found in a study conducted focusing on the diffusion rate for Cl-, HTO, $I^-$,$Na^+$ . This study chose the conservative formation factor of 143 for Boom Clay and the remaining 3 samples for Watervliet clay. This value was chosen due to Opalinus Clay having By choosing a lower-bound estimate, the pore matrix is assumed to be less tortuous in these layers, resulting in upper-bound (overestimated) effective diffusion coefficients (Van Loon et al., 2003).

$D_{eff}$ coefficient values for HTO (liquid electrolyte) in Boom clay was found using a Fractal Model and with experimental plug samples with values ranging from $10^{-10}$ to $10^{-11}$ $m^2/s$ (Busch et al., 2018). However, the anionic tracer Cl- is assumed to have a slightly slower diffusion rate due to anionic exclusion due to surface electrostatic repulsion, size and dead-end pores and the Donnan effect which “limits the movement of anions through interlayer narrow

pores in clay" (Meeussen et al., 2017). On the same note, Opalinus Clay (a marine argillaceous clay similar to Boom Clay) in Mont Terri and Benken had $D_{eff}$ coefficient values (perpendicular to bedding) in the range of $10^{-11}$ to $10^{-12}$ $m^2/s$.

The directly calculated diffusion values from this study were interpreted as vertical (perpendicular to bedding) rather than horizontal (parallel to bedding) values, which can alter the diffusion rate by a factor of approximately 2 to 3, as seen in laboratory diffusion experiments for the neutral tracer HTO (Weetjens et al., 2012, Bruggeman et al., 2013). This anisotropy factor is affected by compaction and consolidation pressure; therefore, an increase of these parameters will likely result in an increase of the anisotropy factor (Bruggeman et al., 2013). An example of an anionic tracer i.e. Iodide also shows direction dependent diffusion values of which can be assumed similar to the 2 to 3 anisotropy factor previously mentioned for HTO (Durce et al., 2024). Vertical transport is slower due to the layered structure and tortuosity of the pore network reducing the overall space for transport; therefore, all samples overall serve as a conservative estimate for diffusion.

### 3.4 Assumptions and limitations

Due to capacity limitations (oven space and limited beakers) and limited opportunities to use the Ion Chromatographer, only a few samples could have both their "0,1" and "0,2" measurements analyzed to find an average value for the IC. Samples with average values are colored orange in Table B3 in the Appendix.

Due to time constraints, the samples were collected from COVRA on two separate days. The resistivity cell was unavailable for use on the first day. Therefore, only samples that were collected on the second day (samples 11-40 and 58-70) could have their bulk resistivity

measured. It was assumed that all NaCl was extracted from the soil samples and present in its porewater after leaching.

For a few samples (Samples 42-52, which are samples consisting of Boom Clay), it was found that the clay stored in the PVC pipes had expanded and hardened over time which made it difficult to collect samples in the standard way. For these samples, one of the two caps of the pipe was cracked and broken open using a hammer (Figure 10). Upon reaching the clay sample by this method, the clay was sprayed with distilled water and allowed to sit for about an hour to loosen up so the samples could be collected with ease. The pipes were resealed using parafilm and duct tape upon completion of sample collection.

*Figure 10: Sample 42 was cracked open with a hammer, sampled with a borer, and then later sealed with parafilm and duct tape.*

Additionally, it was found that sulfate was present in the blanks used for the IC, which led to the conclusion that the distilled water in the Anne lab had sulfate in it. This same distilled water was used for the dilution of the IC samples. The sulfate concentration in the blank, which was found to be 0,197 mol/L, was subtracted from all sample concentrations to ensure the values derived from the IC were only from sulfate in the samples, and not the distilled water.

It was also assumed that all extracted chloride originally came from porewater or exchangeable pools.

# 4 Results

## 4.1 IC results

Upon completing the IC, the calculated concentrations of chloride and sulfate (mg/kg of dry rock) were graphed and displayed below in Graph 1.

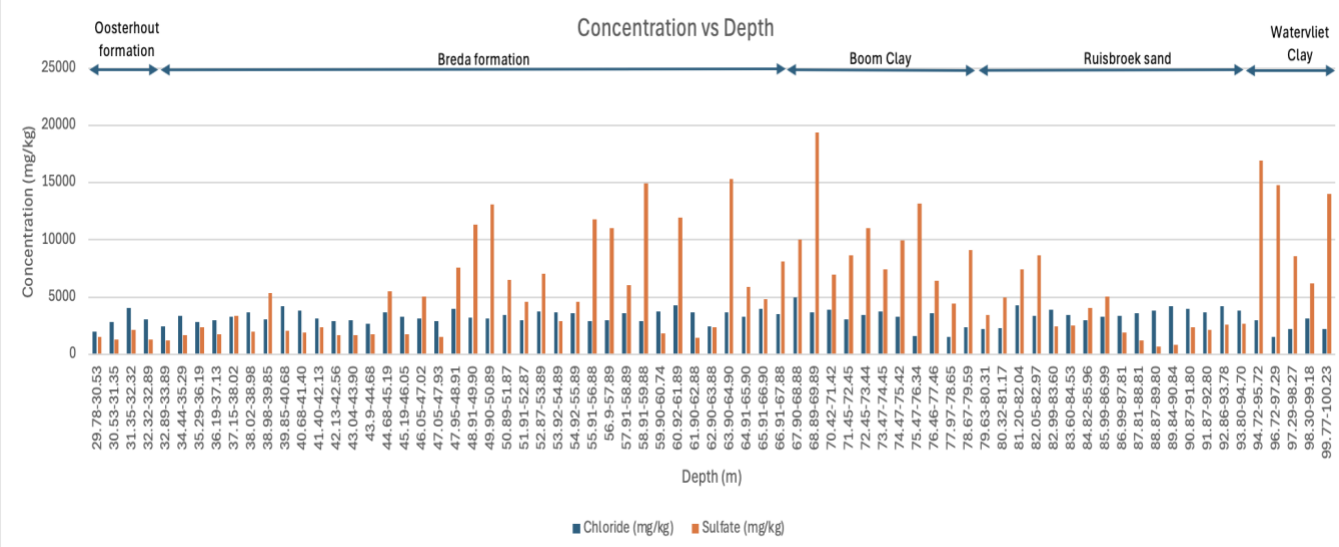


*Graph 1: Chloride and Sulfate profile over depth. The type of formations are indicated at the top of the graph.*

Graph 2 shows that chloride experiences gradual variations with depth, with no extreme changes over small depth intervals except for a few small spikes and drops. The highest peak of chloride is at a depth of 67,90-68,88m where Boom Clay is present. Outside of this peak, it is relatively constant throughout the core. Graph 3 shows a higher concentration of chloride in the porewater content of the clay, while also maintaining a similar pattern as the chloride concentration in the dry sample.

For sulfate (Graph 4), there are much larger spikes in concentration than chloride, with this highest peak at 68,89-69,89m. It can also be noticed that there is a separate region of high sulfate concentration from depth 94,72m onwards, which is where the formation of Watervliet Clay begins. The sulfate levels in the Boom Clay region vary but are regularly higher than chloride.

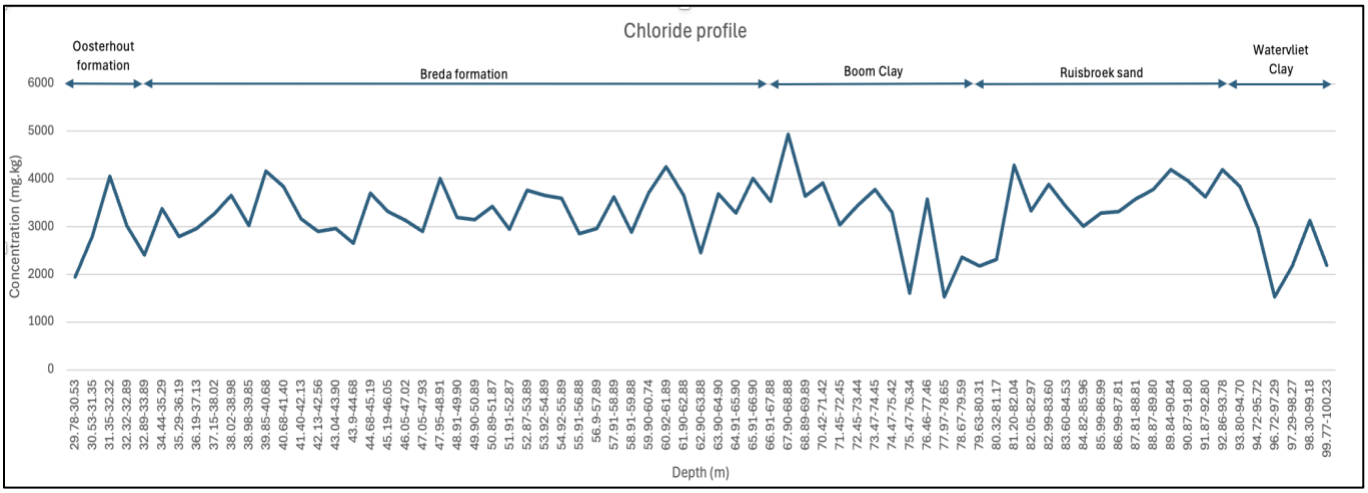


*Graph 2: Chloride profile (mg/kg of dry sample) for all samples with the formation type at the top of the graph.*

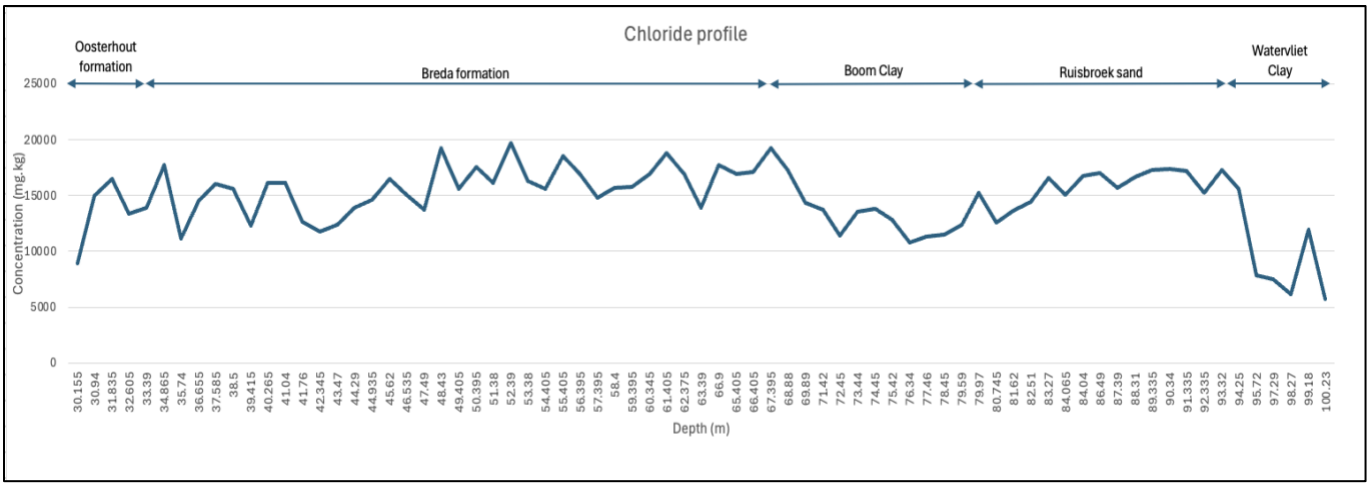


*Graph 3: Chloride profile (mg/kg of porewater) for all samples with the formation type at the top of the graph.*

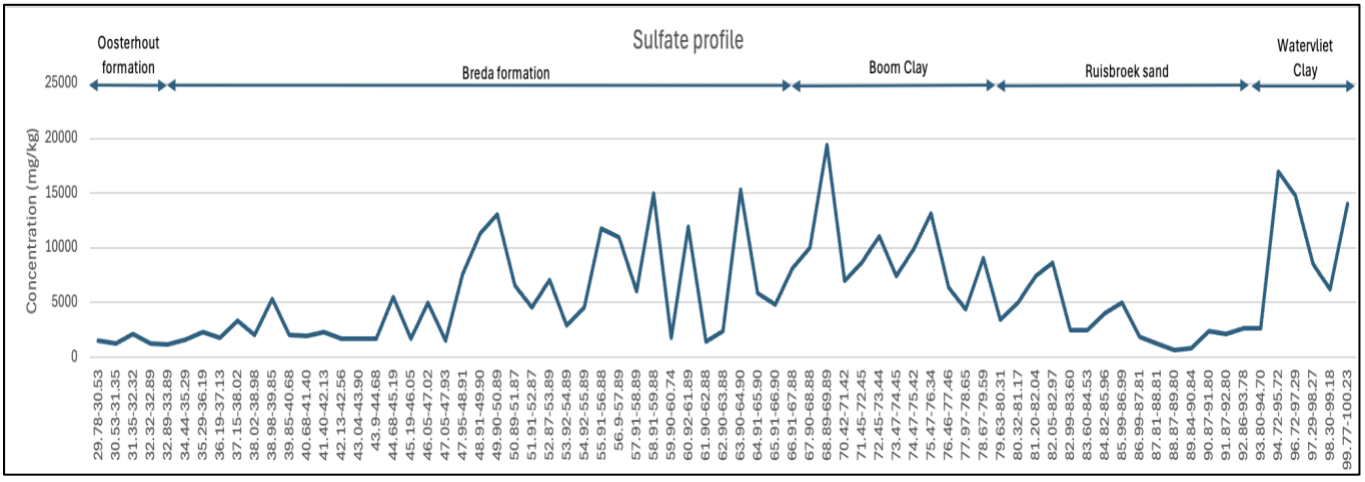


*Graph 4: Sulfate profile with depth for the soil samples with the 1:10 solid to liquid ratio.*

In these soil samples, sulfate seems to dominate as its concentration is much higher than chloride, most probably due to pyrite oxidation. The exact values can be seen in Graph 2 and Table B3 in the Appendix.

## 4.2 EC results

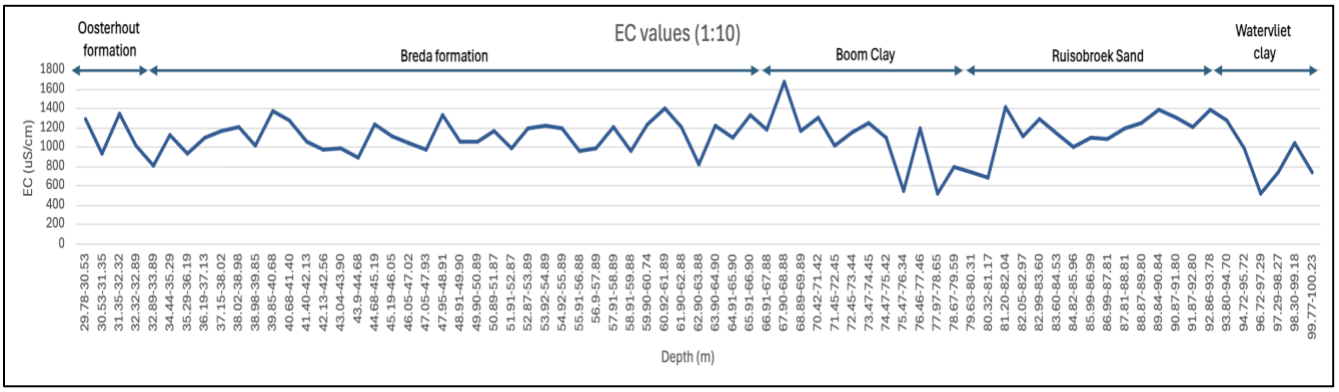


*Graph 5: The electrical conductivity with depth for the extracted porewater (mg/L) with a 1:10 solid to liquid ratio. These EC values were calculated using Geochemist Workbench Professional, using the chloride concentrations derived from the IC, sodium values which were made equal to the values of chloride and pH measurements for all 73 samples.*

Boom Clay and Watervliet Clay extract-based EC values are lower than in the surrounding sandy formations, which is indicative of a fresh to slightly saline extract porewater and partial deviation from original marine composition (Ning et al., 2020). Focusing solely on the porewater inevitably resulted in lower EC values mainly due to the exclusion of mineral surface conduction (Ks), which is the main mechanism to facilitate electrical current in clayey soils at low salinity pore water environments. (Choo et al., 2022). Moreover, anions such as Cl- experience anion exclusion, meaning the accessibility of these ions to move in the pore matrix decreases, which is reflective of the poor ability for these clayey soils to transmit an electrical current (low EC). Nevertheless, these low EC values suggest low ion mobility which points to the retardation of Cl- through adsorption and low permeability, reflective of the low Cl- content at these clay layers.

### 4.3 pH

The pH of the 50 mL distilled water leachate was measured with a pH probe and recorded; Graph 6 shows the results of the pH measurements.

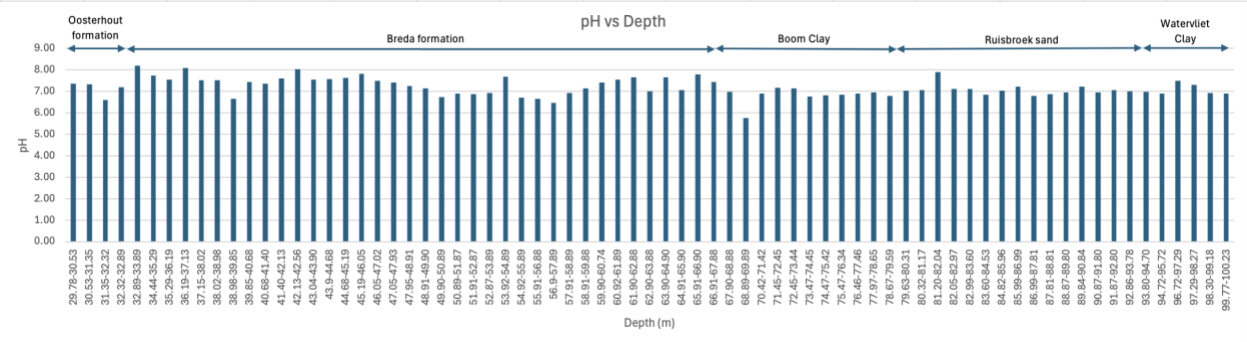


*Graph 6: pH profile across depth*

As seen in Graph 6, the pH stays relatively constant around 7. The most acidic pH was recorded at 68.89-69.89m, which is also the depth with the highest amount of sulfate. This may be due to pyrite oxidation, as pyrite oxidation leads to more acidic conditions if insufficient carbonate minerals are available to buffer the produced acids by pyrite oxidation.

### 4.4 Effective Diffusion Coefficients Results

**Table 3:** Five representative and direct Deff coefficient values for samples 15 to 20 for the Breda Formation, samples 63 to 68 for the Ruisbroek Sand layer and samples 69 and 70 of the Watervliet Clay layer. Opalinus Clay based formation factors were used to calculate the Deff coefficient values for Boom Clay and the remainder of Watervliet Clay samples of which are colored red.

| Samples | Proxy Formation Factor | D0 Molecular Diffusion Coefficient m/s | Effective Diffusion Coefficient |
|---|---|---|---|
| **Breda** | | | |
| 16 | 122,65 | $2,3 \times 10^{-9}$ | $1,9 \times 10^{-11}$ |
| 17 | 150,68 | $2,3 \times 10^{-9}$ | $1,5 \times 10^{-11}$ |
| 18 | 206,70 | $2,3 \times 10^{-9}$ | $1,1 \times 10^{-11}$ |
| 19 | 142,76 | $2,3 \times 10^{-9}$ | $1,6 \times 10^{-11}$ |
| 20 | 169,47 | $2,3 \times 10^{-9}$ | $1,4 \times 10^{-11}$ |
| **Boom Clay** | | | |
| All samples | 143 | $2,3 \times 10^{-9}$ | $1,6 \times 10^{-11}$ |

| | | | |
|---|---|---|---|
| **Ruisbroek Sand** | | | |
| 64 | 221,35 | $2,3 \times 10^{-9}$ | $1,0 \times 10^{-11}$ |
| 65 | 230,30 | $2,3 \times 10^{-9}$ | $1,0 \times 10^{-11}$ |
| 66 | 207,64 | $2,3 \times 10^{-9}$ | $1,1 \times 10^{-11}$ |
| 67 | 282,17 | $2,3 \times 10^{-9}$ | $8,2 \times 10^{-12}$ |
| 68 | 266,68 | $2,3 \times 10^{-9}$ | $8,6 \times 10^{-12}$ |
| **Watervliet Clay** | | | |
| 69 | 137,55 | $2,3 \times 10^{-9}$ | $1,7 \times 10^{-11}$ |
| 70 | 76,11 | $2,3 \times 10^{-9}$ | $3,0 \times 10^{-11}$ |
| 71 | 143 | $2,3 \times 10^{-9}$ | $4,6 \times 10^{-11}$ |
| 72 | 143 | $2,3 \times 10^{-9}$ | $4,6 \times 10^{-11}$ |
| 73 | 143 | $2,3 \times 10^{-9}$ | $4,6 \times 10^{-11}$ |

# 5 Discussion

### 5.1 Determining Diffusion or Advection via ion profiles

The chloride in Graphs 2 and 3 align with the diffusion-dominated shapes described by Mazurek et. al (2011), which explains that diffusion-controlled chloride profiles in clay can appear asymmetric or peaked. The smooth gradients and isolated spikes observed in Graphs 1 and 2 are consistent with the expected patterns for a diffusion-dominated process. Additionally, the smooth curves between 66-72 m, containing a portion of the Boom Clay, and between 94m and 99 m, containing most of the Watervliet Clay, indicate that diffusion is the dominant transport mechanism in both formations.

Additionally, some of the high peaks in sulfate concentration, such as at depths 68,89m-69,89m, 72,45-73,44m, and 75,47-76,34m showed clear signs of pyrite upon sample collection (Figures 11-15). This indicates that the reason for a higher sulfate to chloride ratio, as well as the sudden spikes of sulfate, can be explained by pyrite oxidation.

*Figure 11: Sample 43 (depth 68,89m-69,89m) showing red-brown patches of iron. It has the highest sulfate level of all the samples (19388,9 mg/kg). It has a chloride concentration of 3644,2mg/kg.*

*Figure 12: Sample 46 (depth 72,45-73,44m) showing patches of iron. Sulfate concentration of 11061,1 mg/kg. It has a chloride concentration of 3446,6mg/kg.*

*Figure 13: Sample 49 (depth 75,47-76,34m) bears an orange-ish color and sulfate concentration of 13167,9mg/kg. It has a chloride concentration of 1606,4mg/kg.*

However, there are some exceptions. Samples with low sulfate but higher chloride levels (such as sample 3 in Figure 14) appear considerably redder than those with the highest sulfate concentrations, as shown by comparing Figures 12 and 15. Conversely, a few samples with high sulfate content show little to no redness (Figure 15).

*Figure 14: Sample 3 (depth 31,35-32,32m) with a sulfate concentration of 2130,1 mg/kg and a chloride concentration of 2800,0 mg/kg, It has a chloride concentration of 4059,9mg/kg.*

*Figure 15: Sample 38 (depth 63,90-68,88m) appears to have no signs of pyrite despite having a relatively high sulfate concentration (15311,3 mg/kg). It has a chloride concentration of 3691,9mg/kg.*

## 5.2 Determining Diffusion or Advection via the proxy formation factors and effective diffusion coefficients

### 5.2.1 Comparison of proxy/formation factors and $D_{eff}$ coefficient values between formations

**Table 4:** Average Formation Factor and $D_{eff}$ coefficient values separated by the chosen lower-bound formation factor for Boom Clay and Watervliet Clay from Opalinus Clay and calculated values.

| Formation | Formation Factor | | $D_{eff}$ coefficient values ($m^2/s$) | |
|---|---|---|---|---|
| | Conservative literature based | Avg. calculated (proxy) | Literature based | Avg. calculated |
| Breda | No need for lit. formation factor | 164,8 | No need for a lit. $D_{eff}$ coefficient value | $1,3 \times 10^{-11}$ |
| Boom Clay | 143 | No bulk resistivity measurement; no proxy formation factor | Based on lit. F: $1,6 \times 10^{-11}$<br>Based on lit. $D_{eff}$: $5.70 \pm 0,34 \times 10^{-12}$ | No calculated $D_{eff}$ coefficient value |
| Ruisbroek Sand | No need for lit. formation factor | 238,2 | No need for a lit. $D_{eff}$ coefficient value | $1,2 \times 10^{-11}$ |
| Watervliet Clay | 143 | 106,8 | $1,6 \times 10^{-11}$ | $2,3 \times 10^{-11}$ |

The tortuosity and porosity differences are apparent between formations simply by considering their (literature-based/proxy) formation factors and (literature-based/average) $D_{eff}$ coefficient values. Boom Clay has the slowest literature based $D_{eff}$ coefficient value ($5.70 \pm 0.34 \times 10^{-12}$ $m^2/s$) which infers greatest solute resistance by the soil and pore matrix compared to the other formations, which is reasonable due to its dominance in fine-grained swelling clays such as

illite and smectite which results in much more dead end and narrower pore channels (Beaucaire et al., 2000). On the other hand, another diffusion coefficient of 1,6 x $10^{-11}$ $m^2/s$ is proposed for Boom clay. This value assumes faster diffusion by using the formation factor of 143, which is the lower end of the 143 to 181 range for the Mont Terri opalinus clay in the study by Bruggeman et al. (2013). As Opalinus clay is considered as or has even faster effective diffusion rates due to greater clay content i.e. 40 to 80% depending on the depth and area and is a more rigid claystone, while Boom clay has a clay content of around 60% (at the Mol site) and is a more plastic and indurated claystone, allowing for greater solute transport when compared (Wemaere et al., 2008; De Craen et al., 2004). Both diffusion rates are consistent with the study conducted by Busch et al (2018), where $D_{eff}$ coefficient values for HTO in Boom Clay ranged from $10^{-10}$ to $10^{-11}$ $m^2/s$ pointing towards a diffusion dominated solute system.

The chosen literature-based formation factor for Watervliet clay was also 143 for simplicity, as the main requirement for the resulting estimated Deff was not accuracy but rather for it to be a close approximation to literature-based $D_{eff}$ coefficient values for Watervliet clay. As Watervliet clay and Boom Clay share a high illite/smectite content, similar depositional environment and sediment structure, the use of this formation factor for both layers can be justified. The resulting $D_{eff}$ coefficient value by use of this formation factor 143 was 1,6 x $10^{-11}$ $m^2/s$, like Boom clay. However, in theory diffusion rates should be faster in Watervliet clay layers due to its larger content of sand and silt, yet both are still considered for radioactive nuclear waste due to their low hydraulic conductivity, high sorption capacity and reducing conditions Hoving et al. (2024). In terms of samples 69 and 70, the average formation factor was 106,8 resulting in a $D_{eff}$ coefficient value of 2,3 x $10^{-11}$ $m^2/s$, which is the fastest diffusion rate compared to all formations. This reflects the limited sample availability of this layer where it is

possible locally less tortuous pathways may have been captured, reducing the overall $D_{eff}$ coefficient value. According to Bruggeman et al. (2013), heterogeneity within a unit can be as large as differences between units. Additionally, although clay has a high total porosity, it is possible that not all those voids are accessible for anions like Cl- due to the electrical double layer and Donnan effects, reducing the overall $D_{eff}$ coefficient value (Van Loon et al., 2003; Meeussen et al., 2017).

The Breda formation has an average $D_{eff}$ coefficient value of 1,3 x $10^{-11}$ $m^2/s$ based on the average proxy formation factor of 164,8. This diffusion value is slower than Watervliet clay and the $D_{eff}$ coefficient derived from the literature based formation factor for Boom clay (1,6 x $10^{-11}$ $m^2/s$) and slightly faster than Ruisbroek sand, possibly also due to a greater sample density with bulk resistivity measurements made, unlike Watervliet and Boom clay. Additionally, as this formation mainly consists of fine to medium grained glauconitic sand followed by silt and clay although the exact makeup depends on the area at hand, i.e. the northwest of the Netherlands contains more clay compared to the south, which has a sandier texture and of which these samples come from. This relates to larger more connected pores characteristic of sandy layers and corresponds to the similarity in diffusion rates with Ruisbroek sand. Similarly, well-sorted sand promotes diffusion as pathways would be relatively straight which leads to less heterogeneity, a lower tortuosity and hence a faster $D_{eff}$ coefficient value (Boudreau, 1997).

Ruisbroek sand has the average highest formation factor and lowest calculated $D_{eff}$ coefficient (238,2 and $1.2 \times 10^{-11}$ $m^2/s$). This high proxy formation factor could be a reflection of its fine grained, clayey, and glauconitic composition which can result in the development of microporosity and tortuous diffusion pathways (Beaucaire et al., 2000). The presence of clay coatings and glauconite grains can increase surface conduction and reduce pore connectivity,

resulting in high proxy formation factors and low $D_{eff}$ coefficients, despite the dominance in sand (Boudreau, 1997).

### 5.3 pH variation over the 100m core

The relatively constant pH (±7) observed in Graph 5 demonstrates that the core is well-buffered, most likely due to carbonate or other minerals within the core (Bruggeman & De Craen, 2012; Wang et al., 2023). The localized decrease in pH at 68.89-69.89m, which is where the highest sulfate concentration was, suggests the occurrence of localized redox reactions. This interpretation is supported by Figure 10, which shows discrete patches of pyrite formation. Additionally, the relatively neutral pH across the core provides optimal conditions (pH 6-8) for sulfate reducing bacteria to form the observed pyrite (Tran et al., 2021).

Overall, the stable pH supports the conclusion that chemical conditions are relatively uniform across the 100m core, which is consistent with diffusion-dominated solute movement.

### 5.4 Ratio of Ions in the Core Compared to Sea Water

The overall $Cl^-$ : $SO_4^{2-}$ for the entire core was calculated using the sum of chloride and sulfate concentrations in the sediment at all depths, resulting in a ratio of 0.564 (total chloride = 238209mg/kg, total sulfate = 422363mg/kg). As the obtained ratio is less than 1, sulfate is the more abundant ion in the core porewater. The ratio of $Cl^-$ : $SO_4^{2-}$ at each depth can be seen in the Appendix, Table B2. As Table B2 shows, most samples between 29-43m have a ratio greater than 1, meaning chloride was higher in the shallower layers.

For comparison, the typical $Cl^-$ : $SO_4^2$ ratio in seawater is ~7.06 (Sudaryanto & Naily, 2018), indicating that chloride is higher than sulfate in seawater. The significantly lower ratio observed in the core suggests that geochemical processes, such as limited chloride transport

within the clay and redox reactions leading to pyrite formation, may have influenced porewater chemistry. Although, chloride and sulfate concentrations were found for the chemically altered extract after leaching, these findings still highlight the fact that porewater composition changes over time, and the core is no longer reflective of the original marine conditions.

### 5.5 Possibility of Quantitative Transport Modelling

Quantitative transport modelling is the use of acquired data for predicting the concentrations, fluxes and transport of radionuclides in the future, based on the pre-determined dominant transport mechanism found for the specific soil profile at hand. There is data missing to build a quantitative transport model in this study, yet a summarized table of the elemental parameters needed to construct a quantitative transport model has been put forth. It is important to note that the specific data required can differ based on the baseline transport mechanism that has been determined for the specific soil formation.

For diffusion dominated transport, which is most prominent in low permeable layers such as Boom Clay and Watervliet Clay, the minimum data required is the effective diffusion coefficient, effective porosity (ne), distribution coefficient (Kd), retardation factor and geochemical process such as pH and redox etc. Advection dominated transport includes parameters such as hydraulic conductivity and gradient, Darcy velocity, the dispersion coefficient, porosity and the retardation factor.

Additionally, although these parameters are classified as the minimum data needed to build a quantitative transport model, it is also encouraged to add as much unique details on the chosen soil formation to make it as specific as possible and avoid important data to be neglected. For example, disregarding the incorporation of the ‘Darcy velocity’ would risk the over or under estimation of the velocity of the radionuclide in the soil pore channels. However, as collecting

and processing data can be time-consuming, the minimum number of parameters according to literature cannot be disregarded for a quantitative transport model as shown in Table (5). The corresponding formulas and classification depending on the transport system are made clear.

**Table 5:** Necessary parameters for quantitative transport modelling according to Vandersteen et al. (2013)

| **Parameters for Quantitative Transport Modelling** | | | |
|---|---|---|---|
| Diffusion dominated systems | | Advection dominated systems | |
| **Parameter** | **Formula** | **Parameter** | **Formula** |
| Effective Diffusion Coefficient (De) | $De = D0 \times ne/\tau$ *or* $De = D0 / F$* | Hydraulic Conductivity | No direct formula |
| Effective Porosity (ne) | $n_e = \frac{V_{p,\text{effective}}}{V_t}$ | Hydraulic Gradient | $i = \Delta h / L$ |
| Distribution Coefficient (Kd) | $Kd = \frac{Cs}{Cm}$ | Darcy Velocity | $q = -K * i$ |
| Retardation Factor | $R = 1 + \frac{\rho b \cdot Kd}{\theta}$ | Dispersion Coefficient | $D = \alpha * v + De$ |
| Geochemical Parameters (pH, redox etc.) | No direct formula | Effective Porosity (ne) | $n_e = \frac{V_{p,\text{effective}}}{V_t}$ |
| | | Retardation Factor | $R = 1 + \frac{\rho b \cdot Kd}{\theta}$ |

## 6 Conclusion

There were three direct methods employed to determine the dominant transport mechanism for boom Clay and Watervliet Clay within the 100m soil core, focusing on the depth were first evaluated (Graph 1 and 2), where the smooth concentration gradients observed within both clay formations indicate diffusion-dominated transport. The overall asymmetric patterns and isolated concentration peaks are also consistent with diffusion-controlled systems, as described by Mazurek et al. (2011). In Graph 3, most sulfate concentration peaks coincide with

zones of pyrite formation (Figures 11-124), although some exceptions are present, reflecting localized geochemical processes superimposed on the general diffusive background.

The observation that sulfate concentrations exceed chloride concentrations in the 1:10 soil-water extracts further supports a diffusion-dominated system, as does the vertically variable chloride profile, which is inconsistent with advective flushing and instead suggest slow, gradient-controlled transport. A relatively constant pH of approximately 7 throughout most of the core indicates a well-buffered geochemical system, likely controlled by carbonate equilibrium and clay mineral buffering. Localized pH decreases and elevated sulfate concentrations at depths of 69.89 to 69.89 m suggest redox controlled processes, such as pyrite formation, but these occur only locally and do not dominate the overall transport regime. The general absence of significant pH shifts is consistent with diffusion-dominated transport rather than advective recharge or discharge.

Chloride – sulfate ratios further support this interpretation. Most samples exhibit Cl: $SO_4^{2-}$ ratios below 1, indicating sulfate dominance, whereas shallow depths (29 to 43m) show ratios above 1, reflecting higher chloride contents closer to the surface. Geochemical processes such as redox reactions and limited chloride transport were attributed reasons for an overall shift from the seawater $Cl^-$ : $SO_4^2$ ratio of ~7.06 which indicates $Cl^-$ being the dominant ion to lower $Cl^-$ concentrations. Therefore, this exemplifies the fact that although both Boom Clay and Watervliet Clay are marine originated, over geological time periods these porewater compositions change due to alterations in structure through compaction and diagenesis. Therefore, they are not reflective of the original marine conditions they are derived from.

Proxy formation factors and effective diffusion coefficients derived from extract-based EC values provide quantitative support for the interpreted diffusion-dominated transport

mechanism in the core. The calculated effective diffusion coefficients for Boom clay and Watervliet clay are in the magnitude of $10^{-11}$ to $10^{-12}$ $m^2/s$, which is consistent with the values reported in literature for compacted marine clays i.e. Opalinus clay, reflecting a diffusion-dominated transport system. Although the values used in this study represent proxy estimates as extract resistivity was used in place of true porewater resistivity, literature formation factors and $D_{eff}$ coefficients were used for Boom clay and partially for Watervliet to 'fill in the gaps' and for comparison purposes. These estimates were still useful to quantitively demonstrate that the rate of diffusive transport is slow in these clay layers and thus advective transport is negligible.

Through analysis of the above methods, the overall conclusion is that the two Dutch Paleogene clays, Boom Clay and Watervliet Clay, show consistent diffusion dominated transport patterns. These clays are thus strong candidates for long-term radioactive waste disposal due to their slow migration pathways, thickness, and depth. To further solidify these findings, a quantitative transport model is advised to predict the long-term fluxes, concentration, and transport of the radioactive elements specific to the soil core at hand. In Table (4) the essential characteristics required to build such a model are made clear.

## 7 References

Adrichem, V., & W.P.F Kouwe. (1993). *Stratigraphic nomenclature of the Netherlands, revision and update by RGD and NOGEPA*. *50*.

Allard, E., Passirani, C., & Benoit, J.-P. (2009). Convection-enhanced delivery of nanocarriers for the treatment of brain tumors. *Biomaterials*, *30*(12), 2302–2318. https://doi.org/10.1016/j.biomaterials.2009.01.003

Alwina Hoving, A., Kivits, T., & Griffioen, J. (2024). *Geochemical characterisation of the Watervliet Member and groundwater in Paleogene and other sandy units of Zeeland*. https://www.covra.nl/app/uploads/2025/02/2024-R12632_Geochemical-characterisation-Watervliet-Member-Paleogene-groundwater_FINAL.pdf

Beaucaire, C., Pitsch, H., Toulhoat, P., Motellier, S., & Louvat, D. (2000). Regional fluid characterisation and modelling of water–rock equilibria in the Boom clay Formation and in the Rupelian aquifer at Mol, Belgium. *Applied Geochemistry*, *15*(5), 667–686. https://doi.org/10.1016/s0883-2927(99)00067-0

Boudreau, B. P. (1997). *Diagenetic models and their implementation*. https://doi.org/10.1007/978-3-642-60421-8

Bruggeman, C., & De Craen, M. (2012). *EXTERNAL REPORT SCK•CEN-ER-206 Boom Clay natural organic matter Status Report 2011 SCK•CEN Boeretang 200 BE-2400 Mol Belgium*. https://roma.sckcen.be/ws/portalfiles/portal/250320/ER-206.pdf

Bruggeman, C., Maes, N., Aertsens, M., De Cannière, P., & SCK•CEN. (2013). *Tritiated water retention and migration behaviour in Boom Clay* [Report]. SCK•CEN. https://roma.sckcen.be/ws/portalfiles/portal/92677/ER-248.pdf

Charlet, L., Alt-Epping, P., Wersin, P., & Gilbert, B. (2017). Diffusive transport and reaction in clay rocks: A storage (nuclear waste, CO2, H2), energy (shale gas) and water quality

issue. *Advances in Water Resources*, *106*, 39–59. https://doi.org/10.1016/j.advwatres.2017.03.019

Choo, H., Park, J., Thi, T., DO, & Lee, C. (2022). Estimating the electrical conductivity of clayey soils with varying mineralogy using the index properties of soils. *Applied Clay Science*, *217*, 106388. https://doi.org/10.1016/j.clay.2021.106388

De Craen, M., Wang, L., Van Geet, M., & Moors, H. (2004). *Geochemistry of Boom Clay Pore Water at the Mol site – status 2004*. (SCK CEN Reports; No. BLG-990). SCK CEN.

Durce, D., Aertsens, M., Maes, N., Van Gompel, M., & Brassinnes, S. (2024). Comparison of lab-scale experiments for the determination of non-reactive tracer diffusion coefficients in Boom Clay. *Applied Geochemistry*, *173*, 106101. https://doi.org/10.1016/j.apgeochem.2024.106101

COVRA NV. (2024). *COPERA CLA 2024 A CONDITIONAL SAFETY CASE AND FEASIBILITY STUDY*. www.covra.nl

Gimmi, T., & Churakov, S. V. (2019). Water retention and diffusion in unsaturated clays: Connecting atomistic and pore scale simulations. *Applied Clay Science*, *175*, 169–183. https://doi.org/10.1016/j.clay.2019.03.035

IAEA. (2011). *IAEA Safety Standards for protecting people and the environment Disposal of Radioactive Waste*. https://www-pub.iaea.org/MTCD/Publications/PDF/Pub1449_web.pdf

Jacobs, P., & De Coninck, F. (1992). *Qualitative clay m ineralogy of th e Middle and Upper E ocene in north-western Belgium*.

Jeudy, H. (2017, August 7). *How to Calculate Groundwater Velocity*. Sciencing. https://www.sciencing.com/how-8095052-calculate-groundwater-velocity/

*Journal of Rock Mechanics and Geotechnical Engineering*, *9*(5), 856–876. https://doi.org/10.1016/j.jrmge.2017.05.007

Mazurek, M., Alt-Epping, P., Bath, A., Gimmi, T., Niklaus Waber, H., Buschaert, S., Cannière, P. D., Craen, M. D., Gautschi, A., Savoye, S., Vinsot, A., Wemaere, I., & Wouters, L. (2011). Natural tracer profiles across argillaceous formations. *Applied Geochemistry*, *26*(7), 1035–1064. https://doi.org/10.1016/j.apgeochem.2011.03.124

Meeussen, J., Rosca-Bocancea, E., Schröder, T., Koenen, M., Valega Mackenzie, F., Maes, N., TNO, SCK, & COVRA. (2017). *Model representation of radionuclide diffusion in Boom Clay*. https://www.covra.nl/app/uploads/2019/08/OPERA-PU-NRG6131.pdf

M. Jobmann, A. Bebiolka, V. Burlaka, Herold, P., Jahn, S., A. Lommerzheim, J. Maßmann, A. Meleshyn, S. Mrugalla, Reinhold, K., A. Rübel, Stark, L., & G. Ziefle. (2017). Safety assessment methodology for a German high-level waste repository in clay formations.

Muniruzzaman, M., & Rolle, M. (2019). Multicomponent Ionic Transport Modeling in Physically and Electrostatically Heterogeneous Porous Media With PhreeqcRM Coupling for Geochemical Reactions. *Water Resources Research*, *55*(12), 11121–11143. https://doi.org/10.1029/2019wr026373

NEA. (2019, December 20). *Natural Tracer Profiles Across Argillaceous Formations: The CLAYTRAC Project*. Nuclear Energy Agency (NEA). https://www.oecd-nea.org/jcms/pl_14268/natural-tracer-profiles-across-argillaceous-formations-the-claytrac-project

Ning, S., Zhou, B., Wang, Q., & Tao, W. (2020). Evaluation of irrigation water salinity and leaching fraction on the water productivity for crops. *International Journal of*

*Agricultural and Biological Engineering*, *13*(1), 170–177. https://doi.org/10.25165/j.ijabe.20201301.5047

Paul C. Rizzo Associates, Inc. (2013). *PRELIMINARY GROUND INVESTIGATION REPORT PROJECT KCB2 BORSSELE, THE NETHERLANDS*.

Rumynin, V. G. (2011). Subsurface Solute Transport Models and Case Histories. In *Theory and applications of transport in porous media*. Springer International Publishing. https://doi.org/10.1007/978-94-007-1306-2

Sudaryanto, & Naily, W. (2018). Ratio of Major Ions in Groundwater to Determine Saltwater Intrusion in Coastal Areas. *IOP Conference Series: Earth and Environmental Science*, *118*, 012021. https://doi.org/10.1088/1755-1315/118/1/012021

Sun, S., & Zhang, T. (2020). *Reservoir Simulations*. Gulf Professional Publishing.

Till Bollermann, Yuan, T., Johannes Kulenkampff, Stumpf, T., & Fischer, C. (2022). Pore network and solute flux pattern analysis towards improved predictability of diffusive transport in argillaceous host rocks. *Chemical Geology*, *606*, 120997–120997. https://doi.org/10.1016/j.chemgeo.2022.120997

Tran, T. T. T., Kannoorpatti, K., Padovan, A., & Thennadil, S. (2021). Sulphate-Reducing Bacteria's Response to Extreme pH Environments and the Effect of Their Activities on Microbial Corrosion. *Applied Sciences*, *11*(5), 2201. https://doi.org/10.3390/app11052201

Van Loon, L., Soler, J., Jakob, A., & Bradbury, M. (2003). Effect of confining pressure on the diffusion of HTO, 36Cl− and 125I− in a layered argillaceous rock (Opalinus Clay): diffusion perpendicular to the fabric. *Applied Geochemistry*, *18*(10), 1653–1662. https://doi.org/10.1016/s0883-2927(03)00047-7

Van Loon, L. R., Leupin, O. X., & Cloet, V. (2018). The diffusion of SO42− in Opalinus Clay: Measurements of effective diffusion coefficients and evaluation of their importance in view of microbial mediated reactions in the near field of radioactive waste repositories. *Applied Geochemistry*, *95*, 19–24. https://doi.org/10.1016/j.apgeochem.2018.05.009

Vandersteen, K., Gedeon, M., & De Craen, M. (2013). *Solute Transport in Boom Clay*.

VIS, G.-J., & Verweij, J. M. (2014). *Geological and geohydrological characterization of the Boom Clay and its overburden OPERA-PU-TNO411*. https://www.covra.nl/app/uploads/2019/08/OPERA-PU-TNO411.pdf

Wang, L., Miroslav Honty, Mieke De Craen, & Lander Frederickx. (2023). Boom Clay pore-water geochemistry at the Mol site: Chemical equilibrium constraints on the concentrations of major elements. *Applied Geochemistry*, *148*, 105541–105541. https://doi.org/10.1016/j.apgeochem.2022.105541

Weetjens, E., Govaerts, J., & Aertsens, M. (2012). *Model and parameter validation based on in situ experiments in Boom Clay*. http://hdl.handle.net/10038/7624

Yu, L., Gedeon, M., Wemaere, I., Marivoet, J., & De Craen, M. (2011). *Boom Clay Hydraulic Conductivity A synthesis of 30 years of research*. https://roma.sckcen.be/ws/portalfiles/portal/23523114/Boom_Clay_Hydraulic_Conductivity._A_synthesis_of_30_years_of_research_ER-122.pdf

# 8 Appendix

**Table B1: Post-drying weight of 40 g samples and the corresponding water content loss.** The water content from the 40g soil samples were calculated on a wet basis in the fourth column and the standard gravimetric water content in the fifth column.

| Sample | Depth (m) | Weight after drying 40g (g) | Wet - basis water content (g) | Gravimetric water content (g) | Percentage of Water lost (%) |
|---|---|---|---|---|---|
| 1 | 29,78-30,53 | 32,80 | 7,20 | 0,22 | 21,95 |
| 2 | 30,53-31.35 | 33,70 | 6,30 | 0,19 | 18,69 |
| 3 | 31,35-32,32 | 32,10 | 7,90 | 0,25 | 24,61 |
| 4 | 32,32-32,89 | 32,60 | 7,40 | 0,23 | 22,70 |
| 5 | 32,89-33,89 | 34,10 | 5,90 | 0,17 | 17,30 |
| 6 | 34,44-35,29 | 33,60 | 6,40 | 0,19 | 19,05 |
| 7 | 35,29-36,19 | 32,00 | 8,00 | 0,25 | 25,00 |
| 8 | 36,19-37,13 | 33,20 | 6,80 | 0,20 | 20,48 |
| 9 | 37,15-38,02 | 33,20 | 6,80 | 0,20 | 20,48 |
| 10 | 38,02-38,98 | 32,40 | 7,60 | 0,23 | 23,46 |
| 11 | 38,98-39,85 | 32,10 | 7,90 | 0,25 | 24,61 |
| 12 | 39,85-40,68 | 31,80 | 8,20 | 0,26 | 25,79 |
| 13 | 40,68-41,40 | 32,30 | 7,70 | 0,24 | 23,84 |
| 14 | 41,40-42,13 | 32,00 | 8,00 | 0,25 | 25,00 |
| 15 | 42,13-42,56 | 32,10 | 7,90 | 0,25 | 24,61 |
| 16 | 43,04-43,90 | 32,30 | 7,70 | 0,24 | 23,84 |
| 17 | 43,9-44,68 | 33,60 | 6,40 | 0,19 | 19,05 |
| 18 | 44,68-45,19 | 31,90 | 8,10 | 0,25 | 25,39 |
| 19 | 45,19-46,05 | 33,30 | 6,70 | 0,20 | 20,12 |
| 20 | 46,05-47,02 | 33,10 | 6,90 | 0,21 | 20,85 |
| 21 | 47,05-47,93 | 33,00 | 7,00 | 0,21 | 21,21 |
| 22 | 47,95-48,91 | 33,10 | 6,90 | 0,21 | 20,85 |
| 23 | 48,91-49,90 | 33,20 | 6,80 | 0,20 | 20,48 |
| 24 | 49,90-50,89 | 33,90 | 6,10 | 0,18 | 17,99 |
| 25 | 50,89-51,87 | 33,00 | 7,00 | 0,21 | 21,21 |
| 26 | 51,91-52,87 | 34,80 | 5,20 | 0,15 | 14,94 |
| 27 | 52,87-53,89 | 32,50 | 7,50 | 0,23 | 23,08 |

| | | | | | |
|---|---|---|---|---|---|
| 28 | 53,92-54,89 | 32,40 | 7,60 | 0,23 | 23,46 |
| 29 | 54,92-55,89 | 33,50 | 6,50 | 0,19 | 19,40 |
| 30 | 55,91-56,88 | 34,20 | 5,80 | 0,17 | 16,96 |
| 31 | 56,9-57,89 | 33,30 | 6,70 | 0,20 | 20,12 |
| 32 | 57,91-58,89 | 32,50 | 7,50 | 0,23 | 23,08 |
| 33 | 58,91-59,88 | 33,80 | 6,20 | 0,18 | 18,34 |
| 34 | 59,90-60,74 | 32,80 | 7,20 | 0,22 | 21,95 |
| 35 | 60,92-61,89 | 32,60 | 7,40 | 0,23 | 22,70 |
| 36 | 61,90-62,88 | 32,90 | 7,10 | 0,22 | 21,58 |
| 37 | 62,90-63,88 | 34,00 | 6,00 | 0,18 | 17,65 |
| 38 | 63,90-64,90 | 33,10 | 6,90 | 0,21 | 20,85 |
| 39 | 64,91-65,90 | 33,50 | 6,50 | 0,19 | 19,40 |
| 40 | 65,91-66,90 | 32,40 | 7,60 | 0,23 | 23,46 |
| 41 | 66,91-67,88 | 33,80 | 6,20 | 0,18 | 18,34 |
| 42 | 67,90-68,88 | 31,10 | 8,90 | 0,29 | 28,62 |
| 43 | 68,89-69,89 | 31,90 | 8,10 | 0,25 | 25,39 |
| 44 | 70,42-71,42 | 31,10 | 8,90 | 0,29 | 28,62 |
| 45 | 71,45-72,45 | 31,60 | 8,40 | 0,27 | 26,58 |
| 46 | 72,45-73,44 | 31,90 | 8,10 | 0,25 | 25,39 |
| 47 | 73,47-74,45 | 31,40 | 8,60 | 0,27 | 27,39 |
| 48 | 74,47-75,42 | 31,80 | 8,20 | 0,26 | 25,79 |
| 49 | 75,47-76,34 | 34,80 | 5,20 | 0,15 | 14,94 |
| 50 | 76,46-77,46 | 30,40 | 9,60 | 0,32 | 31,58 |
| 51 | 77,97-78,65 | 35,30 | 4,70 | 0,13 | 13,31 |
| 52 | 78,67-79,59 | 33,60 | 6,40 | 0,19 | 19,05 |
| 53 | 79,63-80,31 | 35,00 | 5,00 | 0,14 | 14,29 |
| 54 | 80,32-81,17 | 33,80 | 6,20 | 0,18 | 18,34 |
| 55 | 81,20-82,04 | 30,40 | 9,60 | 0,32 | 31,58 |
| 56 | 82,05-82,97 | 32,50 | 7,50 | 0,23 | 23,08 |
| 57 | 82,99-83,60 | 32,40 | 7,60 | 0,23 | 23,46 |
| 58 | 83,60-84,53 | 32,60 | 7,40 | 0,23 | 22,70 |
| 59 | 84,82-85,96 | 33,90 | 6,10 | 0,18 | 17,99 |
| 60 | 85,99-86,99 | 33,50 | 6,50 | 0,19 | 19,40 |
| 61 | 86,99-87,81 | 33,00 | 7,00 | 0,21 | 21,21 |
| 62 | 87,81-88,81 | 32,90 | 7,10 | 0,22 | 21,58 |
| 63 | 88,87-89,80 | 32,80 | 7,20 | 0,22 | 21,95 |
| 64 | 89,84-90,84 | 32,20 | 7,80 | 0,24 | 24,22 |
| 65 | 90,87-91,80 | 32,50 | 7,50 | 0,23 | 23,08 |
| 66 | 91,87-92,80 | 32,30 | 7,70 | 0,24 | 23,84 |

| | | | | | |
|---|---|---|---|---|---|
| 67 | 92,86-93,78 | 32,20 | 7,80 | 0,24 | 24,22 |
| 68 | 93,80-94,70 | 32,10 | 7,90 | 0,25 | 24,61 |
| 69 | 94,72-95,72 | 29,00 | 11,00 | 0,38 | 37,93 |
| 70 | 96,72-97,29 | 33,20 | 6,80 | 0,20 | 20,48 |
| 71 | 97,29-98,27 | 29,50 | 10,50 | 0,36 | 35,59 |
| 72 | 98,30-99,18 | 31,70 | 8,30 | 0,26 | 26,18 |
| 73 | 99,77-100,23 | 28,90 | 11,10 | 0,38 | 38,41 |

## Ion Chromatography results

## Below are the IC results of the chloride standards:

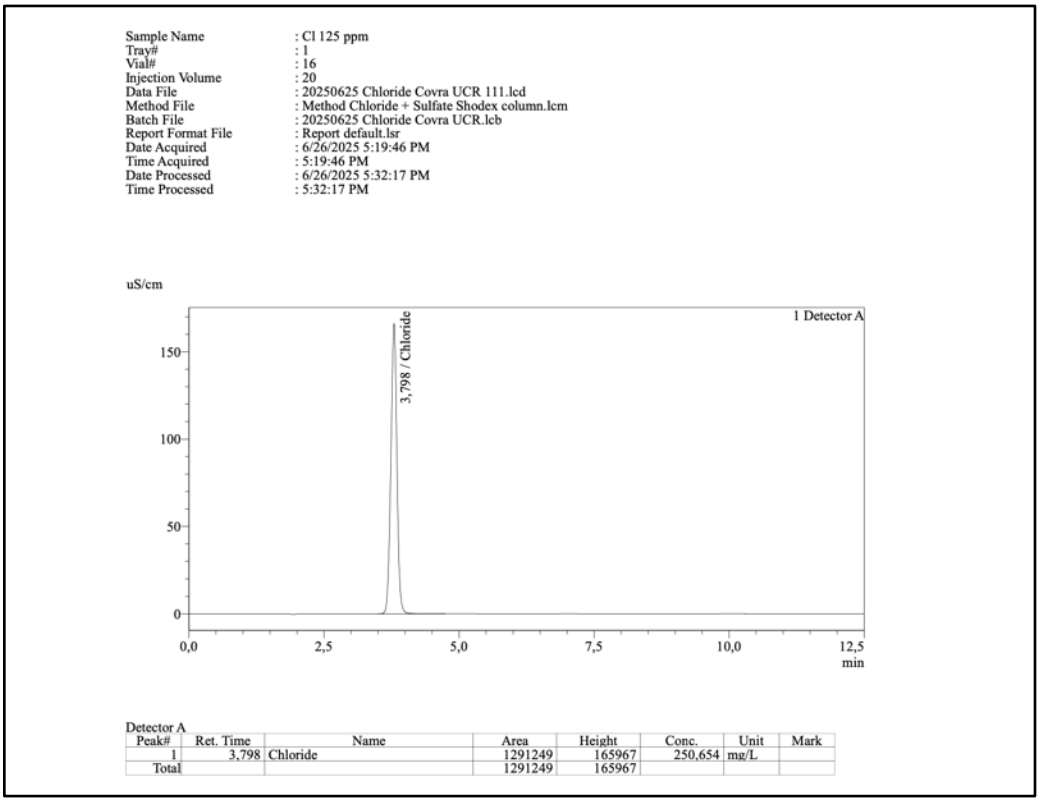

Sample Name : Cl 125 ppm
Tray# : 1
Vial# : 16
Injection Volume : 20
Data File : 20250625 Chloride Covra UCR 111.lcd
Method File : Method Chloride + Sulfate Shodex column.lcm
Batch File : 20250625 Chloride Covra UCR.lcb
Report Format File : Report default.lsr
Date Acquired : 6/26/2025 5:19:46 PM
Time Acquired : 5:19:46 PM
Date Processed : 6/26/2025 5:32:17 PM
Time Processed : 5:32:17 PM



Detector A

| Peak# | Ret. Time | Name | Area | Height | Conc. | Unit | Mark |
|---|---|---|---|---|---|---|---|
| 1 | 3,798 | Chloride | 1291249 | 165967 | 250,654 | mg/L | |
| Total | | | 1291249 | 165967 | | | |

Sample Name : Cl 250 ppm
Tray# : 1
Vial# : 17
Injection Volume : 20
Data File : 20250625 Chloride Covra UCR 112.lcd
Method File : Method Chloride + Sulfate Shodex column.lcm
Batch File : 20250625 Chloride Covra UCR.lcb
Report Format File : Report default.lsr
Date Acquired : 6/26/2025 5:32:52 PM
Time Acquired : 5:32:52 PM
Date Processed : 6/26/2025 5:45:23 PM
Time Processed : 5:45:23 PM

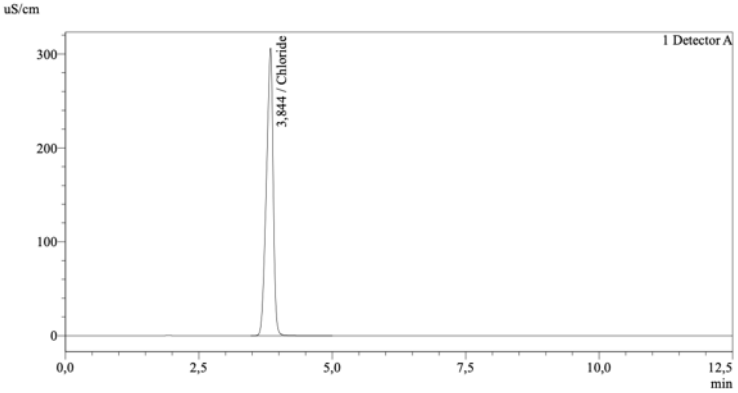


Detector A

| Peak# | Ret. Time | Name | Area | Height | Conc. | Unit | Mark |
|---|---|---|---|---|---|---|---|
| 1 | 3,844 | Chloride | 2700943 | 306009 | 524,300 | mg/L | |
| Total | | | 2700943 | 306009 | | | |

Sample Name : Cl 500 ppm
Tray# : 1
Vial# : 18
Injection Volume : 20
Data File : 20250625 Chloride Covra UCR 113.lcd
Method File : Method Chloride + Sulfate Shodex column.lcm
Batch File : 20250625 Chloride Covra UCR.lcb
Report Format File : Report default.lsr
Date Acquired : 6/26/2025 5:45:59 PM
Time Acquired : 5:45:59 PM
Date Processed : 6/26/2025 5:58:29 PM
Time Processed : 5:58:29 PM

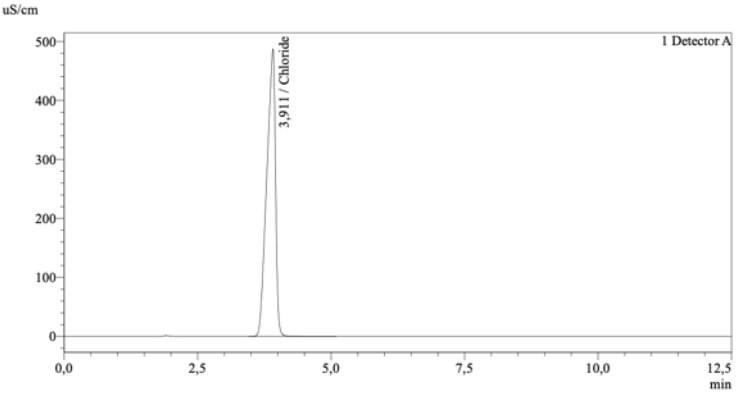


Detector A

| Peak# | Ret. Time | Name | Area | Height | Conc. | Unit | Mark |
|---|---|---|---|---|---|---|---|
| 1 | 3,911 | Chloride | 5537540 | 487340 | 1074,933 | mg/L | |
| Total | | | 5537540 | 487340 | | | |

Sample Name : Cl 750 ppm
Tray# : 1
Vial# : 19
Injection Volume : 20
Data File : 20250625 Chloride Covra UCR 114.lcd
Method File : Method Chloride + Sulfate Shodex column.lcm
Batch File : 20250625 Chloride Covra UCR.lcb
Report Format File : Report default.lsr
Date Acquired : 6/26/2025 5:59:04 PM
Time Acquired : 5:59:04 PM
Date Processed : 6/26/2025 6:11:35 PM
Time Processed : 6:11:35 PM

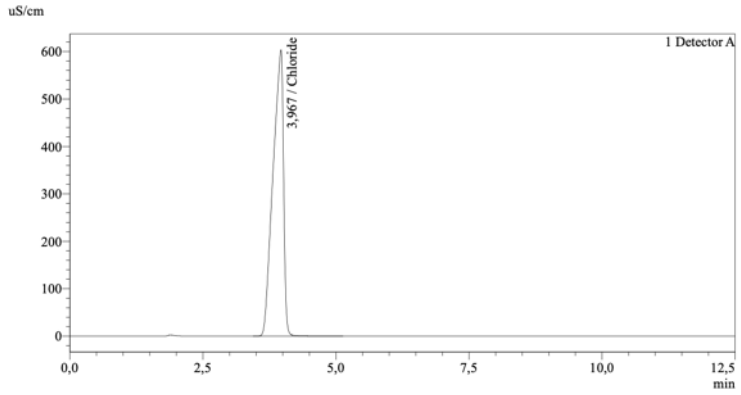


Detector A

| Peak# | Ret. Time | Name | Area | Height | Conc. | Unit | Mark |
|---|---|---|---|---|---|---|---|
| 1 | 3,967 | Chloride | 8272225 | 603110 | 1605,783 | mg/L | |
| Total | | | 8272225 | 603110 | | | |

Sample Name : Cl 1000 ppm
Tray# : 1
Vial# : 20
Injection Volume : 20
Data File : 20250625 Chloride Covra UCR 115.lcd
Method File : Method Chloride + Sulfate Shodex column.lcm
Batch File : 20250625 Chloride Covra UCR.lcb
Report Format File : Report default.lsr
Date Acquired : 6/26/2025 6:12:10 PM
Time Acquired : 6:12:10 PM
Date Processed : 6/26/2025 6:24:41 PM
Time Processed : 6:24:41 PM

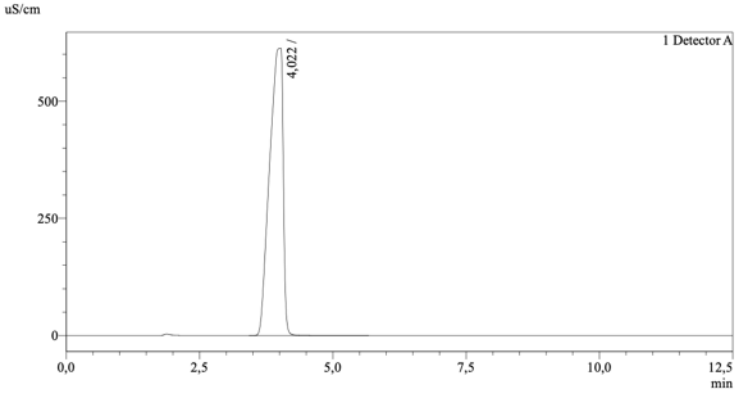


Detector A

| Peak# | Ret. Time | Name | Area | Height | Conc. | Unit | Mark |
|---|---|---|---|---|---|---|---|
| 1 | 4,022 | | 10811839 | 613024 | 0,000 | | |
| Total | | | 10811839 | 613024 | | | |

**Below are the IC results of the sulfate standards:**

Sample Name : 3.125ppm sulfate
Tray# : 1
Vial# : 102
Injection Volume : 20
Data File : 20250625 Chloride Covra UCR 102.lcd
Method File : Method Chloride + Sulfate Shodex column.lcm
Batch File : 20250625 Chloride Covra UCR.lcb
Report Format File : Report default.lsr
Date Acquired : 6/26/2025 3:21:49 PM
Time Acquired : 3:21:49 PM
Date Processed : 6/26/2025 3:34:20 PM
Time Processed : 3:34:20 PM

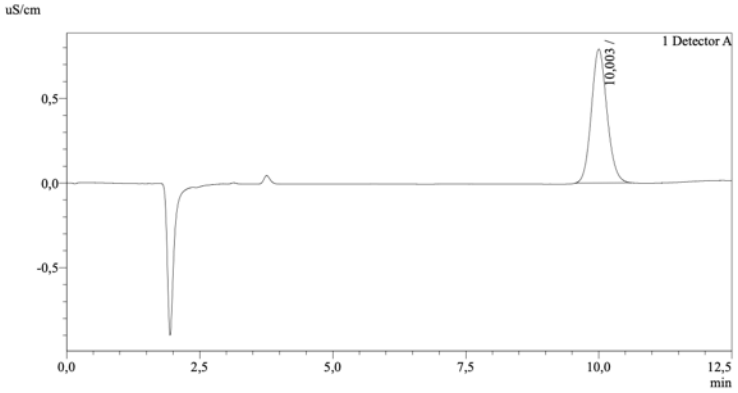


Detector A

| Peak# | Ret. Time | Name | Area | Height | Conc. | Unit | Mark |
|---|---|---|---|---|---|---|---|
| 1 | 10,003 | | 16137 | 791 | 0,000 | | |
| Total | | | 16137 | 791 | | | |

Sample Name : 6.25ppm sulfate
Tray# : 1
Vial# : 103
Injection Volume : 20
Data File : 20250625 Chloride Covra UCR 103.lcd
Method File : Method Chloride + Sulfate Shodex column.lcm
Batch File : 20250625 Chloride Covra UCR.lcb
Report Format File : Report default.lsr
Date Acquired : 6/26/2025 3:34:55 PM
Time Acquired : 3:34:55 PM
Date Processed : 6/26/2025 3:47:26 PM
Time Processed : 3:47:26 PM

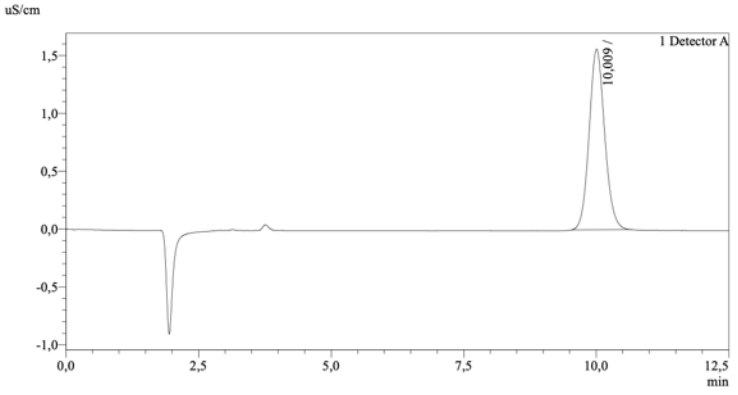


Detector A

| Peak# | Ret. Time | Name | Area | Height | Conc. | Unit | Mark |
|---|---|---|---|---|---|---|---|
| 1 | 10,009 | | 31909 | 1562 | 0,000 | | |
| Total | | | 31909 | 1562 | | | |

Sample Name : 12.5ppm sulfate
Tray# : 1
Vial# : 104
Injection Volume : 20
Data File : 20250625 Chloride Covra UCR 104.lcd
Method File : Method Chloride + Sulfate Shodex column.lcm
Batch File : 20250625 Chloride Covra UCR.lcb
Report Format File : Report default.lsr
Date Acquired : 6/26/2025 3:48:02 PM
Time Acquired : 3:48:02 PM
Date Processed : 6/26/2025 4:00:33 PM
Time Processed : 4:00:33 PM

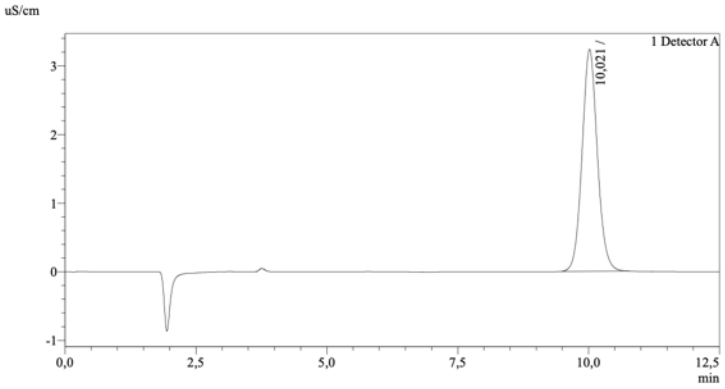


Detector A

| Peak# | Ret. Time | Name | Area | Height | Conc. | Unit | Mark |
|---|---|---|---|---|---|---|---|
| 1 | 10,021 | | 65684 | 3233 | 0,000 | | |
| Total | | | 65684 | 3233 | | | |

Sample Name : 25ppm sulfate
Tray# : 1
Vial# : 105
Injection Volume : 20
Data File : 20250625 Chloride Covra UCR 105.lcd
Method File : Method Chloride + Sulfate Shodex column.lcm
Batch File : 20250625 Chloride Covra UCR.lcb
Report Format File : Report default.lsr
Date Acquired : 6/26/2025 4:01:09 PM
Time Acquired : 4:01:09 PM
Date Processed : 6/26/2025 4:13:40 PM
Time Processed : 4:13:40 PM

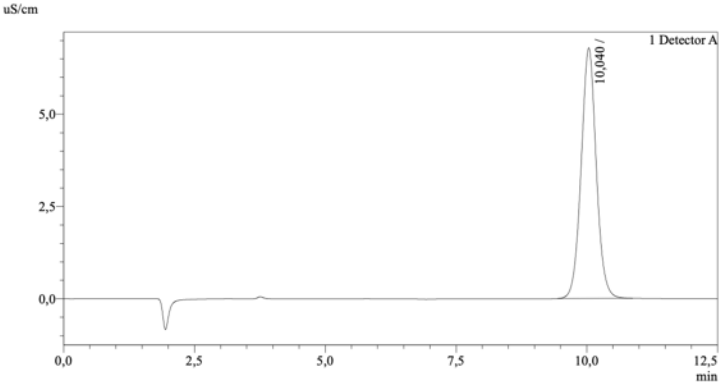


Detector A

| Peak# | Ret. Time | Name | Area | Height | Conc. | Unit | Mark |
|---|---|---|---|---|---|---|---|
| 1 | 10,040 | | 136435 | 6791 | 0,000 | | |
| Total | | | 136435 | 6791 | | | |

Below is the IC result of the blank, followed by the results of the samples. The samples are labeled with either ".1" or ".2" to indicate replicates, allowing for the calculation of an average when both are present. However, the presence of a ".2" sample does not necessarily mean that the corresponding ".1" sample exists and vice versa.

| | |
|---|---|
| Sample Name | : fumehood h2o |
| Tray# | : 1 |
| Vial# | : 50 |
| Injection Volume | : 20 |
| Data File | : 20250625 Chloride Covra UCR 109.lcd |
| Method File | : Method Chloride + Sulfate Shodex column.lcm |
| Batch File | : 20250625 Chloride Covra UCR.lcb |
| Report Format File | : Report default.lsr |
| Date Acquired | : 6/26/2025 4:53:34 PM |
| Time Acquired | : 4:53:34 PM |
| Date Processed | : 6/26/2025 5:06:05 PM |
| Time Processed | : 5:06:05 PM |

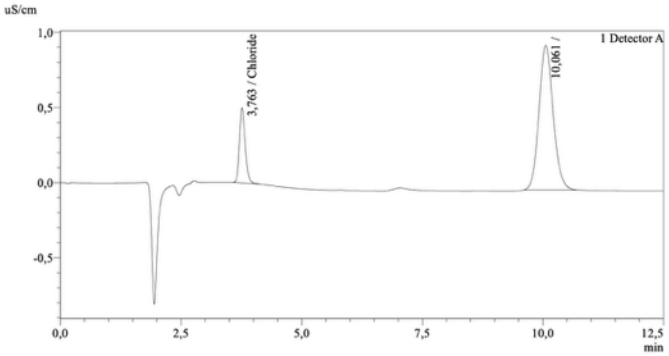


Detector A

| Peak# | Ret. Time | Name | Area | Height | Conc. | Unit | Mark |
|---|---|---|---|---|---|---|---|
| 1 | 3,763 | Chloride | 4141 | 500 | 0,804 | mg/L | |
| 2 | 10,061 | | 19665 | 963 | 0,000 | | |
| Total | | | 23806 | 1463 | | | |

| | |
|---|---|
| Sample Name | : 1.1 |
| Tray# | : 1 |
| Vial# | : 93 |
| Injection Volume | : 20 |
| Data File | : 20250625 Chloride Covra UCR 093.lcd |
| Method File | : Method Chloride + Sulfate Shodex column.lcm |
| Batch File | : 20250625 Chloride Covra UCR.lcb |
| Report Format File | : Report default.lsr |
| Date Acquired | : 6/26/2025 1:23:57 PM |
| Time Acquired | : 1:23:57 PM |
| Date Processed | : 6/26/2025 1:36:27 PM |
| Time Processed | : 1:36:27 PM |

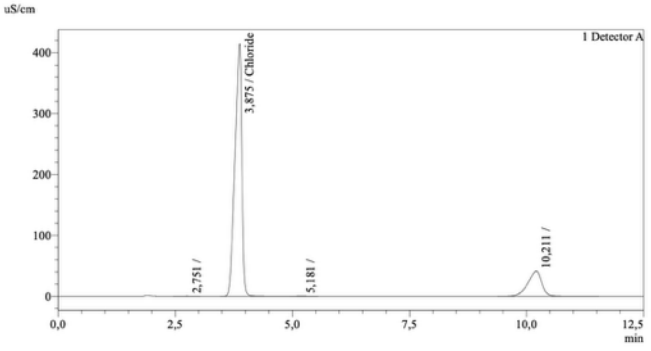


Detector A

| Peak# | Ret. Time | Name | Area | Height | Conc. | Unit | Mark |
|---|---|---|---|---|---|---|---|
| 1 | 2,751 | | 2015 | 179 | 0,000 | | |
| 2 | 3,875 | Chloride | 4237711 | 414100 | 822,614 | mg/L | S |
| 3 | 5,181 | | 3651 | 322 | 0,000 | | T |
| 4 | 10,211 | | 851101 | 41362 | 0,000 | | |
| Total | | | 5094479 | 455962 | | | |

Sample Name : 1.2
Tray# : 1
Vial# : 85
Injection Volume : 20
Data File : 20250625 Chloride Covra UCR 085.lcd
Method File : Method Chloride + Sulfate Shodex column.lcm
Batch File : 20250625 Chloride Covra UCR.lcb
Report Format File : Report default.lsr
Date Acquired : 6/26/2025 11:39:07 AM
Time Acquired : 11:39:07 AM
Date Processed : 6/26/2025 11:51:38 AM
Time Processed : 11:51:38 AM

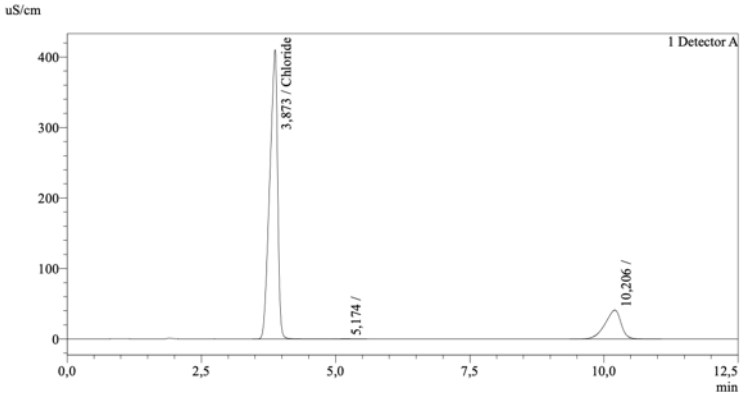


Detector A

| Peak# | Ret. Time | Name | Area | Height | Conc. | Unit | Mark |
|---|---|---|---|---|---|---|---|
| 1 | 3,873 | Chloride | 4180531 | 409903 | 811,514 | mg/L | S |
| 2 | 5,174 | | 3683 | 330 | 0,000 | | T |
| 3 | 10,206 | | 851751 | 40987 | 0,000 | | |
| Total | | | 5035965 | 451221 | | | |

Sample Name : 2.1
Tray# : 1
Vial# : 22
Injection Volume : 20
Data File : 20250625 Chloride Covra UCR 022.lcd
Method File : Method Chloride + Sulfate Shodex column.lcm
Batch File : 20250625 Chloride Covra UCR.lcb
Report Format File : Report default.lsr
Date Acquired : 6/25/2025 7:11:08 PM
Time Acquired : 7:11:08 PM
Date Processed : 6/25/2025 7:23:39 PM
Time Processed : 7:23:39 PM

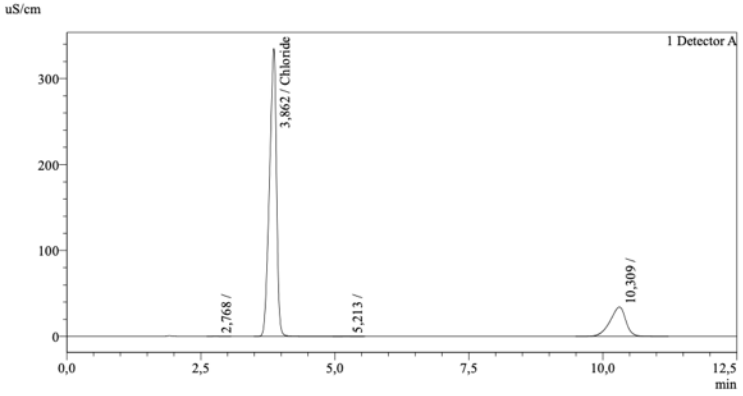


Detector A

| Peak# | Ret. Time | Name | Area | Height | Conc. | Unit | Mark |
|---|---|---|---|---|---|---|---|
| 1 | 2,768 | | 2198 | 266 | 0,000 | | |
| 2 | 3,862 | Chloride | 3046968 | 334314 | 591,470 | mg/L | S |
| 3 | 5,213 | | 2455 | 221 | 0,000 | | T |
| 4 | 10,309 | | 704317 | 34212 | 0,000 | | |
| Total | | | 3755939 | 369013 | | | |

| | |
|---|---|
| Sample Name | : 3.1 |
| Tray# | : 1 |
| Vial# | : 34 |
| Injection Volume | : 20 |
| Data File | : 20250625 Chloride Covra UCR 034.lcd |
| Method File | : Method Chloride + Sulfate Shodex column.lcm |
| Batch File | : 20250625 Chloride Covra UCR.lcb |
| Report Format File | : Report default.lsr |
| Date Acquired | : 6/25/2025 9:48:25 PM |
| Time Acquired | : 9:48:25 PM |
| Date Processed | : 6/25/2025 10:00:56 PM |
| Time Processed | : 10:00:56 PM |

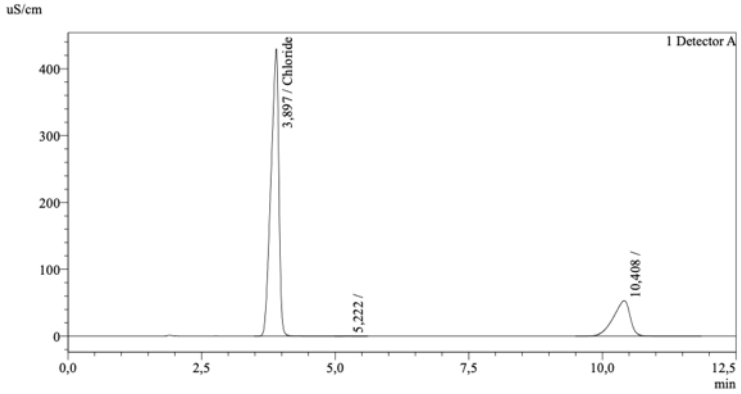


Detector A

| Peak# | Ret. Time | Name | Area | Height | Conc. | Unit | Mark |
|---|---|---|---|---|---|---|---|
| 1 | 3,897 | Chloride | 4422543 | 429736 | 858,493 | mg/L | S |
| 2 | 5,222 | | 3654 | 322 | 0,000 | | T |
| 3 | 10,408 | | 1175032 | 53241 | 0,000 | | |
| Total | | | 5601229 | 483299 | | | |

| | |
|---|---|
| Sample Name | : 4.1 |
| Tray# | : 1 |
| Vial# | : 97 |
| Injection Volume | : 20 |
| Data File | : 20250625 Chloride Covra UCR 097.lcd |
| Method File | : Method Chloride + Sulfate Shodex column.lcm |
| Batch File | : 20250625 Chloride Covra UCR.lcb |
| Report Format File | : Report default.lsr |
| Date Acquired | : 6/26/2025 2:16:19 PM |
| Time Acquired | : 2:16:19 PM |
| Date Processed | : 6/26/2025 2:28:50 PM |
| Time Processed | : 2:28:50 PM |

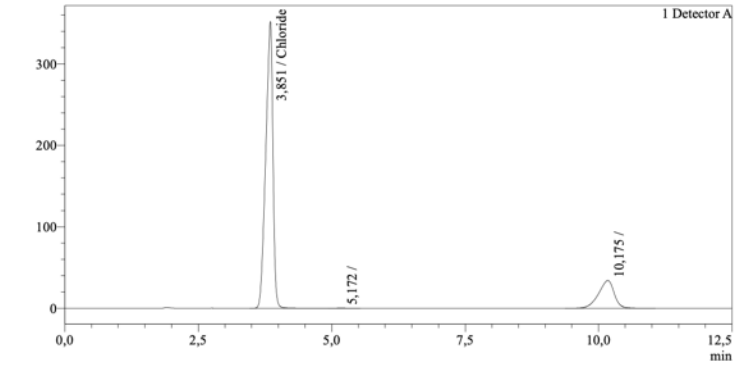


Detector A

| Peak# | Ret. Time | Name | Area | Height | Conc. | Unit | Mark |
|---|---|---|---|---|---|---|---|
| 1 | 3,851 | Chloride | 3294872 | 351903 | 639,592 | mg/L | S |
| 2 | 5,172 | | 2710 | 248 | 0,000 | | T |
| 3 | 10,175 | | 696938 | 34148 | 0,000 | | |
| Total | | | 3994520 | 386298 | | | |

Sample Name : 5.1
Tray# : 1
Vial# : 44
Injection Volume : 20
Data File : 20250625 Chloride Covra UCR 044.lcd
Method File : Method Chloride + Sulfate Shodex column.lcm
Batch File : 20250625 Chloride Covra UCR.lcb
Report Format File : Report default.lsr
Date Acquired : 6/25/2025 11:59:28 PM
Time Acquired : 11:59:28 PM
Date Processed : 6/26/2025 12:11:59 AM
Time Processed : 12:11:59 AM

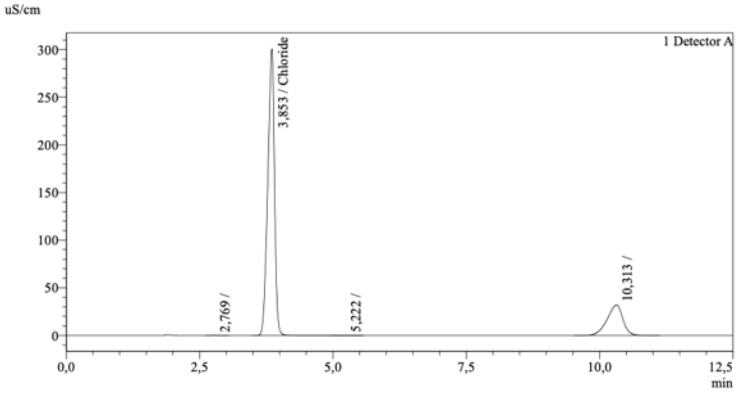


Detector A

| Peak# | Ret. Time | Name | Area | Height | Conc. | Unit | Mark |
|---|---|---|---|---|---|---|---|
| 1 | 2,769 | | 3044 | 353 | 0,000 | | |
| 2 | 3,853 | Chloride | 2617099 | 300398 | 508,025 | mg/L | S |
| 3 | 5,222 | | 2231 | 203 | 0,000 | | T |
| 4 | 10,313 | | 662138 | 31998 | 0,000 | | |
| Total | | | 3284512 | 332952 | | | |

Sample Name : 6.1
Tray# : 1
Vial# : 30
Injection Volume : 20
Data File : 20250625 Chloride Covra UCR 030.lcd
Method File : Method Chloride + Sulfate Shodex column.lcm
Batch File : 20250625 Chloride Covra UCR.lcb
Report Format File : Report default.lsr
Date Acquired : 6/25/2025 8:56:02 PM
Time Acquired : 8:56:02 PM
Date Processed : 6/25/2025 9:08:33 PM
Time Processed : 9:08:33 PM

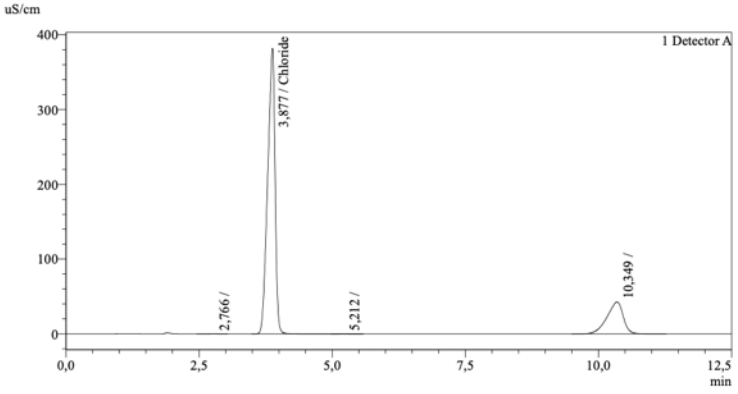


Detector A

| Peak# | Ret. Time | Name | Area | Height | Conc. | Unit | Mark |
|---|---|---|---|---|---|---|---|
| 1 | 2,766 | | 3504 | 356 | 0,000 | | |
| 2 | 3,877 | Chloride | 3680475 | 381609 | 714,444 | mg/L | S |
| 3 | 5,212 | | 3157 | 285 | 0,000 | | T |
| 4 | 10,349 | | 912186 | 42690 | 0,000 | | |
| Total | | | 4599322 | 424940 | | | |

| | |
|---|---|
| Sample Name | : 7.1 |
| Tray# | : 1 |
| Vial# | : 21 |
| Injection Volume | : 20 |
| Data File | : 20250625 Chloride Covra UCR 021.lcd |
| Method File | : Method Chloride + Sulfate Shodex column.lcm |
| Batch File | : 20250625 Chloride Covra UCR.lcb |
| Report Format File | : Report default.lsr |
| Date Acquired | : 6/25/2025 6:58:03 PM |
| Time Acquired | : 6:58:03 PM |
| Date Processed | : 6/25/2025 7:10:33 PM |
| Time Processed | : 7:10:33 PM |

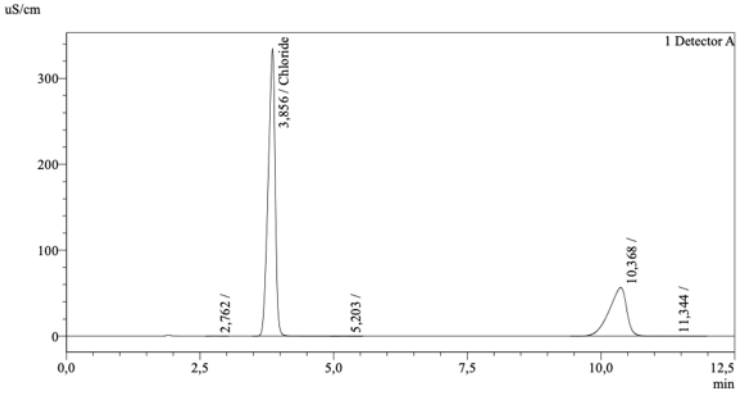


Detector A

| Peak# | Ret. Time | Name | Area | Height | Conc. | Unit | Mark |
|---|---|---|---|---|---|---|---|
| 1 | 2,762 | | 2882 | 330 | 0,000 | | |
| 2 | 3,856 | Chloride | 3039179 | 333987 | 589,958 | mg/L | S |
| 3 | 5,203 | | 2507 | 230 | 0,000 | | T |
| 4 | 10,368 | | 1296149 | 56543 | 0,000 | | |
| 5 | 11,344 | | 2987 | 113 | 0,000 | | V |
| Total | | | 4343705 | 391203 | | | |

| | |
|---|---|
| Sample Name | : 8.1 |
| Tray# | : 1 |
| Vial# | : 82 |
| Injection Volume | : 20 |
| Data File | : 20250625 Chloride Covra UCR 082.lcd |
| Method File | : Method Chloride + Sulfate Shodex column.lcm |
| Batch File | : 20250625 Chloride Covra UCR.lcb |
| Report Format File | : Report default.lsr |
| Date Acquired | : 6/26/2025 10:59:50 AM |
| Time Acquired | : 10:59:50 AM |
| Date Processed | : 6/26/2025 11:12:20 AM |
| Time Processed | : 11:12:20 AM |

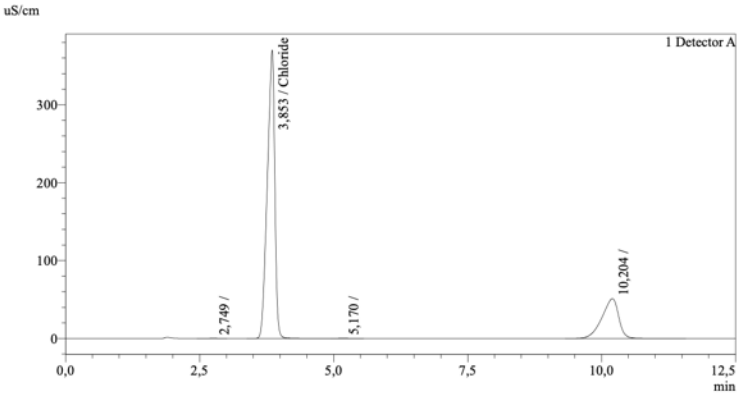


Detector A

| Peak# | Ret. Time | Name | Area | Height | Conc. | Unit | Mark |
|---|---|---|---|---|---|---|---|
| 1 | 2,749 | | 3508 | 329 | 0,000 | | |
| 2 | 3,853 | Chloride | 3578504 | 369848 | 694,650 | mg/L | SV |
| 3 | 5,170 | | 2987 | 269 | 0,000 | | T |
| 4 | 10,204 | | 1113593 | 51182 | 0,000 | | |
| Total | | | 4698592 | 421628 | | | |

Sample Name : 8.2
Tray# : 1
Vial# : 31
Injection Volume : 20
Data File : 20250625 Chloride Covra UCR 031.lcd
Method File : Method Chloride + Sulfate Shodex column.lcm
Batch File : 20250625 Chloride Covra UCR.lcb
Report Format File : Report default.lsr
Date Acquired : 6/25/2025 9:09:08 PM
Time Acquired : 9:09:08 PM
Date Processed : 6/25/2025 9:21:39 PM
Time Processed : 9:21:39 PM

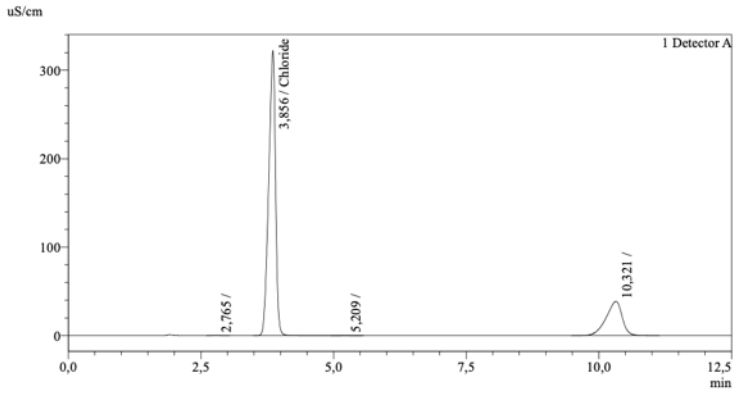


Detector A

| Peak# | Ret. Time | Name | Area | Height | Conc. | Unit | Mark |
|---|---|---|---|---|---|---|---|
| 1 | 2,765 | | 2884 | 329 | 0,000 | | |
| 2 | 3,856 | Chloride | 2883512 | 321726 | 559,740 | mg/L | S |
| 3 | 5,209 | | 2416 | 221 | 0,000 | | T |
| 4 | 10,321 | | 816929 | 38608 | 0,000 | | |
| Total | | | 3705742 | 360885 | | | |

Sample Name : 9.1
Tray# : 1
Vial# : 70
Injection Volume : 20
Data File : 20250625 Chloride Covra UCR 070.lcd
Method File : Method Chloride + Sulfate Shodex column.lcm
Batch File : 20250625 Chloride Covra UCR.lcb
Report Format File : Report default.lsr
Date Acquired : 6/26/2025 5:40:06 AM
Time Acquired : 5:40:06 AM
Date Processed : 6/26/2025 5:52:37 AM
Time Processed : 5:52:37 AM

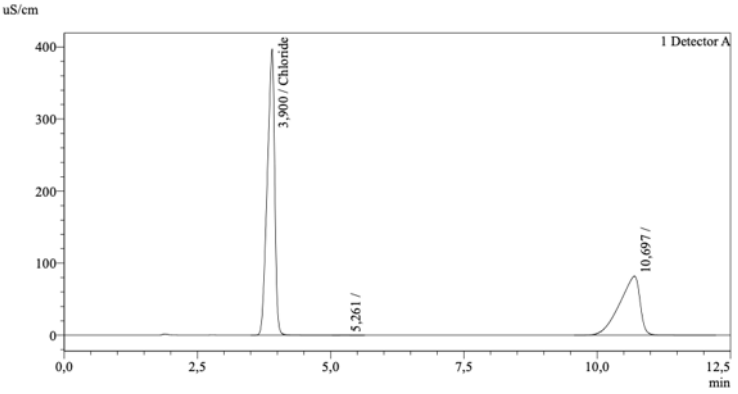


Detector A

| Peak# | Ret. Time | Name | Area | Height | Conc. | Unit | Mark |
|---|---|---|---|---|---|---|---|
| 1 | 3,900 | Chloride | 3829986 | 396665 | 743,467 | mg/L | S |
| 2 | 5,261 | | 3134 | 283 | 0,000 | | T |
| 3 | 10,697 | | 2188954 | 81819 | 0,000 | | |
| Total | | | 6022073 | 478767 | | | |

Sample Name : 9.2
Tray# : 1
Vial# : 23
Injection Volume : 20
Data File : 20250625 Chloride Covra UCR 023.lcd
Method File : Method Chloride + Sulfate Shodex column.lcm
Batch File : 20250625 Chloride Covra UCR.lcb
Report Format File : Report default.lsr
Date Acquired : 6/25/2025 7:24:14 PM
Time Acquired : 7:24:14 PM
Date Processed : 6/25/2025 7:36:45 PM
Time Processed : 7:36:45 PM

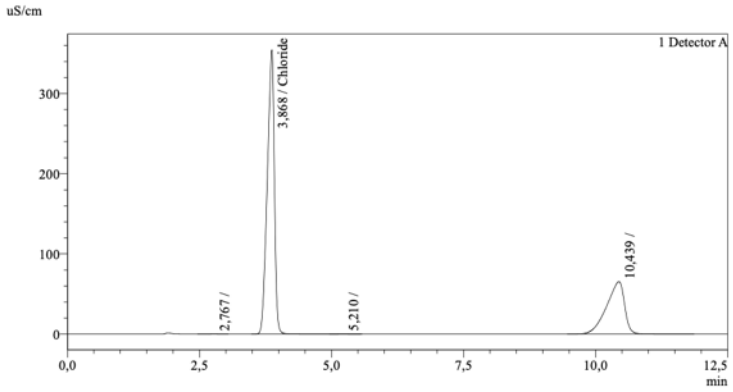


Detector A

| Peak# | Ret. Time | Name | Area | Height | Conc. | Unit | Mark |
|---|---|---|---|---|---|---|---|
| 1 | 2,767 | | 2824 | 240 | 0,000 | | |
| 2 | 3,868 | Chloride | 3305721 | 353857 | 641,698 | mg/L | S |
| 3 | 5,210 | | 2698 | 243 | 0,000 | | T |
| 4 | 10,439 | | 1554288 | 65493 | 0,000 | | |
| Total | | | 4865531 | 419834 | | | |

Sample Name : 10.2
Tray# : 1
Vial# : 33
Injection Volume : 20
Data File : 20250625 Chloride Covra UCR 033.lcd
Method File : Method Chloride + Sulfate Shodex column.lcm
Batch File : 20250625 Chloride Covra UCR.lcb
Report Format File : Report default.lsr
Date Acquired : 6/25/2025 9:35:20 PM
Time Acquired : 9:35:20 PM
Date Processed : 6/25/2025 9:47:50 PM
Time Processed : 9:47:50 PM

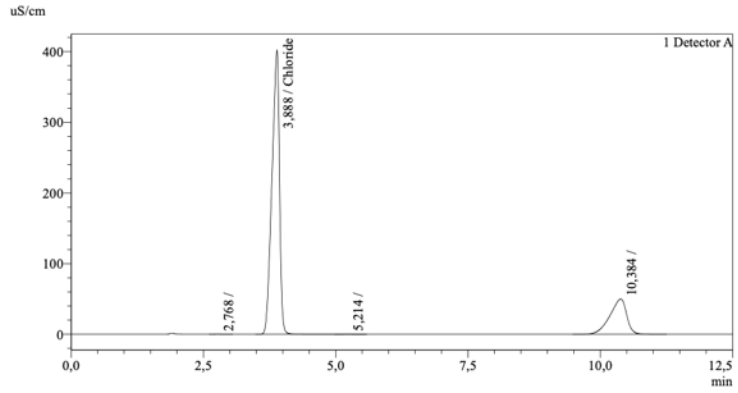


Detector A

| Peak# | Ret. Time | Name | Area | Height | Conc. | Unit | Mark |
|---|---|---|---|---|---|---|---|
| 1 | 2,768 | | 2133 | 252 | 0,000 | | |
| 2 | 3,888 | Chloride | 3980791 | 401517 | 772,741 | mg/L | S |
| 3 | 5,214 | | 3322 | 303 | 0,000 | | T |
| 4 | 10,384 | | 1107662 | 50027 | 0,000 | | |
| Total | | | 5093907 | 452099 | | | |

Sample Name : 11.1
Tray# : 1
Vial# : 14
Injection Volume : 20
Data File : 20250625 Chloride Covra UCR 014.lcd
Method File : Method Chloride + Sulfate Shodex column.lcm
Batch File : 20250625 Chloride Covra UCR.lcb
Report Format File : Report default.lsr
Date Acquired : 6/25/2025 5:26:22 PM
Time Acquired : 5:26:22 PM
Date Processed : 6/25/2025 5:38:53 PM
Time Processed : 5:38:53 PM

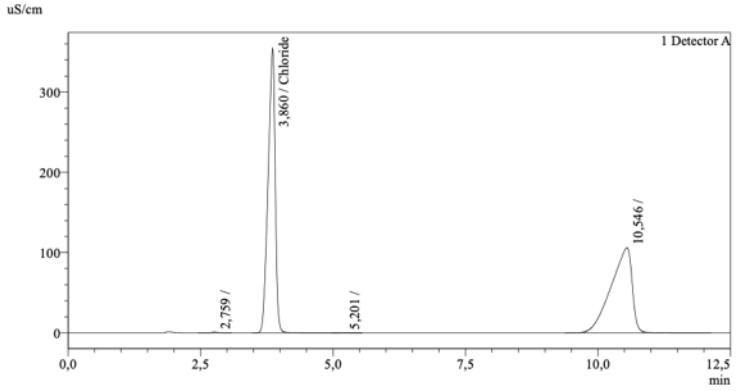


Detector A

| Peak# | Ret. Time | Name | Area | Height | Conc. | Unit | Mark |
|---|---|---|---|---|---|---|---|
| 1 | 2,759 | | 8223 | 957 | 0,000 | | |
| 2 | 3,860 | Chloride | 3301707 | 354008 | 640,919 | mg/L | S |
| 3 | 5,201 | | 2729 | 247 | 0,000 | | T |
| 4 | 10,546 | | 2947865 | 106043 | 0,000 | | |
| Total | | | 6260524 | 461255 | | | |

Sample Name : 12.1
Tray# : 1
Vial# : 90
Injection Volume : 20
Data File : 20250625 Chloride Covra UCR 090.lcd
Method File : Method Chloride + Sulfate Shodex column.lcm
Batch File : 20250625 Chloride Covra UCR.lcb
Report Format File : Report default.lsr
Date Acquired : 6/26/2025 12:44:40 PM
Time Acquired : 12:44:40 PM
Date Processed : 6/26/2025 12:57:11 PM
Time Processed : 12:57:11 PM

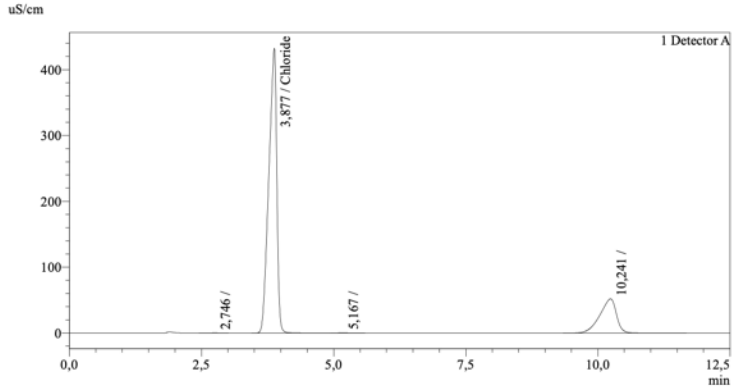


Detector A

| Peak# | Ret. Time | Name | Area | Height | Conc. | Unit | Mark |
|---|---|---|---|---|---|---|---|
| 1 | 2,746 | | 2869 | 281 | 0,000 | | |
| 2 | 3,877 | Chloride | 4538512 | 431934 | 881,004 | mg/L | S |
| 3 | 5,167 | | 3801 | 345 | 0,000 | | T |
| 4 | 10,241 | | 1134718 | 51889 | 0,000 | | |
| Total | | | 5679900 | 484450 | | | |

Sample Name : 13.1
Tray# : 1
Vial# : 38
Injection Volume : 20
Data File : 20250625 Chloride Covra UCR 038.lcd
Method File : Method Chloride + Sulfate Shodex column.lcm
Batch File : 20250625 Chloride Covra UCR.lcb
Report Format File : Report default.lsr
Date Acquired : 6/25/2025 10:40:49 PM
Time Acquired : 10:40:49 PM
Date Processed : 6/25/2025 10:53:19 PM
Time Processed : 10:53:19 PM

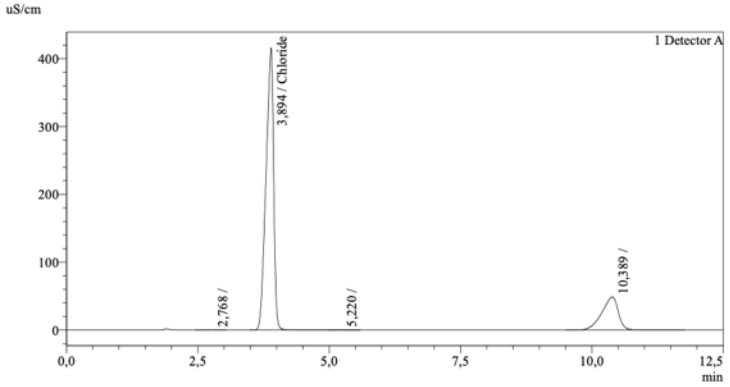


Detector A

| Peak# | Ret. Time | Name | Area | Height | Conc. | Unit | Mark |
|---|---|---|---|---|---|---|---|
| 1 | 2,768 | | 2996 | 287 | 0,000 | | |
| 2 | 3,894 | Chloride | 4187157 | 415379 | 812,800 | mg/L | S |
| 3 | 5,220 | | 3605 | 326 | 0,000 | | T |
| 4 | 10,389 | | 1068311 | 48779 | 0,000 | | |
| Total | | | 5262069 | 464770 | | | |

Sample Name : 14.1
Tray# : 1
Vial# : 87
Injection Volume : 20
Data File : 20250625 Chloride Covra UCR 087.lcd
Method File : Method Chloride + Sulfate Shodex column.lcm
Batch File : 20250625 Chloride Covra UCR.lcb
Report Format File : Report default.lsr
Date Acquired : 6/26/2025 12:05:22 PM
Time Acquired : 12:05:22 PM
Date Processed : 6/26/2025 12:17:52 PM
Time Processed : 12:17:52 PM

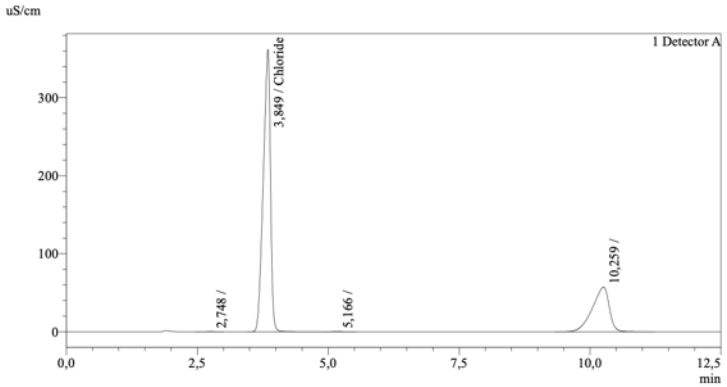


Detector A

| Peak# | Ret. Time | Name | Area | Height | Conc. | Unit | Mark |
|---|---|---|---|---|---|---|---|
| 1 | 2,748 | | 3388 | 332 | 0,000 | | |
| 2 | 3,849 | Chloride | 3446635 | 361480 | 669,052 | mg/L | S |
| 3 | 5,166 | | 2853 | 260 | 0,000 | | T |
| 4 | 10,259 | | 1284431 | 57232 | 0,000 | | |
| Total | | | 4737306 | 419302 | | | |

Sample Name : 15.1
Tray# : 1
Vial# : 68
Injection Volume : 20
Data File : 20250625 Chloride Covra UCR 068.lcd
Method File : Method Chloride + Sulfate Shodex column.lcm
Batch File : 20250625 Chloride Covra UCR.lcb
Report Format File : Report default.lsr
Date Acquired : 6/26/2025 5:13:53 AM
Time Acquired : 5:13:53 AM
Date Processed : 6/26/2025 5:26:24 AM
Time Processed : 5:26:24 AM

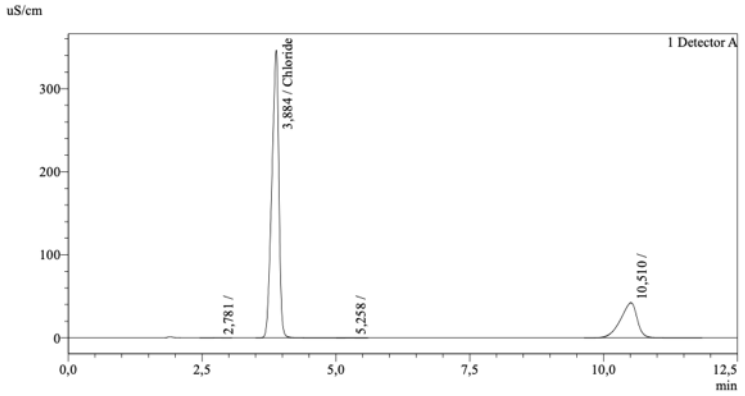


Detector A

| Peak# | Ret. Time | Name | Area | Height | Conc. | Unit | Mark |
|---|---|---|---|---|---|---|---|
| 1 | 2,781 | | 3714 | 358 | 0,000 | | |
| 2 | 3,884 | Chloride | 3150719 | 346526 | 611,609 | mg/L | S |
| 3 | 5,258 | | 2773 | 251 | 0,000 | | T |
| 4 | 10,510 | | 914571 | 42191 | 0,000 | | |
| Total | | | 4071777 | 389326 | | | |

Sample Name : 16.1
Tray# : 1
Vial# : 55
Injection Volume : 20
Data File : 20250625 Chloride Covra UCR 055.lcd
Method File : Method Chloride + Sulfate Shodex column.lcm
Batch File : 20250625 Chloride Covra UCR.lcb
Report Format File : Report default.lsr
Date Acquired : 6/26/2025 2:23:38 AM
Time Acquired : 2:23:38 AM
Date Processed : 6/26/2025 2:36:08 AM
Time Processed : 2:36:08 AM

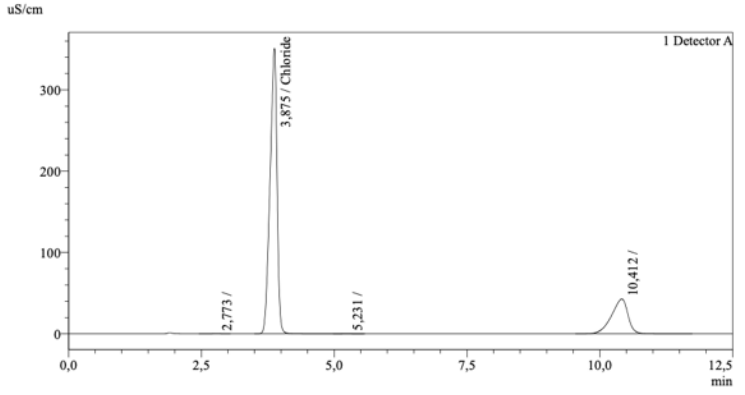


Detector A

| Peak# | Ret. Time | Name | Area | Height | Conc. | Unit | Mark |
|---|---|---|---|---|---|---|---|
| 1 | 2,773 | | 3712 | 346 | 0,000 | | |
| 2 | 3,875 | Chloride | 3223609 | 350166 | 625,759 | mg/L | S |
| 3 | 5,231 | | 2768 | 252 | 0,000 | | T |
| 4 | 10,412 | | 926128 | 42876 | 0,000 | | |
| Total | | | 4156218 | 393641 | | | |

Sample Name : 17.1
Tray# : 1
Vial# : 48
Injection Volume : 20
Data File : 20250625 Chloride Covra UCR 048.lcd
Method File : Method Chloride + Sulfate Shodex column.lcm
Batch File : 20250625 Chloride Covra UCR.lcb
Report Format File : Report default.lsr
Date Acquired : 6/26/2025 12:51:53 AM
Time Acquired : 12:51:53 AM
Date Processed : 6/26/2025 1:04:24 AM
Time Processed : 1:04:24 AM

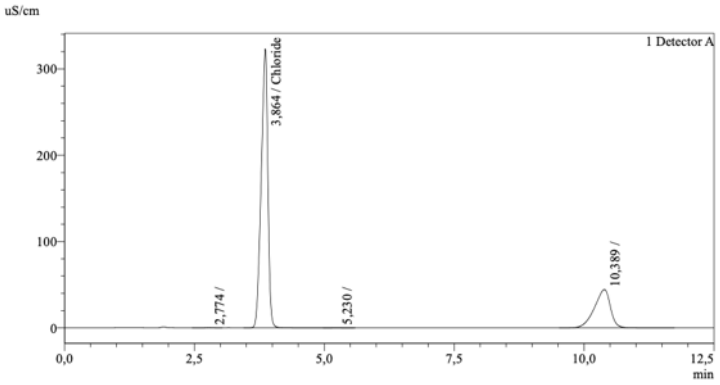


Detector A

| Peak# | Ret. Time | Name | Area | Height | Conc. | Unit | Mark |
|---|---|---|---|---|---|---|---|
| 1 | 2,774 | | 4957 | 443 | 0,000 | | |
| 2 | 3,864 | Chloride | 2883195 | 322806 | 559,678 | mg/L | SV |
| 3 | 5,230 | | 2486 | 225 | 0,000 | | T |
| 4 | 10,389 | | 957498 | 44423 | 0,000 | | |
| Total | | | 3848137 | 367897 | | | |

Sample Name : 18.1
Tray# : 1
Vial# : 52
Injection Volume : 20
Data File : 20250625 Chloride Covra UCR 052.lcd
Method File : Method Chloride + Sulfate Shodex column.lcm
Batch File : 20250625 Chloride Covra UCR.lcb
Report Format File : Report default.lsr
Date Acquired : 6/26/2025 1:44:18 AM
Time Acquired : 1:44:18 AM
Date Processed : 6/26/2025 1:56:49 AM
Time Processed : 1:56:49 AM

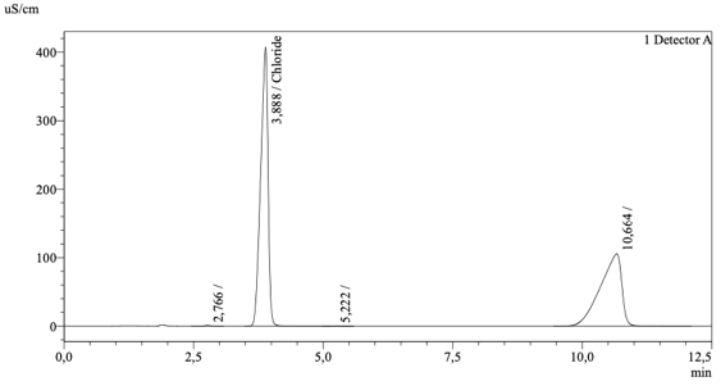


Detector A

| Peak# | Ret. Time | Name | Area | Height | Conc. | Unit | Mark |
|---|---|---|---|---|---|---|---|
| 1 | 2,766 | | 10825 | 1093 | 0,000 | | |
| 2 | 3,888 | Chloride | 4032726 | 406407 | 782,822 | mg/L | S |
| 3 | 5,222 | | 3296 | 298 | 0,000 | | T |
| 4 | 10,664 | | 3033717 | 105423 | 0,000 | | |
| Total | | | 7080564 | 513221 | | | |

Sample Name : 19.1
Tray# : 1
Vial# : 66
Injection Volume : 20
Data File : 20250625 Chloride Covra UCR 066.lcd
Method File : Method Chloride + Sulfate Shodex column.lcm
Batch File : 20250625 Chloride Covra UCR.lcb
Report Format File : Report default.lsr
Date Acquired : 6/26/2025 4:47:43 AM
Time Acquired : 4:47:43 AM
Date Processed : 6/26/2025 5:00:14 AM
Time Processed : 5:00:14 AM

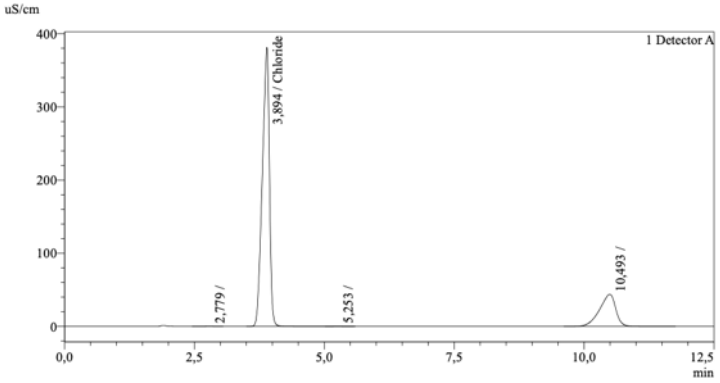


Detector A

| Peak# | Ret. Time | Name | Area | Height | Conc. | Unit | Mark |
|---|---|---|---|---|---|---|---|
| 1 | 2,779 | | 3561 | 341 | 0,000 | | |
| 2 | 3,894 | Chloride | 3616342 | 380525 | 701,995 | mg/L | S |
| 3 | 5,253 | | 2629 | 240 | 0,000 | | T |
| 4 | 10,493 | | 956799 | 43884 | 0,000 | | |
| Total | | | 4579331 | 424990 | | | |

Sample Name : 20.1
Tray# : 1
Vial# : 40
Injection Volume : 20
Data File : 20250625 Chloride Covra UCR 040.lcd
Method File : Method Chloride + Sulfate Shodex column.lcm
Batch File : 20250625 Chloride Covra UCR.lcb
Report Format File : Report default.lsr
Date Acquired : 6/25/2025 11:07:01 PM
Time Acquired : 11:07:01 PM
Date Processed : 6/25/2025 11:19:31 PM
Time Processed : 11:19:31 PM

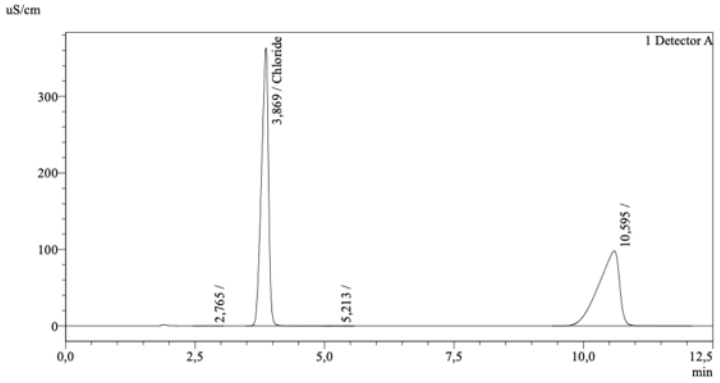


Detector A

| Peak# | Ret. Time | Name | Area | Height | Conc. | Unit | Mark |
|---|---|---|---|---|---|---|---|
| 1 | 2,765 | | 3084 | 290 | 0,000 | | |
| 2 | 3,869 | Chloride | 3408865 | 362567 | 661,720 | mg/L | S |
| 3 | 5,213 | | 2962 | 269 | 0,000 | | T |
| 4 | 10,595 | | 2767281 | 98146 | 0,000 | | |
| Total | | | 6182192 | 461273 | | | |

Sample Name : 21.1
Tray# : 1
Vial# : 24
Injection Volume : 20
Data File : 20250625 Chloride Covra UCR 024.lcd
Method File : Method Chloride + Sulfate Shodex column.lcm
Batch File : 20250625 Chloride Covra UCR.lcb
Report Format File : Report default.lsr
Date Acquired : 6/25/2025 7:37:21 PM
Time Acquired : 7:37:21 PM
Date Processed : 6/25/2025 7:49:51 PM
Time Processed : 7:49:51 PM

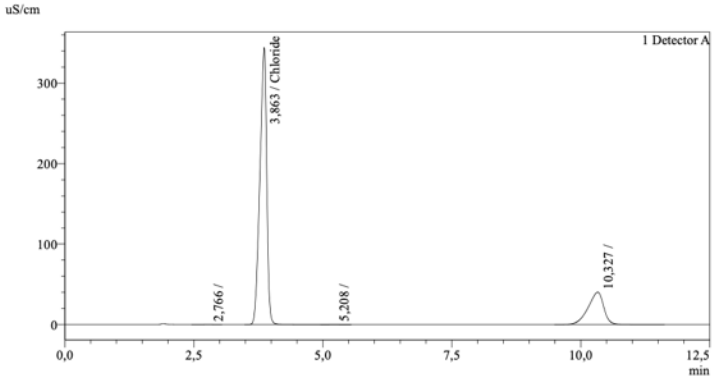


Detector A

| Peak# | Ret. Time | Name | Area | Height | Conc. | Unit | Mark |
|---|---|---|---|---|---|---|---|
| 1 | 2,766 | | 3565 | 309 | 0,000 | | |
| 2 | 3,863 | Chloride | 3164164 | 343808 | 614,219 | mg/L | S |
| 3 | 5,208 | | 2582 | 234 | 0,000 | | T |
| 4 | 10,327 | | 854149 | 40281 | 0,000 | | |
| Total | | | 4024460 | 384632 | | | |

Sample Name : 22.1
Tray# : 1
Vial# : 63
Injection Volume : 20
Data File : 20250625 Chloride Covra UCR 063.lcd
Method File : Method Chloride + Sulfate Shodex column.lcm
Batch File : 20250625 Chloride Covra UCR.lcb
Report Format File : Report default.lsr
Date Acquired : 6/26/2025 4:08:27 AM
Time Acquired : 4:08:27 AM
Date Processed : 6/26/2025 4:20:58 AM
Time Processed : 4:20:58 AM

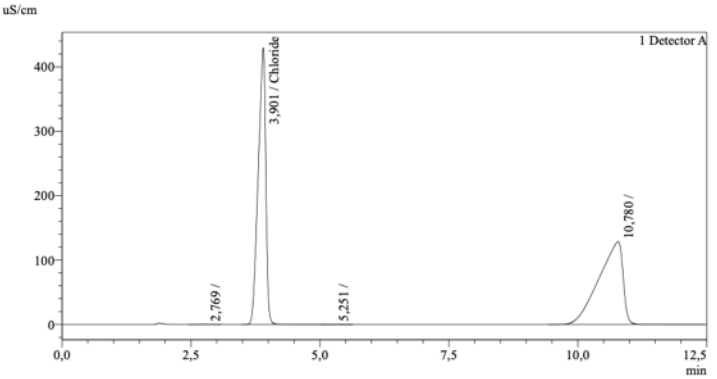


Detector A

| Peak# | Ret. Time | Name | Area | Height | Conc. | Unit | Mark |
|---|---|---|---|---|---|---|---|
| 1 | 2,769 | | 5855 | 569 | 0,000 | | |
| 2 | 3,901 | Chloride | 4361386 | 428669 | 846,621 | mg/L | S |
| 3 | 5,251 | | 3724 | 331 | 0,000 | | T |
| 4 | 10,780 | | 4193105 | 128598 | 0,000 | | |
| Total | | | 8564070 | 558167 | | | |

Sample Name : 23.1
Tray# : 1
Vial# : 67
Injection Volume : 20
Data File : 20250625 Chloride Covra UCR 067.lcd
Method File : Method Chloride + Sulfate Shodex column.lcm
Batch File : 20250625 Chloride Covra UCR.lcb
Report Format File : Report default.lsr
Date Acquired : 6/26/2025 5:00:49 AM
Time Acquired : 5:00:49 AM
Date Processed : 6/26/2025 5:13:18 AM
Time Processed : 5:13:18 AM

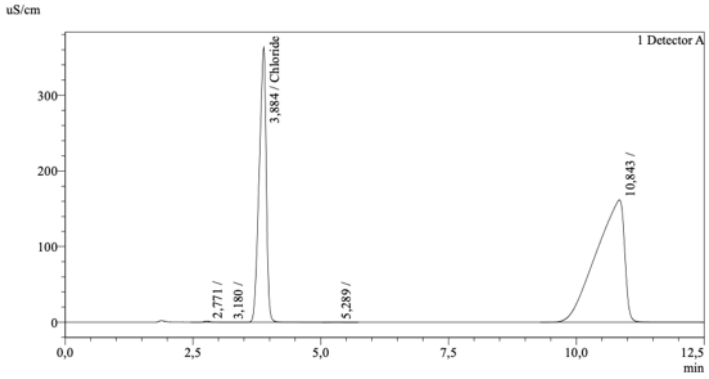


Detector A

| Peak# | Ret. Time | Name | Area | Height | Conc. | Unit | Mark |
|---|---|---|---|---|---|---|---|
| 1 | 2,771 | | 16217 | 1565 | 0,000 | | |
| 2 | 3,180 | | 2426 | 128 | 0,000 | | V |
| 3 | 3,884 | Chloride | 3471375 | 362949 | 673,854 | mg/L | SV |
| 4 | 5,289 | | 2867 | 252 | 0,000 | | T |
| 5 | 10,843 | | 6252218 | 161763 | 0,000 | | |
| Total | | | 9745103 | 526656 | | | |

Sample Name : 24.1
Tray# : 1
Vial# : 69
Injection Volume : 20
Data File : 20250625 Chloride Covra UCR 069.lcd
Method File : Method Chloride + Sulfate Shodex column.lcm
Batch File : 20250625 Chloride Covra UCR.lcb
Report Format File : Report default.lsr
Date Acquired : 6/26/2025 5:26:59 AM
Time Acquired : 5:26:59 AM
Date Processed : 6/26/2025 5:39:30 AM
Time Processed : 5:39:30 AM

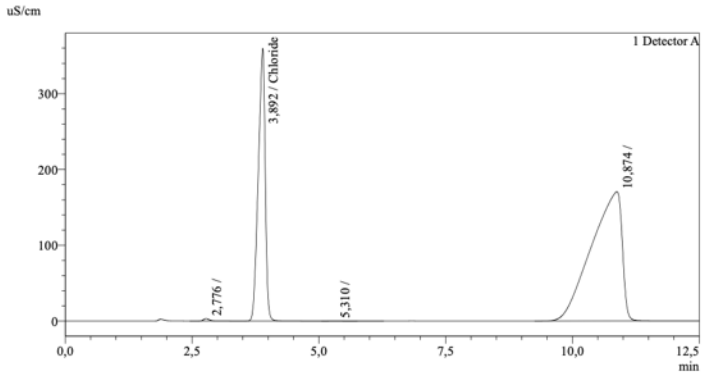


Detector A

| Peak# | Ret. Time | Name | Area | Height | Conc. | Unit | Mark |
|---|---|---|---|---|---|---|---|
| 1 | 2,776 | | 33754 | 3177 | 0,000 | | |
| 2 | 3,892 | Chloride | 3428328 | 359851 | 665,498 | mg/L | SV |
| 3 | 5,310 | | 2871 | 250 | 0,000 | | T |
| 4 | 10,874 | | 7223877 | 170665 | 0,000 | | |
| Total | | | 10688831 | 533942 | | | |

Sample Name : 25.1
Tray# : 1
Vial# : 11
Injection Volume : 20
Data File : 20250625 Chloride Covra UCR 011.lcd
Method File : Method Chloride + Sulfate Shodex column.lcm
Batch File : 20250625 Chloride Covra UCR.lcb
Report Format File : Report default.lsr
Date Acquired : 6/25/2025 4:47:03 PM
Time Acquired : 4:47:03 PM
Date Processed : 6/25/2025 4:59:34 PM
Time Processed : 4:59:34 PM

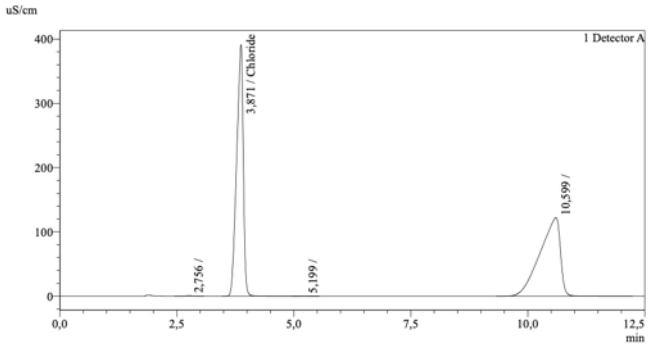


Detector A

| Peak# | Ret. Time | Name | Area | Height | Conc. | Unit | Mark |
|---|---|---|---|---|---|---|---|
| 1 | 2,756 | | 7205 | 826 | 0,000 | | |
| 2 | 3,871 | Chloride | 3834647 | 391227 | 744,372 | mg/L | S |
| 3 | 5,199 | | 3176 | 287 | 0,000 | | T |
| 4 | 10,599 | | 3711180 | 122288 | 0,000 | | |
| Total | | | 7556207 | 514628 | | | |

Sample Name : 25.2
Tray# : 1
Vial# : 36
Injection Volume : 20
Data File : 20250625 Chloride Covra UCR 036.lcd
Method File : Method Chloride + Sulfate Shodex column.lcm
Batch File : 20250625 Chloride Covra UCR.lcb
Report Format File : Report default.lsr
Date Acquired : 6/25/2025 10:14:36 PM
Time Acquired : 10:14:36 PM
Date Processed : 6/25/2025 10:27:07 PM
Time Processed : 10:27:07 PM

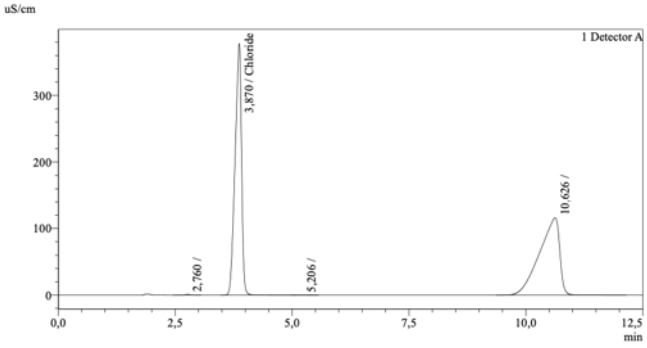


Detector A

| Peak# | Ret. Time | Name | Area | Height | Conc. | Unit | Mark |
|---|---|---|---|---|---|---|---|
| 1 | 2,760 | | 9241 | 1041 | 0,000 | | |
| 2 | 3,870 | Chloride | 3614356 | 377671 | 701,609 | mg/L | S |
| 3 | 5,206 | | 3061 | 280 | 0,000 | | T |
| 4 | 10,626 | | 3494886 | 116258 | 0,000 | | |
| Total | | | 7121544 | 495250 | | | |

Sample Name : 26.1
Tray# : 1
Vial# : 12
Injection Volume : 20
Data File : 20250625 Chloride Covra UCR 012.lcd
Method File : Method Chloride + Sulfate Shodex column.lcm
Batch File : 20250625 Chloride Covra UCR.lcb
Report Format File : Report default.lsr
Date Acquired : 6/25/2025 5:00:10 PM
Time Acquired : 5:00:10 PM
Date Processed : 6/25/2025 5:12:40 PM
Time Processed : 5:12:40 PM

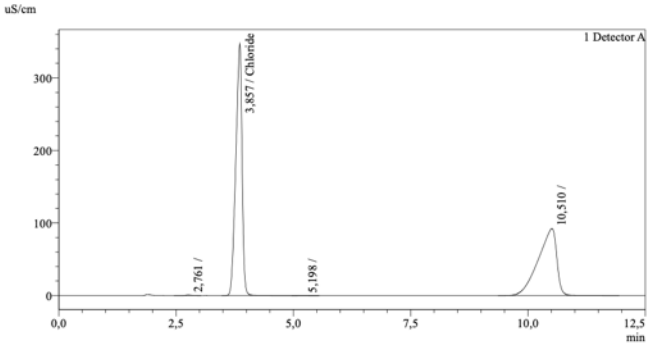


Detector A

| Peak# | Ret. Time | Name | Area | Height | Conc. | Unit | Mark |
|---|---|---|---|---|---|---|---|
| 1 | 2,761 | | 8955 | 889 | 0,000 | | |
| 2 | 3,857 | Chloride | 3207725 | 346828 | 622,675 | mg/L | S |
| 3 | 5,198 | | 2584 | 234 | 0,000 | | T |
| 4 | 10,510 | | 2539764 | 92399 | 0,000 | | |
| Total | | | 5759029 | 440350 | | | |

Sample Name : 27.1
Tray# : 1
Vial# : 95
Injection Volume : 20
Data File : 20250625 Chloride Covra UCR 095.lcd
Method File : Method Chloride + Sulfate Shodex column.lcm
Batch File : 20250625 Chloride Covra UCR.lcb
Report Format File : Report default.lsr
Date Acquired : 6/26/2025 1:50:08 PM
Time Acquired : 1:50:08 PM
Date Processed : 6/26/2025 2:02:39 PM
Time Processed : 2:02:39 PM

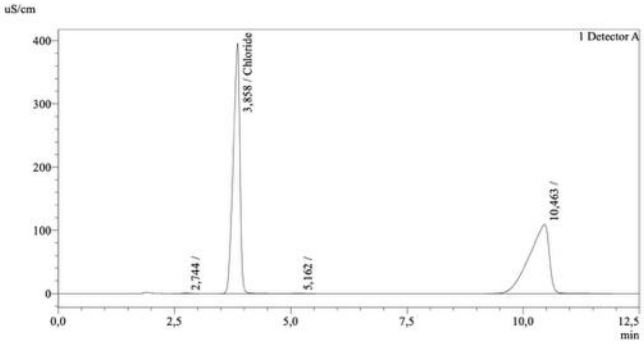


Detector A

| Peak# | Ret. Time | Name | Area | Height | Conc. | Unit | Mark |
|---|---|---|---|---|---|---|---|
| 1 | 2,744 | | 8616 | 842 | 0,000 | | |
| 2 | 3,858 | Chloride | 3931333 | 395616 | 763,140 | mg/L | S |
| 3 | 5,162 | | 3313 | 303 | 0,000 | | T |
| 4 | 10,463 | | 3269506 | 109716 | 0,000 | | |
| Total | | | 7212769 | 506477 | | | |

Sample Name : 27.2
Tray# : 1
Vial# : 26
Injection Volume : 20
Data File : 20250625 Chloride Covra UCR 026.lcd
Method File : Method Chloride + Sulfate Shodex column.lcm
Batch File : 20250625 Chloride Covra UCR.lcb
Report Format File : Report default.lsr
Date Acquired : 6/25/2025 8:03:33 PM
Time Acquired : 8:03:33 PM
Date Processed : 6/25/2025 8:16:04 PM
Time Processed : 8:16:04 PM

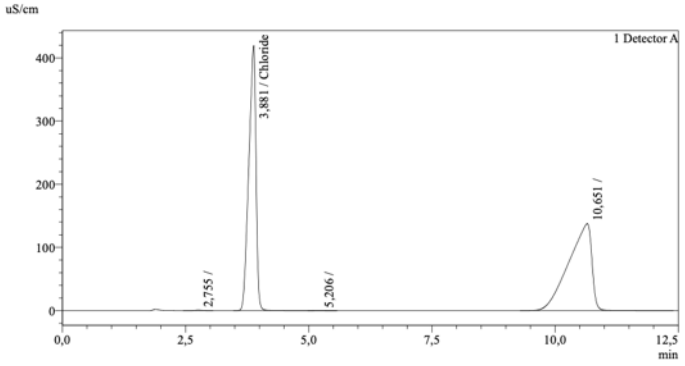


Detector A

| Peak# | Ret. Time | Name | Area | Height | Conc. | Unit | Mark |
|---|---|---|---|---|---|---|---|
| 1 | 2,755 | | 7387 | 801 | 0,000 | | |
| 2 | 3,881 | Chloride | 4254855 | 418827 | 825,941 | mg/L | S |
| 3 | 5,206 | | 3467 | 314 | 0,000 | | T |
| 4 | 10,651 | | 4504551 | 137566 | 0,000 | | |
| Total | | | 8770261 | 557507 | | | |

Sample Name : 28.1
Tray# : 1
Vial# : 100
Injection Volume : 20
Data File : 20250625 Chloride Covra UCR 100.lcd
Method File : Method Chloride + Sulfate Shodex column.lcm
Batch File : 20250625 Chloride Covra UCR.lcb
Report Format File : Report default.lsr
Date Acquired : 6/26/2025 2:55:37 PM
Time Acquired : 2:55:37 PM
Date Processed : 6/26/2025 3:08:08 PM
Time Processed : 3:08:08 PM

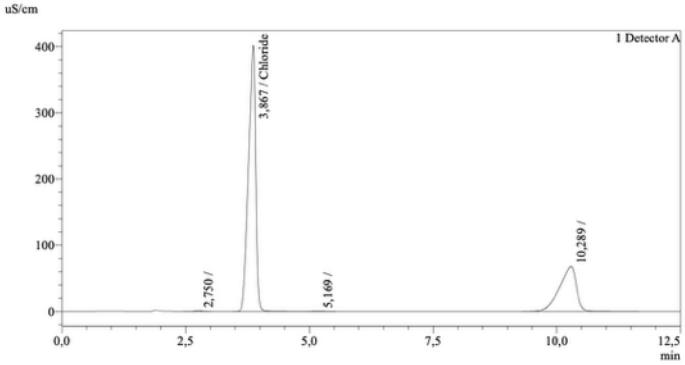


Detector A

| Peak# | Ret. Time | Name | Area | Height | Conc. | Unit | Mark |
|---|---|---|---|---|---|---|---|
| 1 | 2,750 | | 12079 | 1270 | 0,000 | | |
| 2 | 3,867 | Chloride | 4024068 | 401343 | 781,142 | mg/L | S |
| 3 | 5,169 | | 3306 | 304 | 0,000 | | T |
| 4 | 10,289 | | 1609327 | 67836 | 0,000 | | |
| Total | | | 5648779 | 470752 | | | |

Sample Name : 28.2
Tray# : 1
Vial# : 54
Injection Volume : 20
Data File : 20250625 Chloride Covra UCR 054.lcd
Method File : Method Chloride + Sulfate Shodex column.lcm
Batch File : 20250625 Chloride Covra UCR.lcb
Report Format File : Report default.lsr
Date Acquired : 6/26/2025 2:10:30 AM
Time Acquired : 2:10:30 AM
Date Processed : 6/26/2025 2:23:01 AM
Time Processed : 2:23:01 AM

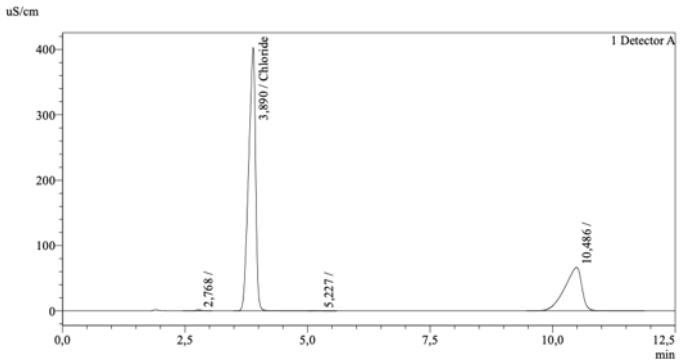


Detector A

| Peak# | Ret. Time | Name | Area | Height | Conc. | Unit | Mark |
|---|---|---|---|---|---|---|---|
| 1 | 2,768 | | 12234 | 1416 | 0,000 | | |
| 2 | 3,890 | Chloride | 3956148 | 402685 | 767,957 | mg/L | S |
| 3 | 5,227 | | 3202 | 294 | 0,000 | | T |
| 4 | 10,486 | | 1627850 | 66570 | 0,000 | | |
| Total | | | 5599435 | 470965 | | | |

Sample Name : 29.1
Tray# : 1
Vial# : 86
Injection Volume : 20
Data File : 20250625 Chloride Covra UCR 086.lcd
Method File : Method Chloride + Sulfate Shodex column.lcm
Batch File : 20250625 Chloride Covra UCR.lcb
Report Format File : Report default.lsr
Date Acquired : 6/26/2025 11:52:14 AM
Time Acquired : 11:52:14 AM
Date Processed : 6/26/2025 12:04:45 PM
Time Processed : 12:04:45 PM

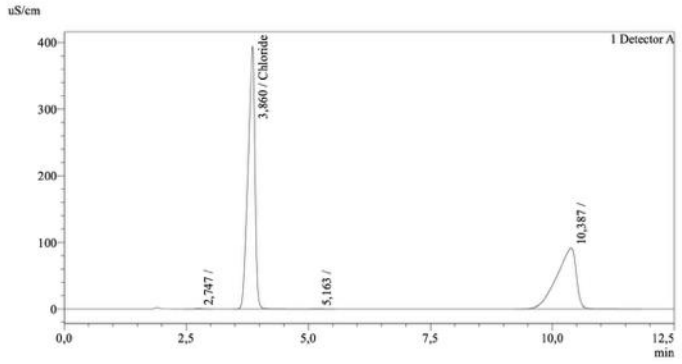


Detector A

| Peak# | Ret. Time | Name | Area | Height | Conc. | Unit | Mark |
|---|---|---|---|---|---|---|---|
| 1 | 2,747 | | 10600 | 1074 | 0,000 | | |
| 2 | 3,860 | Chloride | 3919793 | 393777 | 760,900 | mg/L | S |
| 3 | 5,163 | | 3348 | 306 | 0,000 | | T |
| 4 | 10,387 | | 2539161 | 91786 | 0,000 | | |
| Total | | | 6472902 | 486943 | | | |

Sample Name : 30.1
Tray# : 1
Vial# : 13
Injection Volume : 20
Data File : 20250625 Chloride Covra UCR 013.lcd
Method File : Method Chloride + Sulfate Shodex column.lcm
Batch File : 20250625 Chloride Covra UCR.lcb
Report Format File : Report default.lsr
Date Acquired : 6/25/2025 5:13:15 PM
Time Acquired : 5:13:15 PM
Date Processed : 6/25/2025 5:25:46 PM
Time Processed : 5:25:46 PM

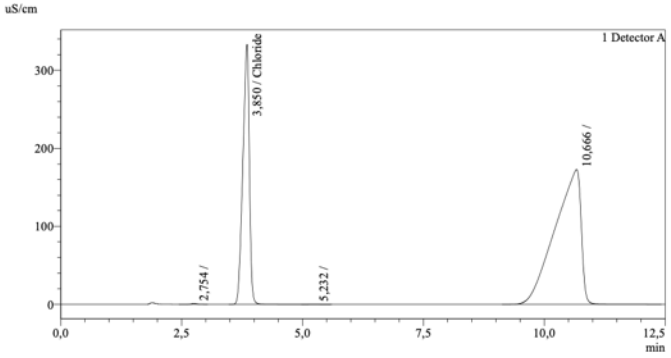


Detector A

| Peak# | Ret. Time | Name | Area | Height | Conc. | Unit | Mark |
|---|---|---|---|---|---|---|---|
| 1 | 2,754 | | 10575 | 1151 | 0,000 | | |
| 2 | 3,850 | Chloride | 3115263 | 332902 | 604,727 | mg/L | SV |
| 3 | 5,232 | | 2613 | 236 | 0,000 | | T |
| 4 | 10,666 | | 6514578 | 172963 | 0,000 | | |
| Total | | | 9643029 | 507253 | | | |

Sample Name : 31.1
Tray# : 1
Vial# : 53
Injection Volume : 20
Data File : 20250625 Chloride Covra UCR 053.lcd
Method File : Method Chloride + Sulfate Shodex column.lcm
Batch File : 20250625 Chloride Covra UCR.lcb
Report Format File : Report default.lsr
Date Acquired : 6/26/2025 1:57:24 AM
Time Acquired : 1:57:24 AM
Date Processed : 6/26/2025 2:09:55 AM
Time Processed : 2:09:55 AM

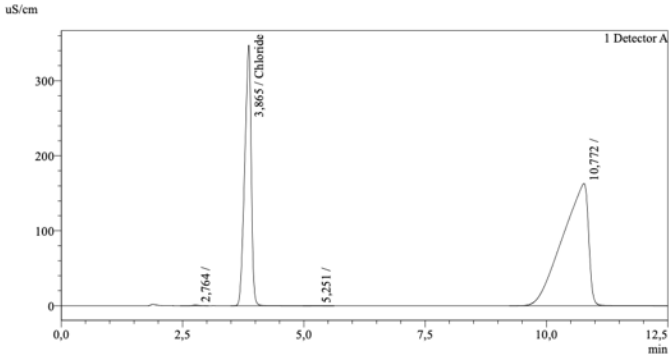


Detector A

| Peak# | Ret. Time | Name | Area | Height | Conc. | Unit | Mark |
|---|---|---|---|---|---|---|---|
| 1 | 2,764 | | 10124 | 1116 | 0,000 | | |
| 2 | 3,865 | Chloride | 3229317 | 347324 | 626,867 | mg/L | SV |
| 3 | 5,251 | | 2671 | 242 | 0,000 | | T |
| 4 | 10,772 | | 6076559 | 163191 | 0,000 | | |
| Total | | | 9318670 | 511873 | | | |

Sample Name : 32.1
Tray# : 1
Vial# : 73
Injection Volume : 20
Data File : 20250625 Chloride Covra UCR 073.lcd
Method File : Method Chloride + Sulfate Shodex column.lcm
Batch File : 20250625 Chloride Covra UCR.lcb
Report Format File : Report default.lsr
Date Acquired : 6/26/2025 9:01:57 AM
Time Acquired : 9:01:57 AM
Date Processed : 6/26/2025 9:14:28 AM
Time Processed : 9:14:28 AM

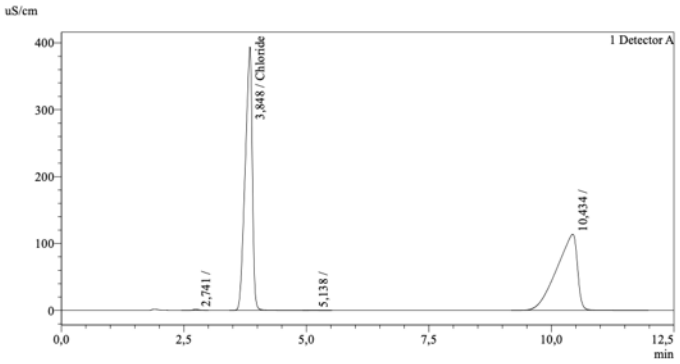


Detector A

| Peak# | Ret. Time | Name | Area | Height | Conc. | Unit | Mark |
|---|---|---|---|---|---|---|---|
| 1 | 2,741 | | 14957 | 1654 | 0,000 | | |
| 2 | 3,848 | Chloride | 3944241 | 393105 | 765,646 | mg/L | SV |
| 3 | 5,138 | | 3262 | 296 | 0,000 | | T |
| 4 | 10,434 | | 3353446 | 113782 | 0,000 | | |
| Total | | | 7315905 | 508837 | | | |

Sample Name : 33.1
Tray# : 1
Vial# : 78
Injection Volume : 20
Data File : 20250625 Chloride Covra UCR 078.lcd
Method File : Method Chloride + Sulfate Shodex column.lcm
Batch File : 20250625 Chloride Covra UCR.lcb
Report Format File : Report default.lsr
Date Acquired : 6/26/2025 10:07:29 AM
Time Acquired : 10:07:29 AM
Date Processed : 6/26/2025 10:20:00 AM
Time Processed : 10:20:00 AM

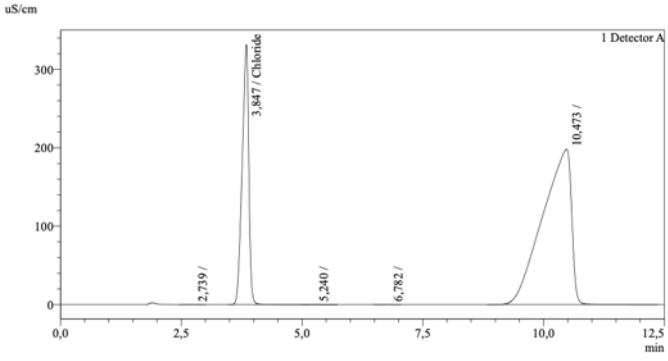


Detector A

| Peak# | Ret. Time | Name | Area | Height | Conc. | Unit | Mark |
|---|---|---|---|---|---|---|---|
| 1 | 2,739 | | 2480 | 251 | 0,000 | | |
| 2 | 3,847 | Chloride | 3140707 | 331113 | 609,666 | mg/L | S |
| 3 | 5,240 | | 3147 | 250 | 0,000 | | T |
| 4 | 6,782 | | 2172 | 142 | 0,000 | | |
| 5 | 10,473 | | 8250810 | 198226 | 0,000 | | |
| Total | | | 11399316 | 529982 | | | |

Sample Name : 34.1
Tray# : 1
Vial# : 20
Injection Volume : 20
Data File : 20250625 Chloride Covra UCR 020.lcd
Method File : Method Chloride + Sulfate Shodex column.lcm
Batch File : 20250625 Chloride Covra UCR.lcb
Report Format File : Report default.lsr
Date Acquired : 6/25/2025 6:44:58 PM
Time Acquired : 6:44:58 PM
Date Processed : 6/25/2025 6:57:28 PM
Time Processed : 6:57:28 PM

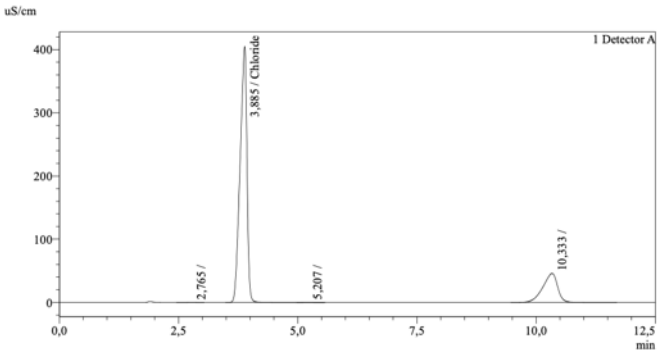


Detector A

| Peak# | Ret. Time | Name | Area | Height | Conc. | Unit | Mark |
|---|---|---|---|---|---|---|---|
| 1 | 2,765 | | 4816 | 429 | 0,000 | | |
| 2 | 3,885 | Chloride | 4036441 | 405088 | 783,543 | mg/L | S |
| 3 | 5,207 | | 3470 | 316 | 0,000 | | T |
| 4 | 10,333 | | 994691 | 45954 | 0,000 | | |
| Total | | | 5039418 | 451786 | | | |

Sample Name : 35.1
Tray# : 1
Vial# : 92
Injection Volume : 20
Data File : 20250625 Chloride Covra UCR 092.lcd
Method File : Method Chloride + Sulfate Shodex column.lcm
Batch File : 20250625 Chloride Covra UCR.lcb
Report Format File : Report default.lsr
Date Acquired : 6/26/2025 1:10:51 PM
Time Acquired : 1:10:51 PM
Date Processed : 6/26/2025 1:23:21 PM
Time Processed : 1:23:21 PM

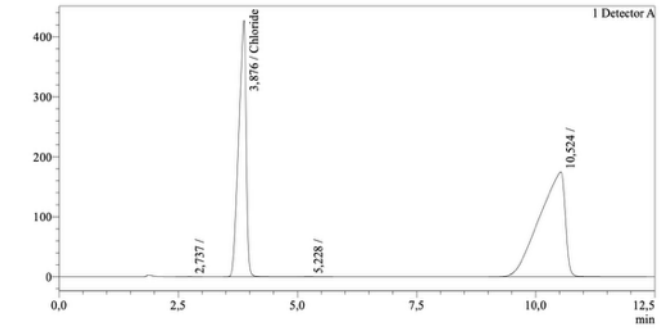


Detector A

| Peak# | Ret. Time | Name | Area | Height | Conc. | Unit | Mark |
|---|---|---|---|---|---|---|---|
| 1 | 2,737 | | 2164 | 212 | 0,000 | | |
| 2 | 3,876 | Chloride | 4641564 | 427190 | 901,008 | mg/L | S |
| 3 | 5,228 | | 3964 | 333 | 0,000 | | T |
| 4 | 10,524 | | 6581392 | 174716 | 0,000 | | |
| Total | | | 11229084 | 602451 | | | |

Sample Name : 36.1
Tray# : 1
Vial# : 16
Injection Volume : 20
Data File : 20250625 Chloride Covra UCR 016.lcd
Method File : Method Chloride + Sulfate Shodex column.lcm
Batch File : 20250625 Chloride Covra UCR.lcb
Report Format File : Report default.lsr
Date Acquired : 6/25/2025 5:52:36 PM
Time Acquired : 5:52:36 PM
Date Processed : 6/25/2025 6:05:06 PM
Time Processed : 6:05:06 PM

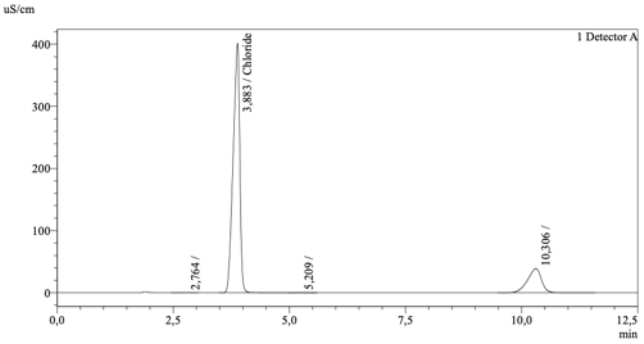


Detector A

| Peak# | Ret. Time | Name | Area | Height | Conc. | Unit | Mark |
|---|---|---|---|---|---|---|---|
| 1 | 2,764 | | 4408 | 459 | 0,000 | | |
| 2 | 3,883 | Chloride | 3976542 | 400934 | 771,916 | mg/L | S |
| 3 | 5,209 | | 3401 | 306 | 0,000 | | T |
| 4 | 10,306 | | 815289 | 38803 | 0,000 | | |
| Total | | | 4799639 | 440502 | | | |

Sample Name : 37.1
Tray# : 1
Vial# : 29
Injection Volume : 20
Data File : 20250625 Chloride Covra UCR 029.lcd
Method File : Method Chloride + Sulfate Shodex column.lcm
Batch File : 20250625 Chloride Covra UCR.lcb
Report Format File : Report default.lsr
Date Acquired : 6/25/2025 8:42:55 PM
Time Acquired : 8:42:55 PM
Date Processed : 6/25/2025 8:55:25 PM
Time Processed : 8:55:25 PM

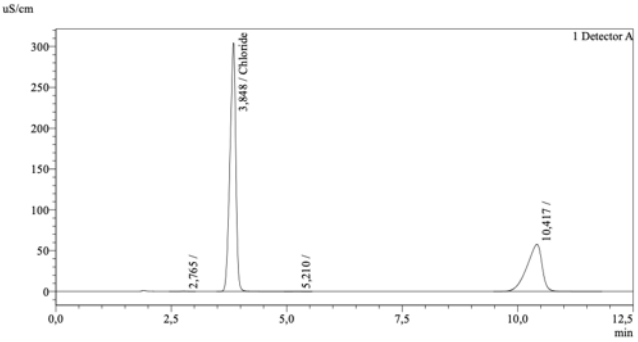


Detector A

| Peak# | Ret. Time | Name | Area | Height | Conc. | Unit | Mark |
|---|---|---|---|---|---|---|---|
| 1 | 2,765 | | 4023 | 408 | 0,000 | | |
| 2 | 3,848 | Chloride | 2672653 | 303963 | 518,809 | mg/L | S |
| 3 | 5,210 | | 2173 | 197 | 0,000 | | T |
| 4 | 10,417 | | 1318359 | 57690 | 0,000 | | |
| Total | | | 3997208 | 362258 | | | |

| | |
|---|---|
| Sample Name | : 38.1 |
| Tray# | : 1 |
| Vial# | : 51 |
| Injection Volume | : 20 |
| Data File | : 20250625 Chloride Covra UCR 051.lcd |
| Method File | : Method Chloride + Sulfate Shodex column.lcm |
| Batch File | : 20250625 Chloride Covra UCR.lcb |
| Report Format File | : Report default.lsr |
| Date Acquired | : 6/26/2025 1:31:13 AM |
| Time Acquired | : 1:31:13 AM |
| Date Processed | : 6/26/2025 1:43:43 AM |
| Time Processed | : 1:43:43 AM |

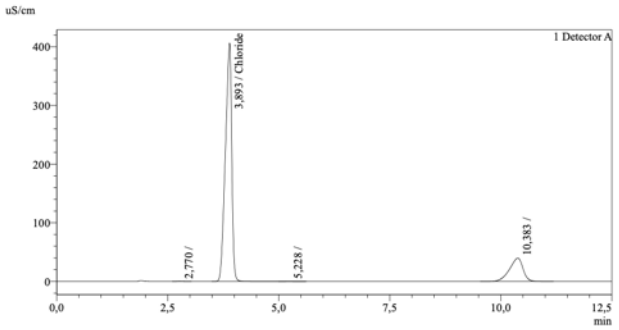


Detector A

| Peak# | Ret. Time | Name | Area | Height | Conc. | Unit | Mark |
|---|---|---|---|---|---|---|---|
| 1 | 2,770 | | 4519 | 518 | 0,000 | | |
| 2 | 3,893 | Chloride | 4020485 | 405956 | 780,446 | mg/L | S |
| 3 | 5,228 | | 3345 | 304 | 0,000 | | T |
| 4 | 10,383 | | 845276 | 39794 | 0,000 | | |
| Total | | | 4873625 | 446573 | | | |

| | |
|---|---|
| Sample Name | : 39.1 |
| Tray# | : 1 |
| Vial# | : 46 |
| Injection Volume | : 20 |
| Data File | : 20250625 Chloride Covra UCR 046.lcd |
| Method File | : Method Chloride + Sulfate Shodex column.lcm |
| Batch File | : 20250625 Chloride Covra UCR.lcb |
| Report Format File | : Report default.lsr |
| Date Acquired | : 6/26/2025 12:25:41 AM |
| Time Acquired | : 12:25:41 AM |
| Date Processed | : 6/26/2025 12:38:11 AM |
| Time Processed | : 12:38:11 AM |

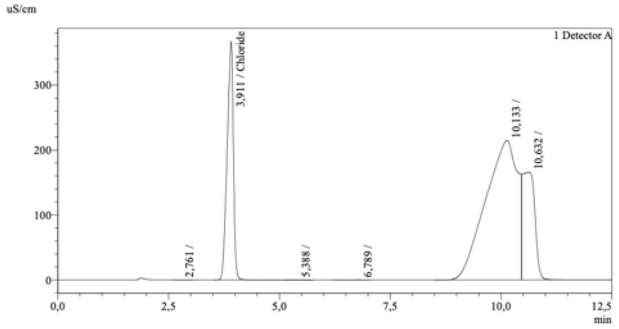


Detector A

| Peak# | Ret. Time | Name | Area | Height | Conc. | Unit | Mark |
|---|---|---|---|---|---|---|---|
| 1 | 2,761 | | 2359 | 251 | 0,000 | | |
| 2 | 3,911 | Chloride | 3577643 | 366707 | 694,483 | mg/L | S |
| 3 | 5,388 | | 3004 | 247 | 0,000 | | T |
| 4 | 6,789 | | 9659 | 439 | 0,000 | | |
| 5 | 10,133 | | 10785972 | 215002 | 0,000 | | |
| 6 | 10,632 | | 3258927 | 166099 | 0,000 | | V |
| Total | | | 17637564 | 748746 | | | |

Sample Name : 40.1
Tray# : 1
Vial# : 41
Injection Volume : 20
Data File : 20250625 Chloride Covra UCR 041.lcd
Method File : Method Chloride + Sulfate Shodex column.lcm
Batch File : 20250625 Chloride Covra UCR.lcb
Report Format File : Report default.lsr
Date Acquired : 6/25/2025 11:20:06 PM
Time Acquired : 11:20:06 PM
Date Processed : 6/25/2025 11:32:37 PM
Time Processed : 11:32:37 PM

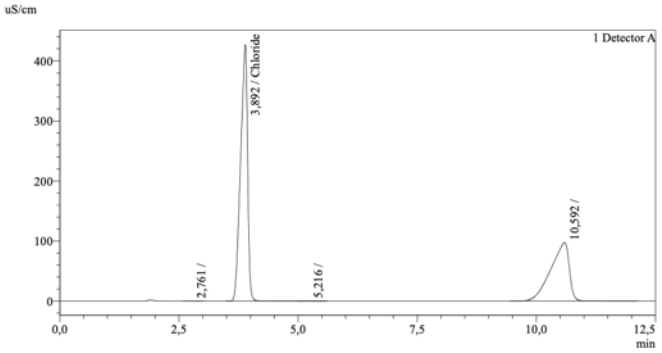


Detector A

| Peak# | Ret. Time | Name | Area | Height | Conc. | Unit | Mark |
|---|---|---|---|---|---|---|---|
| 1 | 2,761 | | 3430 | 389 | 0,000 | | |
| 2 | 3,892 | Chloride | 4366649 | 426964 | 847,642 | mg/L | S |
| 3 | 5,216 | | 3715 | 334 | 0,000 | | T |
| 4 | 10,592 | | 2644518 | 97328 | 0,000 | | |
| Total | | | 7018311 | 525016 | | | |

Sample Name : 41.2
Tray# : 1
Vial# : 79
Injection Volume : 20
Data File : 20250625 Chloride Covra UCR 079.lcd
Method File : Method Chloride + Sulfate Shodex column.lcm
Batch File : 20250625 Chloride Covra UCR.lcb
Report Format File : Report default.lsr
Date Acquired : 6/26/2025 10:20:34 AM
Time Acquired : 10:20:34 AM
Date Processed : 6/26/2025 10:33:05 AM
Time Processed : 10:33:05 AM

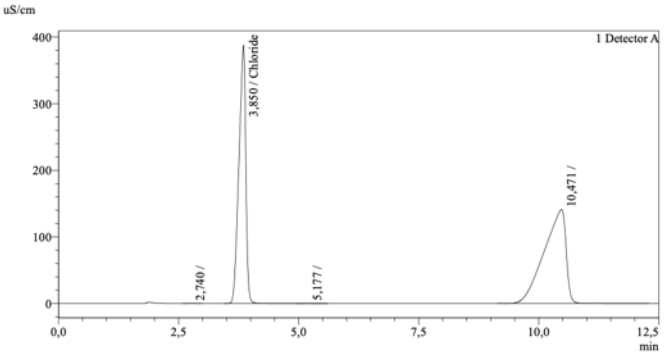


Detector A

| Peak# | Ret. Time | Name | Area | Height | Conc. | Unit | Mark |
|---|---|---|---|---|---|---|---|
| 1 | 2,740 | | 3034 | 341 | 0,000 | | |
| 2 | 3,850 | Chloride | 3847258 | 387341 | 746,820 | mg/L | S |
| 3 | 5,177 | | 2572 | 229 | 0,000 | | T |
| 4 | 10,471 | | 4487907 | 141117 | 0,000 | | |
| Total | | | 8340770 | 529028 | | | |

Sample Name : 42.1
Tray# : 1
Vial# : 99
Injection Volume : 20
Data File : 20250625 Chloride Covra UCR 099.lcd
Method File : Method Chloride + Sulfate Shodex column.lcm
Batch File : 20250625 Chloride Covra UCR.lcb
Report Format File : Report default.lsr
Date Acquired : 6/26/2025 2:42:30 PM
Time Acquired : 2:42:30 PM
Date Processed : 6/26/2025 2:55:01 PM
Time Processed : 2:55:01 PM

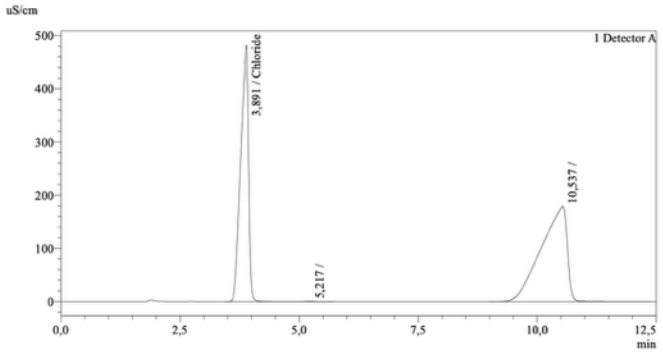


Detector A

| Peak# | Ret. Time | Name | Area | Height | Conc. | Unit | Mark |
|---|---|---|---|---|---|---|---|
| 1 | 3,891 | Chloride | 5547664 | 481741 | 1076,898 | mg/L | S |
| 2 | 5,217 | | 4894 | 422 | 0,000 | | T |
| 3 | 10,537 | | 6777511 | 178746 | 0,000 | | |
| Total | | | 12330069 | 660909 | | | |

Sample Name : 42.2
Tray# : 1
Vial# : 84
Injection Volume : 20
Data File : 20250625 Chloride Covra UCR 084.lcd
Method File : Method Chloride + Sulfate Shodex column.lcm
Batch File : 20250625 Chloride Covra UCR.lcb
Report Format File : Report default.lsr
Date Acquired : 6/26/2025 11:26:03 AM
Time Acquired : 11:26:03 AM
Date Processed : 6/26/2025 11:38:33 AM
Time Processed : 11:38:33 AM

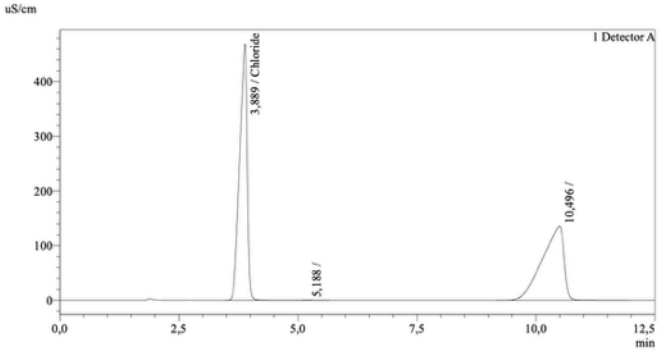


Detector A

| Peak# | Ret. Time | Name | Area | Height | Conc. | Unit | Mark |
|---|---|---|---|---|---|---|---|
| 1 | 3,889 | Chloride | 5216081 | 468282 | 1012,532 | mg/L | S |
| 2 | 5,188 | | 4399 | 391 | 0,000 | | T |
| 3 | 10,496 | | 4291895 | 135575 | 0,000 | | |
| Total | | | 9512376 | 604249 | | | |

Sample Name : 43.1
Tray# : 1
Vial# : 25
Injection Volume : 20
Data File : 20250625 Chloride Covra UCR 025.lcd
Method File : Method Chloride + Sulfate Shodex column.lcm
Batch File : 20250625 Chloride Covra UCR.lcb
Report Format File : Report default.lsr
Date Acquired : 6/25/2025 7:50:27 PM
Time Acquired : 7:50:27 PM
Date Processed : 6/25/2025 8:02:57 PM
Time Processed : 8:02:57 PM

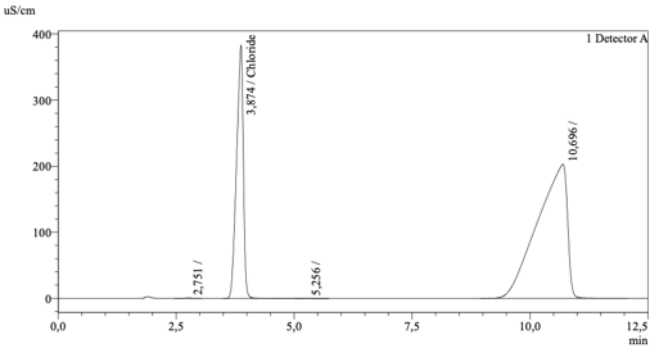


Detector A

| Peak# | Ret. Time | Name | Area | Height | Conc. | Unit | Mark |
|---|---|---|---|---|---|---|---|
| 1 | 2,751 | | 7985 | 773 | 0,000 | | |
| 2 | 3,874 | Chloride | 3800465 | 382537 | 737,736 | mg/L | SV |
| 3 | 5,256 | | 3026 | 264 | 0,000 | | T |
| 4 | 10,696 | | 8971489 | 202912 | 0,000 | | |
| Total | | | 12782964 | 586487 | | | |

Sample Name : 43.2
Tray# : 1
Vial# : 18
Injection Volume : 20
Data File : 20250625 Chloride Covra UCR 018.lcd
Method File : Method Chloride + Sulfate Shodex column.lcm
Batch File : 20250625 Chloride Covra UCR.lcb
Report Format File : Report default.lsr
Date Acquired : 6/25/2025 6:18:46 PM
Time Acquired : 6:18:46 PM
Date Processed : 6/25/2025 6:31:17 PM
Time Processed : 6:31:17 PM

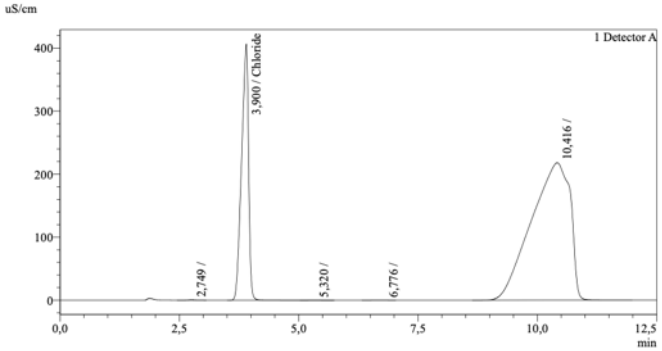


Detector A

| Peak# | Ret. Time | Name | Area | Height | Conc. | Unit | Mark |
|---|---|---|---|---|---|---|---|
| 1 | 2,749 | | 8926 | 801 | 0,000 | | |
| 2 | 3,900 | Chloride | 4136340 | 405980 | 802,936 | mg/L | SV |
| 3 | 5,320 | | 3267 | 270 | 0,000 | | T |
| 4 | 6,776 | | 5707 | 312 | 0,000 | | |
| 5 | 10,416 | | 12436800 | 218271 | 0,000 | | |
| Total | | | 16591039 | 625635 | | | |

| | |
|---|---|
| Sample Name | : 44.1 |
| Tray# | : 1 |
| Vial# | : 91 |
| Injection Volume | : 20 |
| Data File | : 20250625 Chloride Covra UCR 091.lcd |
| Method File | : Method Chloride + Sulfate Shodex column.lcm |
| Batch File | : 20250625 Chloride Covra UCR.lcb |
| Report Format File | : Report default.lsr |
| Date Acquired | : 6/26/2025 12:57:46 PM |
| Time Acquired | : 12:57:46 PM |
| Date Processed | : 6/26/2025 1:10:16 PM |
| Time Processed | : 1:10:16 PM |

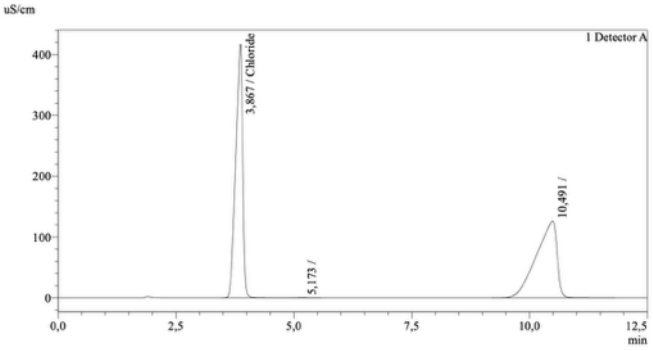


Detector A

| Peak# | Ret. Time | Name | Area | Height | Conc. | Unit | Mark |
|---|---|---|---|---|---|---|---|
| 1 | 3,867 | Chloride | 4276912 | 416496 | 830,223 | mg/L | S |
| 2 | 5,173 | | 3705 | 333 | 0,000 | | T |
| 3 | 10,491 | | 3853373 | 126247 | 0,000 | | |
| Total | | | 8133989 | 543076 | | | |

| | |
|---|---|
| Sample Name | : 45.1 |
| Tray# | : 1 |
| Vial# | : 43 |
| Injection Volume | : 20 |
| Data File | : 20250625 Chloride Covra UCR 043.lcd |
| Method File | : Method Chloride + Sulfate Shodex column.lcm |
| Batch File | : 20250625 Chloride Covra UCR.lcb |
| Report Format File | : Report default.lsr |
| Date Acquired | : 6/25/2025 11:46:21 PM |
| Time Acquired | : 11:46:21 PM |
| Date Processed | : 6/25/2025 11:58:52 PM |
| Time Processed | : 11:58:52 PM |

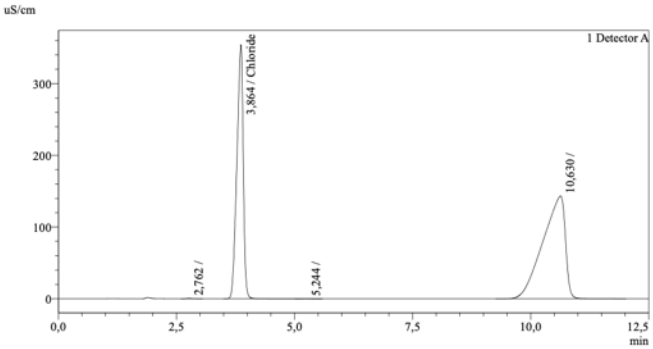


Detector A

| Peak# | Ret. Time | Name | Area | Height | Conc. | Unit | Mark |
|---|---|---|---|---|---|---|---|
| 1 | 2,762 | | 5974 | 681 | 0,000 | | |
| 2 | 3,864 | Chloride | 3310506 | 354197 | 642,627 | mg/L | S |
| 3 | 5,244 | | 2643 | 238 | 0,000 | | T |
| 4 | 10,630 | | 4756090 | 143436 | 0,000 | | |
| Total | | | 8075214 | 498552 | | | |

Sample Name : 46.1
Tray# : 1
Vial# : 15
Injection Volume : 20
Data File : 20250625 Chloride Covra UCR 015.lcd
Method File : Method Chloride + Sulfate Shodex column.lcm
Batch File : 20250625 Chloride Covra UCR.lcb
Report Format File : Report default.lsr
Date Acquired : 6/25/2025 5:39:29 PM
Time Acquired : 5:39:29 PM
Date Processed : 6/25/2025 5:51:59 PM
Time Processed : 5:51:59 PM

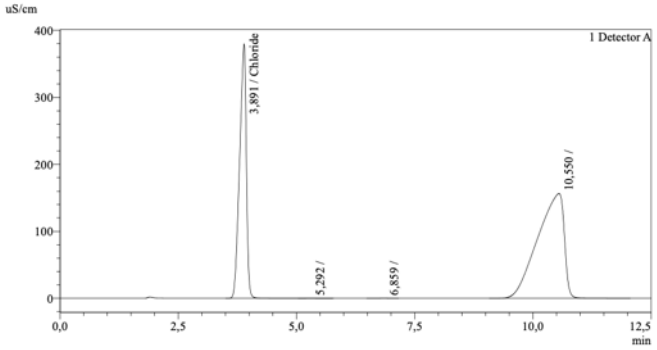


Detector A

| Peak# | Ret. Time | Name | Area | Height | Conc. | Unit | Mark |
|---|---|---|---|---|---|---|---|
| 1 | 3,891 | Chloride | 3752494 | 379707 | 728,424 | mg/L | S |
| 2 | 5,292 | | 3475 | 295 | 0,000 | | T |
| 3 | 6,859 | | 3224 | 189 | 0,000 | | |
| 4 | 10,550 | | 6106019 | 156556 | 0,000 | | |
| Total | | | 9865212 | 536747 | | | |

Sample Name : 47.1
Tray# : 1
Vial# : 49
Injection Volume : 20
Data File : 20250625 Chloride Covra UCR 049.lcd
Method File : Method Chloride + Sulfate Shodex column.lcm
Batch File : 20250625 Chloride Covra UCR.lcb
Report Format File : Report default.lsr
Date Acquired : 6/26/2025 1:04:59 AM
Time Acquired : 1:04:59 AM
Date Processed : 6/26/2025 1:17:30 AM
Time Processed : 1:17:30 AM

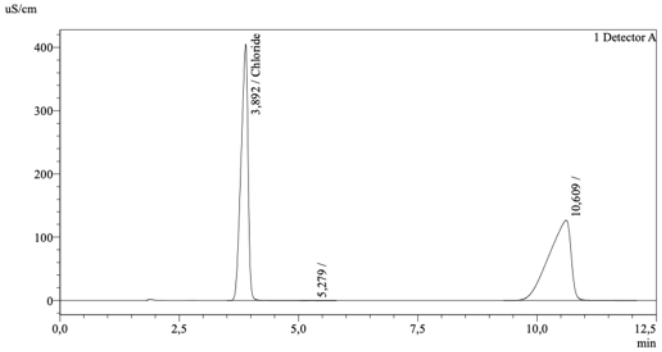


Detector A

| Peak# | Ret. Time | Name | Area | Height | Conc. | Unit | Mark |
|---|---|---|---|---|---|---|---|
| 1 | 3,892 | Chloride | 4113839 | 404785 | 798,568 | mg/L | S |
| 2 | 5,279 | | 3527 | 305 | 0,000 | | T |
| 3 | 10,609 | | 4098242 | 126701 | 0,000 | | |
| Total | | | 8215608 | 531790 | | | |

Sample Name : 48.1
Tray# : 1
Vial# : 35
Injection Volume : 20
Data File : 20250625 Chloride Covra UCR 035.lcd
Method File : Method Chloride + Sulfate Shodex column.lcm
Batch File : 20250625 Chloride Covra UCR.lcb
Report Format File : Report default.lsr
Date Acquired : 6/25/2025 10:01:31 PM
Time Acquired : 10:01:31 PM
Date Processed : 6/25/2025 10:14:02 PM
Time Processed : 10:14:02 PM

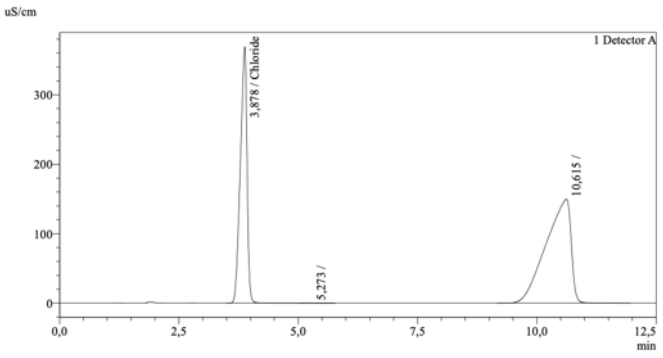


Detector A

| Peak# | Ret. Time | Name | Area | Height | Conc. | Unit | Mark |
|---|---|---|---|---|---|---|---|
| 1 | 3,878 | Chloride | 3594541 | 368866 | 697,763 | mg/L | S |
| 2 | 5,273 | | 3189 | 275 | 0,000 | | T |
| 3 | 10,615 | | 5473788 | 149714 | 0,000 | | |
| Total | | | 9071518 | 518855 | | | |

Sample Name : 49.1
Tray# : 1
Vial# : 58
Injection Volume : 20
Data File : 20250625 Chloride Covra UCR 058.lcd
Method File : Method Chloride + Sulfate Shodex column.lcm
Batch File : 20250625 Chloride Covra UCR.lcb
Report Format File : Report default.lsr
Date Acquired : 6/26/2025 3:02:55 AM
Time Acquired : 3:02:55 AM
Date Processed : 6/26/2025 3:15:26 AM
Time Processed : 3:15:26 AM

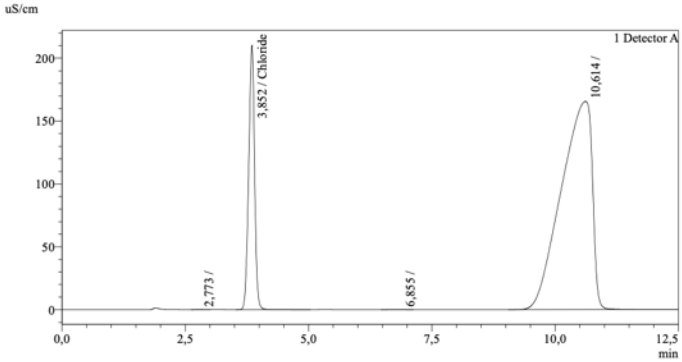


Detector A

| Peak# | Ret. Time | Name | Area | Height | Conc. | Unit | Mark |
|---|---|---|---|---|---|---|---|
| 1 | 2,773 | | 2535 | 292 | 0,000 | | |
| 2 | 3,852 | Chloride | 1742109 | 210356 | 338,174 | mg/L | |
| 3 | 6,855 | | 3449 | 205 | 0,000 | | |
| 4 | 10,614 | | 7269356 | 165691 | 0,000 | | |
| Total | | | 9017449 | 376545 | | | |

Sample Name : 50.1
Tray# : 1
Vial# : 42
Injection Volume : 20
Data File : 20250625 Chloride Covra UCR 042.lcd
Method File : Method Chloride + Sulfate Shodex column.lcm
Batch File : 20250625 Chloride Covra UCR.lcb
Report Format File : Report default.lsr
Date Acquired : 6/25/2025 11:33:14 PM
Time Acquired : 11:33:14 PM
Date Processed : 6/25/2025 11:45:45 PM
Time Processed : 11:45:45 PM

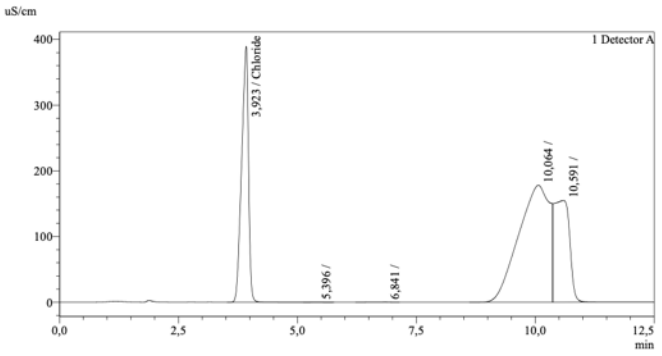


Detector A

| Peak# | Ret. Time | Name | Area | Height | Conc. | Unit | Mark |
|---|---|---|---|---|---|---|---|
| 1 | 3,923 | Chloride | 3904811 | 388927 | 757,992 | mg/L | S |
| 2 | 5,396 | | 3395 | 278 | 0,000 | | T |
| 3 | 6,841 | | 10179 | 441 | 0,000 | | |
| 4 | 10,064 | | 8091707 | 178219 | 0,000 | | |
| 5 | 10,591 | | 3533382 | 154922 | 0,000 | | V |
| Total | | | 15543474 | 722787 | | | |

Sample Name : 51.1
Tray# : 1
Vial# : 96
Injection Volume : 20
Data File : 20250625 Chloride Covra UCR 096.lcd
Method File : Method Chloride + Sulfate Shodex column.lcm
Batch File : 20250625 Chloride Covra UCR.lcb
Report Format File : Report default.lsr
Date Acquired : 6/26/2025 2:03:13 PM
Time Acquired : 2:03:13 PM
Date Processed : 6/26/2025 2:15:44 PM
Time Processed : 2:15:44 PM

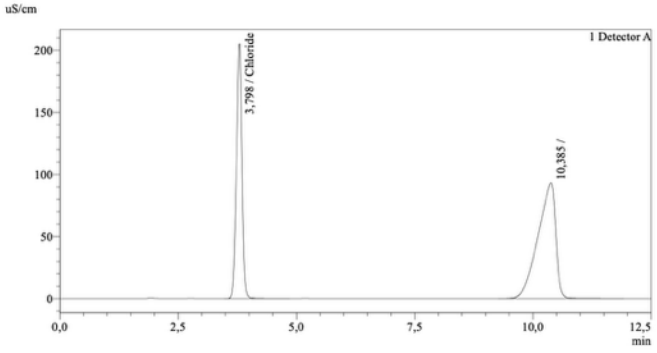


Detector A

| Peak# | Ret. Time | Name | Area | Height | Conc. | Unit | Mark |
|---|---|---|---|---|---|---|---|
| 1 | 3,798 | Chloride | 1655423 | 205215 | 321,346 | mg/L | |
| 2 | 10,385 | | 2437090 | 93376 | 0,000 | | |
| Total | | | 4092513 | 298591 | | | |

Sample Name : 52.1
Tray# : 1
Vial# : 57
Injection Volume : 20
Data File : 20250625 Chloride Covra UCR 057.lcd
Method File : Method Chloride + Sulfate Shodex column.lcm
Batch File : 20250625 Chloride Covra UCR.lcb
Report Format File : Report default.lsr
Date Acquired : 6/26/2025 2:49:49 AM
Time Acquired : 2:49:49 AM
Date Processed : 6/26/2025 3:02:20 AM
Time Processed : 3:02:20 AM

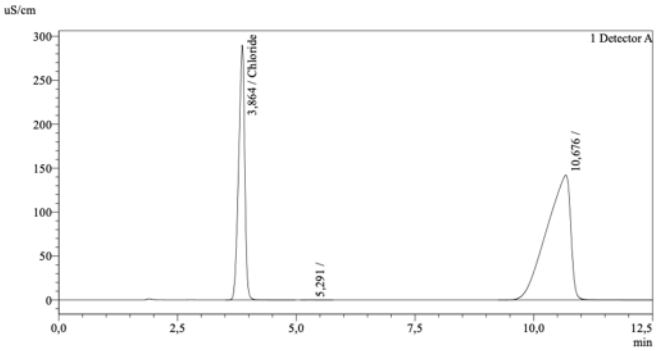


Detector A

| Peak# | Ret. Time | Name | Area | Height | Conc. | Unit | Mark |
|---|---|---|---|---|---|---|---|
| 1 | 3,864 | Chloride | 2565355 | 289772 | 497,980 | mg/L | |
| 2 | 5,291 | | 2205 | 191 | 0,000 | | |
| 3 | 10,676 | | 5013724 | 142251 | 0,000 | | |
| Total | | | 7581284 | 432215 | | | |

Sample Name : 53.1
Tray# : 1
Vial# : 89
Injection Volume : 20
Data File : 20250625 Chloride Covra UCR 089.lcd
Method File : Method Chloride + Sulfate Shodex column.lcm
Batch File : 20250625 Chloride Covra UCR.lcb
Report Format File : Report default.lsr
Date Acquired : 6/26/2025 12:31:34 PM
Time Acquired : 12:31:34 PM
Date Processed : 6/26/2025 12:44:04 PM
Time Processed : 12:44:04 PM

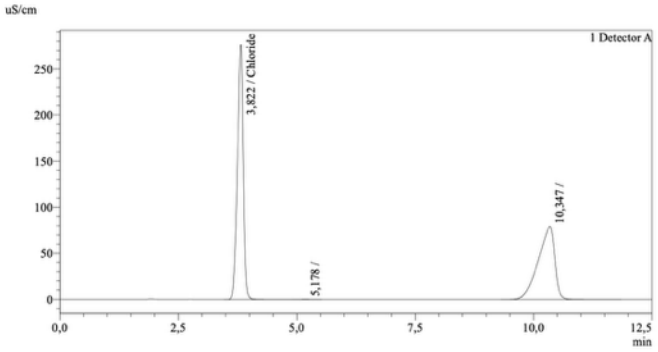


Detector A

| Peak# | Ret. Time | Name | Area | Height | Conc. | Unit | Mark |
|---|---|---|---|---|---|---|---|
| 1 | 3,822 | Chloride | 2370272 | 275577 | 460,111 | mg/L | S |
| 2 | 5,178 | | 2055 | 185 | 0,000 | | T |
| 3 | 10,347 | | 1916765 | 78996 | 0,000 | | |
| Total | | | 4289093 | 354757 | | | |

Sample Name : 54.1
Tray# : 1
Vial# : 56
Injection Volume : 20
Data File : 20250625 Chloride Covra UCR 056.lcd
Method File : Method Chloride + Sulfate Shodex column.lcm
Batch File : 20250625 Chloride Covra UCR.lcb
Report Format File : Report default.lsr
Date Acquired : 6/26/2025 2:36:43 AM
Time Acquired : 2:36:43 AM
Date Processed : 6/26/2025 2:49:14 AM
Time Processed : 2:49:14 AM

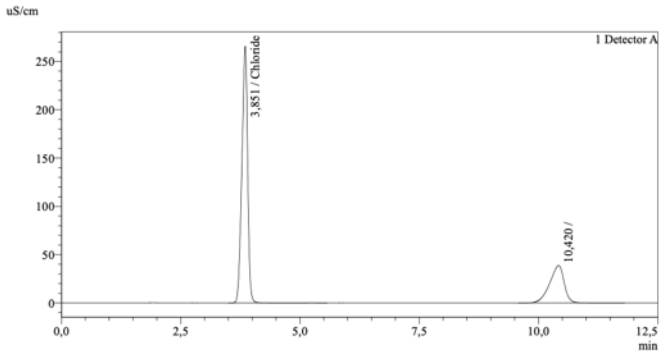


Detector A

| Peak# | Ret. Time | Name | Area | Height | Conc. | Unit | Mark |
|---|---|---|---|---|---|---|---|
| 1 | 3,851 | Chloride | 2224982 | 265662 | 431,908 | mg/L | S |
| 2 | 10,420 | | 824100 | 38804 | 0,000 | | |
| Total | | | 3049083 | 304466 | | | |

Sample Name : 54.2
Tray# : 1
Vial# : 75
Injection Volume : 20
Data File : 20250625 Chloride Covra UCR 075.lcd
Method File : Method Chloride + Sulfate Shodex column.lcm
Batch File : 20250625 Chloride Covra UCR.lcb
Report Format File : Report default.lsr
Date Acquired : 6/26/2025 9:28:10 AM
Time Acquired : 9:28:10 AM
Date Processed : 6/26/2025 9:40:41 AM
Time Processed : 9:40:41 AM

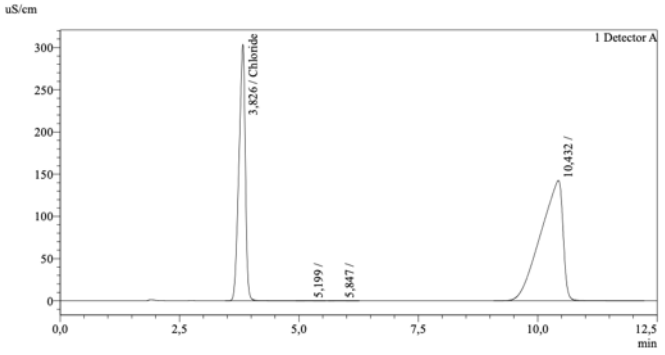


Detector A

| Peak# | Ret. Time | Name | Area | Height | Conc. | Unit | Mark |
|---|---|---|---|---|---|---|---|
| 1 | 3,826 | Chloride | 2801000 | 303464 | 543,723 | mg/L | S |
| 2 | 5,199 | | 2403 | 215 | 0,000 | | T |
| 3 | 5,847 | | 4001 | 306 | 0,000 | | T |
| 4 | 10,432 | | 4661677 | 142548 | 0,000 | | |
| Total | | | 7469082 | 446533 | | | |

Sample Name : 55.1
Tray# : 1
Vial# : 76
Injection Volume : 20
Data File : 20250625 Chloride Covra UCR 076.lcd
Method File : Method Chloride + Sulfate Shodex column.lcm
Batch File : 20250625 Chloride Covra UCR.lcb
Report Format File : Report default.lsr
Date Acquired : 6/26/2025 9:41:16 AM
Time Acquired : 9:41:16 AM
Date Processed : 6/26/2025 9:53:47 AM
Time Processed : 9:53:47 AM

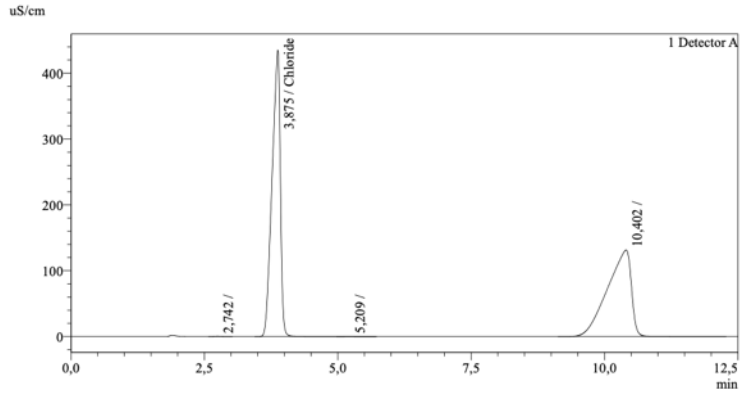


Detector A

| Peak# | Ret. Time | Name | Area | Height | Conc. | Unit | Mark |
|---|---|---|---|---|---|---|---|
| 1 | 2,742 | | 4231 | 487 | 0,000 | | |
| 2 | 3,875 | Chloride | 4680525 | 434240 | 908,571 | mg/L | S |
| 3 | 5,209 | | 4083 | 348 | 0,000 | | T |
| 4 | 10,402 | | 4090805 | 131315 | 0,000 | | |
| Total | | | 8779644 | 566390 | | | |

Sample Name : 56.1
Tray# : 1
Vial# : 9
Injection Volume : 20
Data File : 20250625 Chloride Covra UCR 009.lcd
Method File : Method Chloride + Sulfate Shodex column.lcm
Batch File : 20250625 Chloride Covra UCR.lcb
Report Format File : Report default.lsr
Date Acquired : 6/25/2025 4:20:51 PM
Time Acquired : 4:20:51 PM
Date Processed : 6/25/2025 4:33:21 PM
Time Processed : 4:33:21 PM

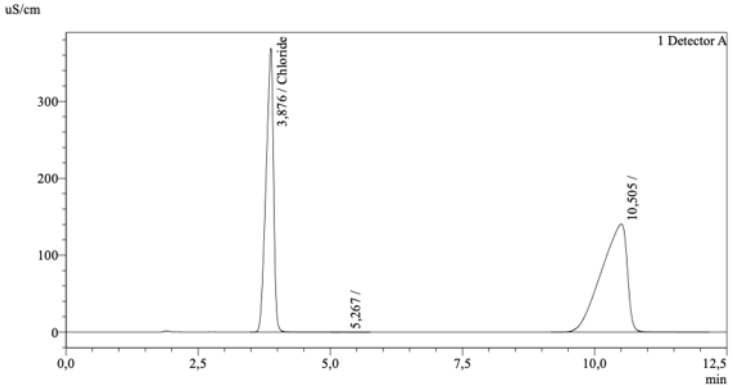


Detector A

| Peak# | Ret. Time | Name | Area | Height | Conc. | Unit | Mark |
|---|---|---|---|---|---|---|---|
| 1 | 3,876 | Chloride | 3625722 | 368405 | 703,816 | mg/L | S |
| 2 | 5,267 | | 3139 | 270 | 0,000 | | T |
| 3 | 10,505 | | 4775024 | 140742 | 0,000 | | |
| Total | | | 8403886 | 509417 | | | |

Sample Name : 57.1
Tray# : 1
Vial# : 88
Injection Volume : 20
Data File : 20250625 Chloride Covra UCR 088.lcd
Method File : Method Chloride + Sulfate Shodex column.lcm
Batch File : 20250625 Chloride Covra UCR.lcb
Report Format File : Report default.lsr
Date Acquired : 6/26/2025 12:18:28 PM
Time Acquired : 12:18:28 PM
Date Processed : 6/26/2025 12:30:59 PM
Time Processed : 12:30:59 PM

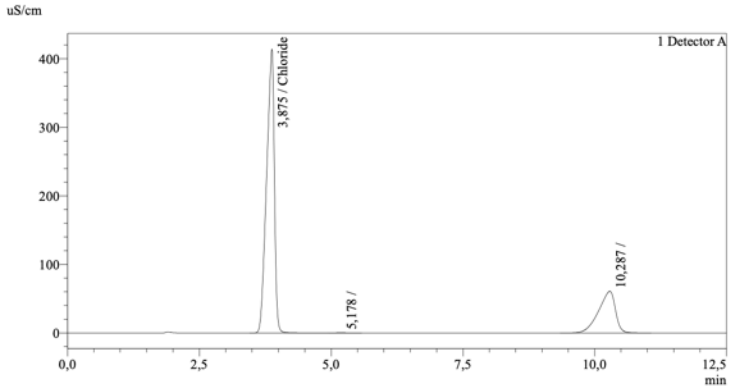


Detector A

| Peak# | Ret. Time | Name | Area | Height | Conc. | Unit | Mark |
|---|---|---|---|---|---|---|---|
| 1 | 3,875 | Chloride | 4234359 | 412992 | 821,963 | mg/L | S |
| 2 | 5,178 | | 3468 | 310 | 0,000 | | T |
| 3 | 10,287 | | 1351546 | 60820 | 0,000 | | |
| Total | | | 5589373 | 474122 | | | |

Sample Name : 58.1
Tray# : 1
Vial# : 62
Injection Volume : 20
Data File : 20250625 Chloride Covra UCR 062.lcd
Method File : Method Chloride + Sulfate Shodex column.lcm
Batch File : 20250625 Chloride Covra UCR.lcb
Report Format File : Report default.lsr
Date Acquired : 6/26/2025 3:55:22 AM
Time Acquired : 3:55:22 AM
Date Processed : 6/26/2025 4:07:53 AM
Time Processed : 4:07:53 AM

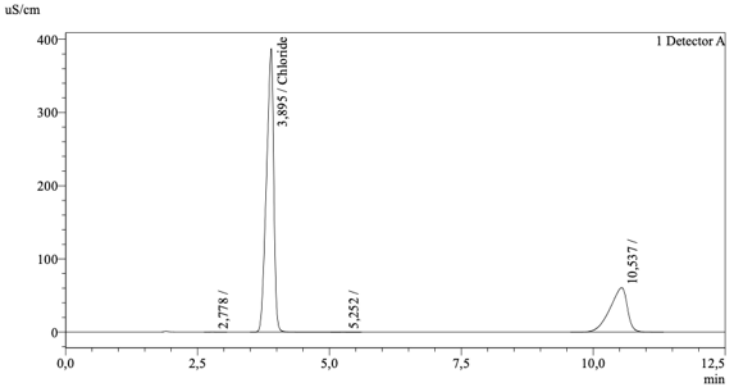


Detector A

| Peak# | Ret. Time | Name | Area | Height | Conc. | Unit | Mark |
|---|---|---|---|---|---|---|---|
| 1 | 2,778 | | 2027 | 233 | 0,000 | | |
| 2 | 3,895 | Chloride | 3717110 | 386559 | 721,556 | mg/L | S |
| 3 | 5,252 | | 2261 | 202 | 0,000 | | T |
| 4 | 10,537 | | 1392393 | 60714 | 0,000 | | |
| Total | | | 5113791 | 447708 | | | |

Sample Name : 59.1
Tray# : 1
Vial# : 74
Injection Volume : 20
Data File : 20250625 Chloride Covra UCR 074.lcd
Method File : Method Chloride + Sulfate Shodex column.lcm
Batch File : 20250625 Chloride Covra UCR.lcb
Report Format File : Report default.lsr
Date Acquired : 6/26/2025 9:15:03 AM
Time Acquired : 9:15:03 AM
Date Processed : 6/26/2025 9:27:34 AM
Time Processed : 9:27:34 AM

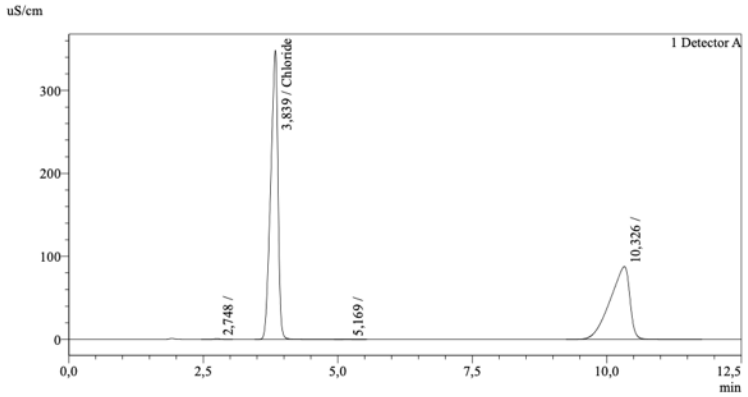


Detector A

| Peak# | Ret. Time | Name | Area | Height | Conc. | Unit | Mark |
|---|---|---|---|---|---|---|---|
| 1 | 2,748 | | 7227 | 870 | 0,000 | | |
| 2 | 3,839 | Chloride | 3274807 | 348002 | 635,697 | mg/L | S |
| 3 | 5,169 | | 2775 | 245 | 0,000 | | T |
| 4 | 10,326 | | 2247585 | 87795 | 0,000 | | |
| Total | | | 5532395 | 436913 | | | |

Sample Name : 60.1
Tray# : 1
Vial# : 80
Injection Volume : 20
Data File : 20250625 Chloride Covra UCR 080.lcd
Method File : Method Chloride + Sulfate Shodex column.lcm
Batch File : 20250625 Chloride Covra UCR.lcb
Report Format File : Report default.lsr
Date Acquired : 6/26/2025 10:33:40 AM
Time Acquired : 10:33:40 AM
Date Processed : 6/26/2025 10:46:11 AM
Time Processed : 10:46:11 AM

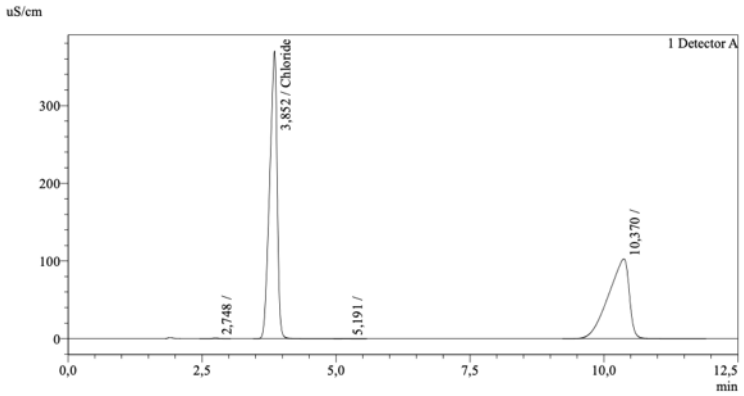


Detector A

| Peak# | Ret. Time | Name | Area | Height | Conc. | Unit | Mark |
|---|---|---|---|---|---|---|---|
| 1 | 2,748 | | 7719 | 927 | 0,000 | | |
| 2 | 3,852 | Chloride | 3584720 | 369977 | 695,857 | mg/L | S |
| 3 | 5,191 | | 3154 | 279 | 0,000 | | T |
| 4 | 10,370 | | 2774301 | 102717 | 0,000 | | |
| Total | | | 6369894 | 473900 | | | |

Sample Name : 61.1
Tray# : 1
Vial# : 71
Injection Volume : 20
Data File : 20250625 Chloride Covra UCR 071.lcd
Method File : Method Chloride + Sulfate Shodex column.lcm
Batch File : 20250625 Chloride Covra UCR.lcb
Report Format File : Report default.lsr
Date Acquired : 6/26/2025 5:53:12 AM
Time Acquired : 5:53:12 AM
Date Processed : 6/26/2025 6:05:43 AM
Time Processed : 6:05:43 AM

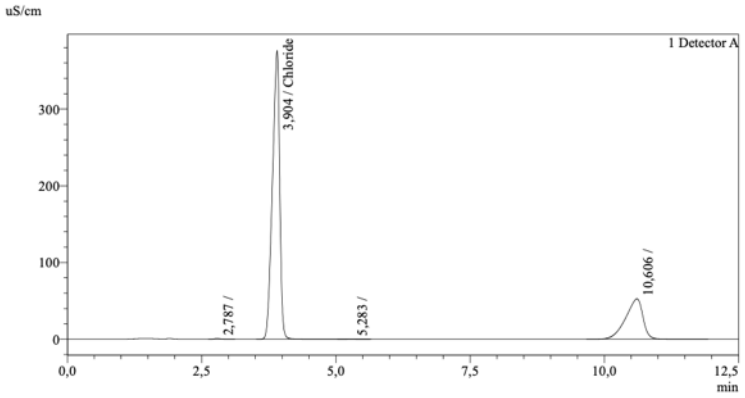


Detector A

| Peak# | Ret. Time | Name | Area | Height | Conc. | Unit | Mark |
|---|---|---|---|---|---|---|---|
| 1 | 2,787 | | 7256 | 900 | 0,000 | | |
| 2 | 3,904 | Chloride | 3529486 | 375870 | 685,135 | mg/L | S |
| 3 | 5,283 | | 3062 | 270 | 0,000 | | T |
| 4 | 10,606 | | 1184486 | 52592 | 0,000 | | |
| Total | | | 4724290 | 429631 | | | |

Sample Name : 61.2
Tray# : 1
Vial# : 98
Injection Volume : 20
Data File : 20250625 Chloride Covra UCR 098.lcd
Method File : Method Chloride + Sulfate Shodex column.lcm
Batch File : 20250625 Chloride Covra UCR.lcb
Report Format File : Report default.lsr
Date Acquired : 6/26/2025 2:29:25 PM
Time Acquired : 2:29:25 PM
Date Processed : 6/26/2025 2:41:56 PM
Time Processed : 2:41:56 PM

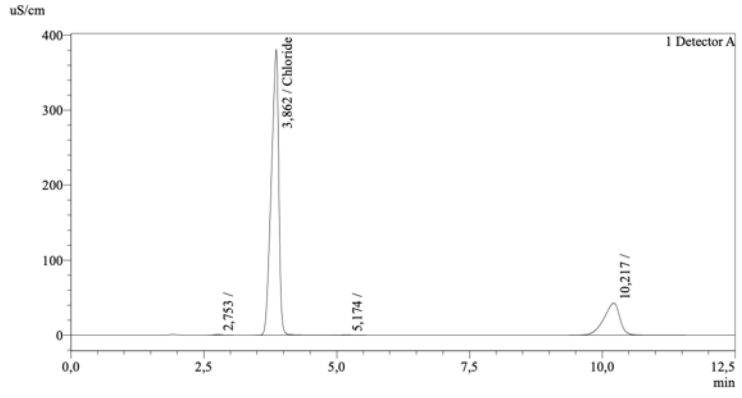


Detector A

| Peak# | Ret. Time | Name | Area | Height | Conc. | Unit | Mark |
|---|---|---|---|---|---|---|---|
| 1 | 2,753 | | 8243 | 997 | 0,000 | | |
| 2 | 3,862 | Chloride | 3707211 | 380364 | 719,634 | mg/L | S |
| 3 | 5,174 | | 3274 | 297 | 0,000 | | T |
| 4 | 10,217 | | 887504 | 42671 | 0,000 | | |
| Total | | | 4606232 | 424328 | | | |

Sample Name : 62.1
Tray# : 1
Vial# : 19
Injection Volume : 20
Data File : 20250625 Chloride Covra UCR 019.lcd
Method File : Method Chloride + Sulfate Shodex column.lcm
Batch File : 20250625 Chloride Covra UCR.lcb
Report Format File : Report default.lsr
Date Acquired : 6/25/2025 6:31:53 PM
Time Acquired : 6:31:53 PM
Date Processed : 6/25/2025 6:44:23 PM
Time Processed : 6:44:23 PM

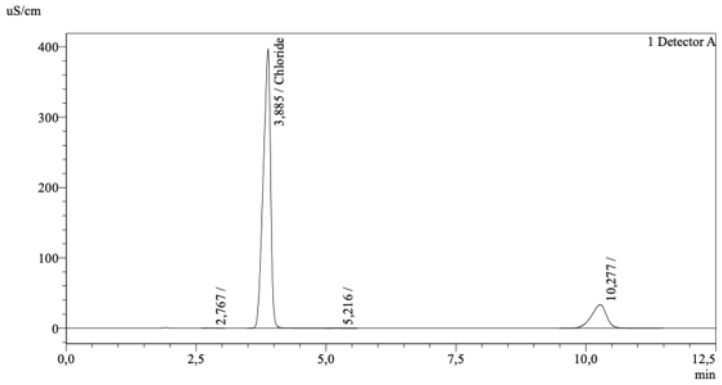


Detector A

| Peak# | Ret. Time | Name | Area | Height | Conc. | Unit | Mark |
|---|---|---|---|---|---|---|---|
| 1 | 2,767 | | 3435 | 419 | 0,000 | | |
| 2 | 3,885 | Chloride | 3906062 | 396764 | 758,235 | mg/L | S |
| 3 | 5,216 | | 3446 | 307 | 0,000 | | T |
| 4 | 10,277 | | 687122 | 33539 | 0,000 | | |
| Total | | | 4600065 | 431029 | | | |

Sample Name : 63.1
Tray# : 1
Vial# : 27
Injection Volume : 20
Data File : 20250625 Chloride Covra UCR 027.lcd
Method File : Method Chloride + Sulfate Shodex column.lcm
Batch File : 20250625 Chloride Covra UCR.lcb
Report Format File : Report default.lsr
Date Acquired : 6/25/2025 8:16:40 PM
Time Acquired : 8:16:40 PM
Date Processed : 6/25/2025 8:29:11 PM
Time Processed : 8:29:11 PM

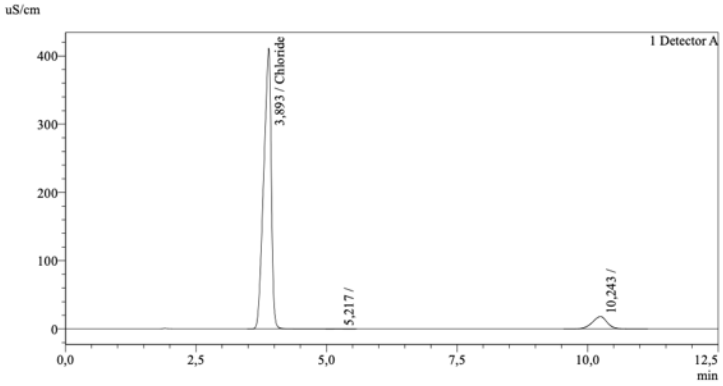


Detector A

| Peak# | Ret. Time | Name | Area | Height | Conc. | Unit | Mark |
|---|---|---|---|---|---|---|---|
| 1 | 3,893 | Chloride | 4121824 | 410918 | 800,118 | mg/L | S |
| 2 | 5,217 | | 3660 | 330 | 0,000 | | T |
| 3 | 10,243 | | 363863 | 18177 | 0,000 | | |
| Total | | | 4489347 | 429425 | | | |

Sample Name : 64.1
Tray# : 1
Vial# : 77
Injection Volume : 20
Data File : 20250625 Chloride Covra UCR 077.lcd
Method File : Method Chloride + Sulfate Shodex column.lcm
Batch File : 20250625 Chloride Covra UCR.lcb
Report Format File : Report default.lsr
Date Acquired : 6/26/2025 9:54:23 AM
Time Acquired : 9:54:23 AM
Date Processed : 6/26/2025 10:06:54 AM
Time Processed : 10:06:54 AM

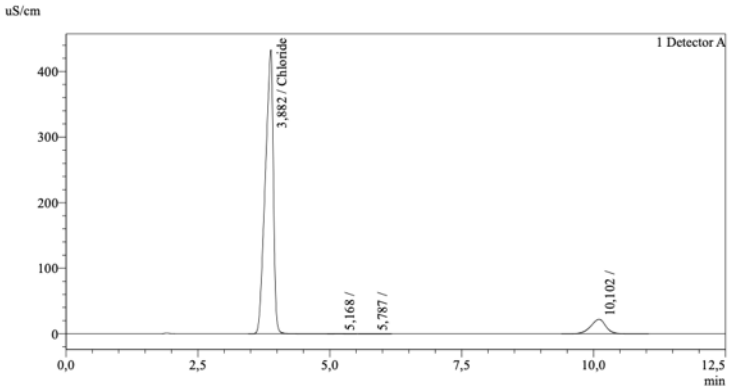


Detector A

| Peak# | Ret. Time | Name | Area | Height | Conc. | Unit | Mark |
|---|---|---|---|---|---|---|---|
| 1 | 3,882 | Chloride | 4578687 | 432166 | 888,803 | mg/L | S |
| 2 | 5,168 | | 4119 | 371 | 0,000 | | T |
| 3 | 5,787 | | 2291 | 175 | 0,000 | | T |
| 4 | 10,102 | | 440315 | 22150 | 0,000 | | |
| Total | | | 5025413 | 454862 | | | |

Sample Name : 65.1
Tray# : 1
Vial# : 32
Injection Volume : 20
Data File : 20250625 Chloride Covra UCR 032.lcd
Method File : Method Chloride + Sulfate Shodex column.lcm
Batch File : 20250625 Chloride Covra UCR.lcb
Report Format File : Report default.lsr
Date Acquired : 6/25/2025 9:22:15 PM
Time Acquired : 9:22:15 PM
Date Processed : 6/25/2025 9:34:45 PM
Time Processed : 9:34:45 PM

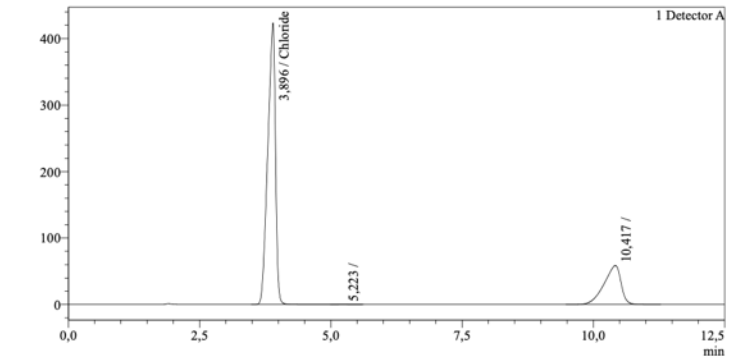


Detector A

| Peak# | Ret. Time | Name | Area | Height | Conc. | Unit | Mark |
|---|---|---|---|---|---|---|---|
| 1 | 3,896 | Chloride | 4322309 | 422900 | 839,035 | mg/L | S |
| 2 | 5,223 | | 3677 | 325 | 0,000 | | T |
| 3 | 10,417 | | 1323307 | 58616 | 0,000 | | |
| Total | | | 5649293 | 481841 | | | |

| | |
|---|---|
| Sample Name | : 66.1 |
| Tray# | : 1 |
| Vial# | : 65 |
| Injection Volume | : 20 |
| Data File | : 20250625 Chloride Covra UCR 065.lcd |
| Method File | : Method Chloride + Sulfate Shodex column.lcm |
| Batch File | : 20250625 Chloride Covra UCR.lcb |
| Report Format File | : Report default.lsr |
| Date Acquired | : 6/26/2025 4:34:38 AM |
| Time Acquired | : 4:34:38 AM |
| Date Processed | : 6/26/2025 4:47:09 AM |
| Time Processed | : 4:47:09 AM |

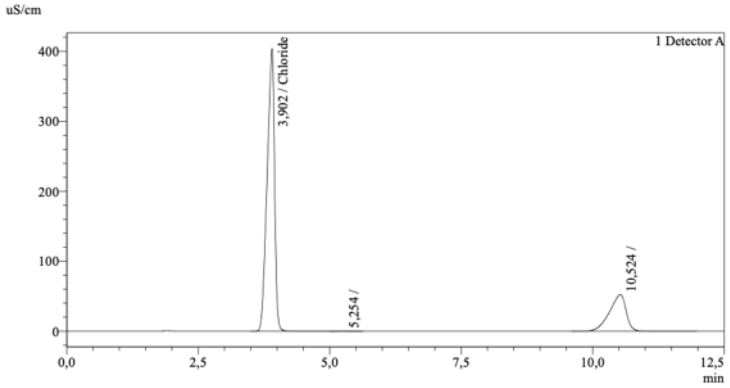


Detector A

| Peak# | Ret. Time | Name | Area | Height | Conc. | Unit | Mark |
|---|---|---|---|---|---|---|---|
| 1 | 3,902 | Chloride | 3953658 | 403170 | 767,474 | mg/L | S |
| 2 | 5,254 | | 3509 | 313 | 0,000 | | T |
| 3 | 10,524 | | 1163246 | 52331 | 0,000 | | |
| Total | | | 5120413 | 455813 | | | |

| | |
|---|---|
| Sample Name | : 67.1 |
| Tray# | : 1 |
| Vial# | : 64 |
| Injection Volume | : 20 |
| Data File | : 20250625 Chloride Covra UCR 064.lcd |
| Method File | : Method Chloride + Sulfate Shodex column.lcm |
| Batch File | : 20250625 Chloride Covra UCR.lcb |
| Report Format File | : Report default.lsr |
| Date Acquired | : 6/26/2025 4:21:33 AM |
| Time Acquired | : 4:21:33 AM |
| Date Processed | : 6/26/2025 4:34:04 AM |
| Time Processed | : 4:34:04 AM |

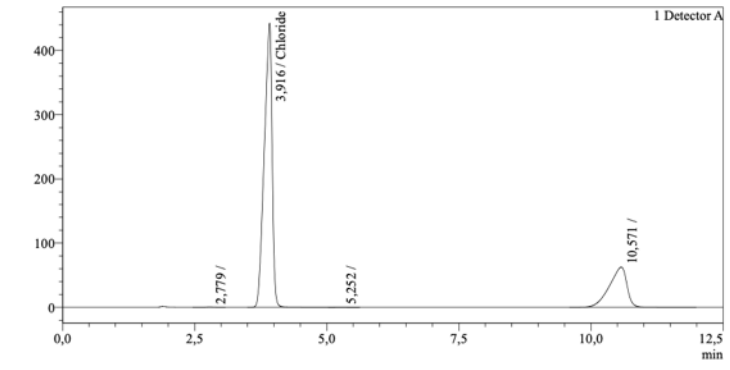


Detector A

| Peak# | Ret. Time | Name | Area | Height | Conc. | Unit | Mark |
|---|---|---|---|---|---|---|---|
| 1 | 2,779 | | 6664 | 692 | 0,000 | | |
| 2 | 3,916 | Chloride | 4565889 | 441984 | 886,319 | mg/L | S |
| 3 | 5,252 | | 3897 | 346 | 0,000 | | T |
| 4 | 10,571 | | 1450442 | 62662 | 0,000 | | |
| Total | | | 6026892 | 505684 | | | |

Sample Name : 68.1
Tray# : 1
Vial# : 59
Injection Volume : 20
Data File : 20250625 Chloride Covra UCR 059.lcd
Method File : Method Chloride + Sulfate Shodex column.lcm
Batch File : 20250625 Chloride Covra UCR.lcb
Report Format File : Report default.lsr
Date Acquired : 6/26/2025 3:16:03 AM
Time Acquired : 3:16:03 AM
Date Processed : 6/26/2025 3:28:34 AM
Time Processed : 3:28:34 AM

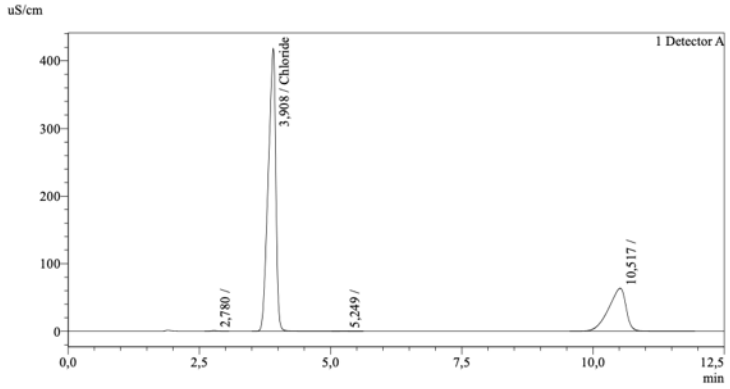


Detector A

| Peak# | Ret. Time | Name | Area | Height | Conc. | Unit | Mark |
|---|---|---|---|---|---|---|---|
| 1 | 2,780 | | 7645 | 890 | 0,000 | | |
| 2 | 3,908 | Chloride | 4176482 | 417153 | 810,728 | mg/L | S |
| 3 | 5,249 | | 3592 | 323 | 0,000 | | T |
| 4 | 10,517 | | 1472954 | 63633 | 0,000 | | |
| Total | | | 5660673 | 482000 | | | |

Sample Name : 69.1
Tray# : 1
Vial# : 8
Injection Volume : 20
Data File : 20250625 Chloride Covra UCR 008.lcd
Method File : Method Chloride + Sulfate Shodex column.lcm
Batch File : 20250625 Chloride Covra UCR.lcb
Report Format File : Report default.lsr
Date Acquired : 6/25/2025 4:07:44 PM
Time Acquired : 4:07:44 PM
Date Processed : 6/25/2025 4:20:15 PM
Time Processed : 4:20:15 PM

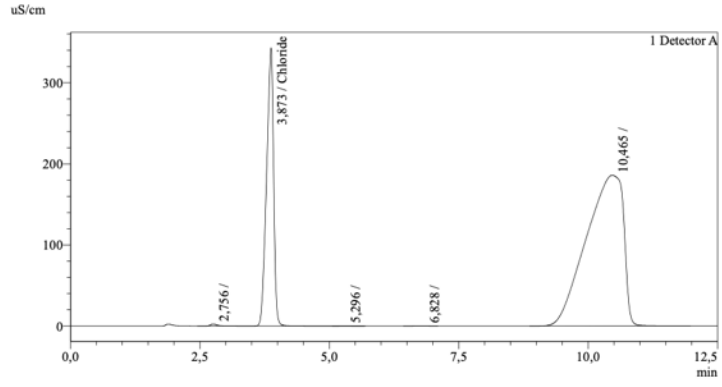


Detector A

| Peak# | Ret. Time | Name | Area | Height | Conc. | Unit | Mark |
|---|---|---|---|---|---|---|---|
| 1 | 2,756 | | 29012 | 2490 | 0,000 | | |
| 2 | 3,873 | Chloride | 3239251 | 342613 | 628,795 | mg/L | SV |
| 3 | 5,296 | | 2758 | 233 | 0,000 | | T |
| 4 | 6,828 | | 4043 | 236 | 0,000 | | |
| 5 | 10,465 | | 9350712 | 186030 | 0,000 | | |
| Total | | | 12625776 | 531601 | | | |

Sample Name : 70.1
Tray# : 1
Vial# : 81
Injection Volume : 20
Data File : 20250625 Chloride Covra UCR 081.lcd
Method File : Method Chloride + Sulfate Shodex column.lcm
Batch File : 20250625 Chloride Covra UCR.lcb
Report Format File : Report default.lsr
Date Acquired : 6/26/2025 10:46:46 AM
Time Acquired : 10:46:46 AM
Date Processed : 6/26/2025 10:59:16 AM
Time Processed : 10:59:16 AM

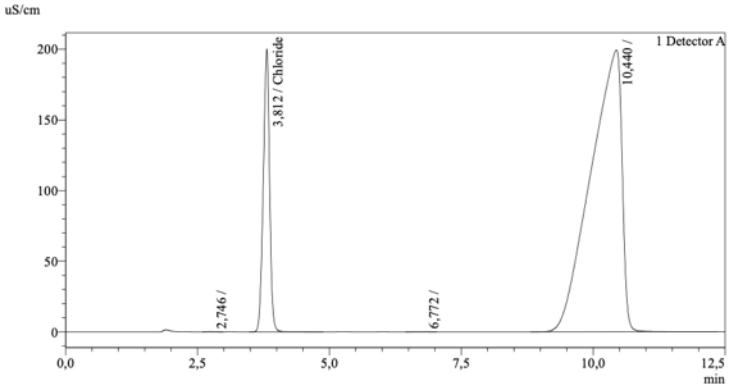


Detector A

| Peak# | Ret. Time | Name | Area | Height | Conc. | Unit | Mark |
|---|---|---|---|---|---|---|---|
| 1 | 2,746 | | 2110 | 246 | 0,000 | | |
| 2 | 3,812 | Chloride | 1665705 | 200271 | 323,342 | mg/L | |
| 3 | 6,772 | | 2566 | 164 | 0,000 | | |
| 4 | 10,440 | | 8177113 | 199504 | 0,000 | | |
| Total | | | 9847494 | 400185 | | | |

Sample Name : 71.1
Tray# : 1
Vial# : 47
Injection Volume : 20
Data File : 20250625 Chloride Covra UCR 047.lcd
Method File : Method Chloride + Sulfate Shodex column.lcm
Batch File : 20250625 Chloride Covra UCR.lcb
Report Format File : Report default.lsr
Date Acquired : 6/26/2025 12:38:47 AM
Time Acquired : 12:38:47 AM
Date Processed : 6/26/2025 12:51:18 AM
Time Processed : 12:51:18 AM

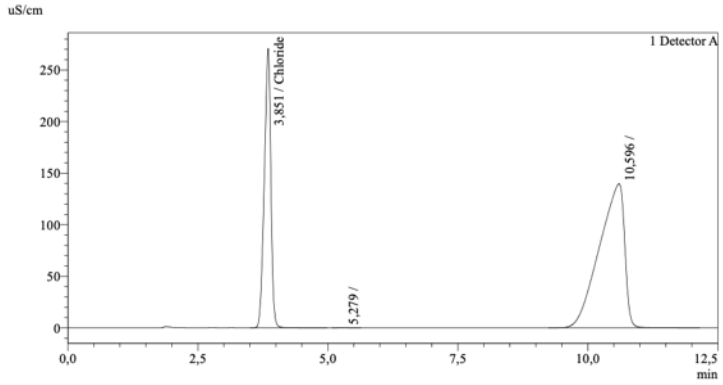


Detector A

| Peak# | Ret. Time | Name | Area | Height | Conc. | Unit | Mark |
|---|---|---|---|---|---|---|---|
| 1 | 3,851 | Chloride | 2367172 | 270779 | 459,509 | mg/L | |
| 2 | 5,279 | | 2108 | 186 | 0,000 | | |
| 3 | 10,596 | | 4719172 | 139663 | 0,000 | | |
| Total | | | 7088452 | 410628 | | | |

Sample Name : 72.1
Tray# : 1
Vial# : 37
Injection Volume : 20
Data File : 20250625 Chloride Covra UCR 037.lcd
Method File : Method Chloride + Sulfate Shodex column.lcm
Batch File : 20250625 Chloride Covra UCR.lcb
Report Format File : Report default.lsr
Date Acquired : 6/25/2025 10:27:42 PM
Time Acquired : 10:27:42 PM
Date Processed : 6/25/2025 10:40:13 PM
Time Processed : 10:40:13 PM

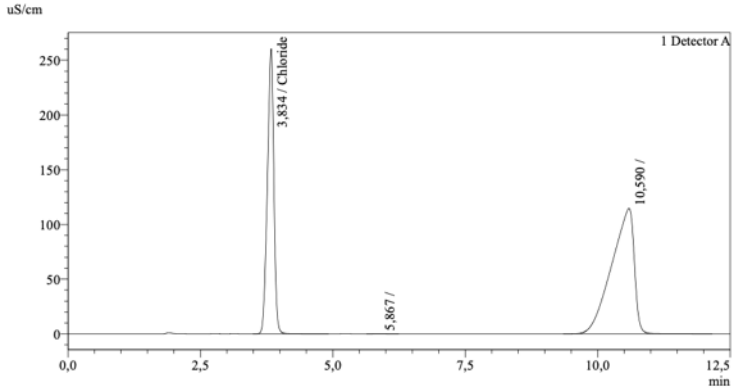


Detector A

| Peak# | Ret. Time | Name | Area | Height | Conc. | Unit | Mark |
|---|---|---|---|---|---|---|---|
| 1 | 3,834 | Chloride | 2201607 | 260159 | 427,370 | mg/L | |
| 2 | 5,867 | | 2959 | 234 | 0,000 | | |
| 3 | 10,590 | | 3413229 | 114754 | 0,000 | | |
| Total | | | 5617795 | 375147 | | | |

Sample Name : 73.1
Tray# : 1
Vial# : 7
Injection Volume : 20
Data File : 20250625 Chloride Covra UCR 007.lcd
Method File : Method Chloride + Sulfate Shodex column.lcm
Batch File : 20250625 Chloride Covra UCR.lcb
Report Format File : Report default.lsr
Date Acquired : 6/25/2025 3:54:38 PM
Time Acquired : 3:54:38 PM
Date Processed : 6/25/2025 4:07:09 PM
Time Processed : 4:07:09 PM

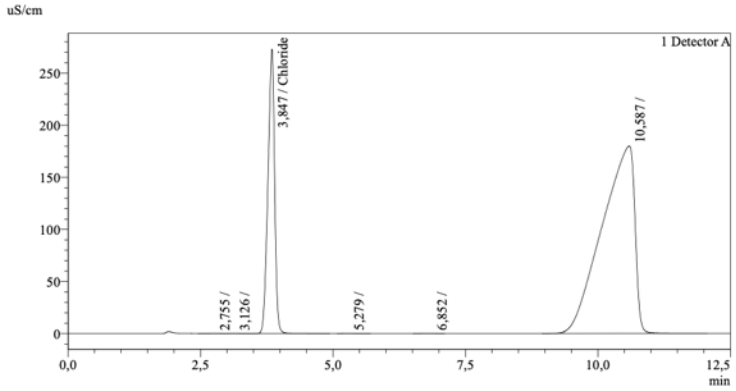


Detector A

| Peak# | Ret. Time | Name | Area | Height | Conc. | Unit | Mark |
|---|---|---|---|---|---|---|---|
| 1 | 2,755 | | 2365 | 198 | 0,000 | | |
| 2 | 3,126 | | 2072 | 182 | 0,000 | | V |
| 3 | 3,847 | Chloride | 2393084 | 272569 | 464,539 | mg/L | V |
| 4 | 5,279 | | 2007 | 170 | 0,000 | | |
| 5 | 6,852 | | 2971 | 187 | 0,000 | | |
| 6 | 10,587 | | 7754629 | 180014 | 0,000 | | |
| Total | | | 10157127 | 453320 | | | |

**IC Calibration curves**

Below are the calibration curves obtained from the Chloride and Sulfate standards.

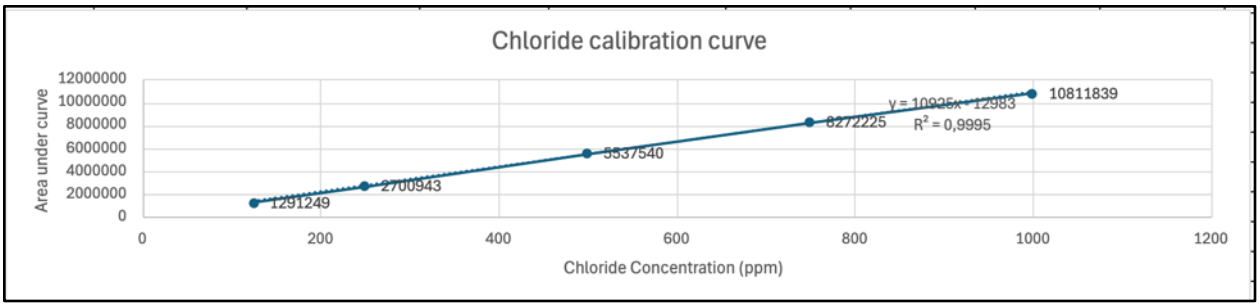


*Graph B1 – Chloride calibration curve.*

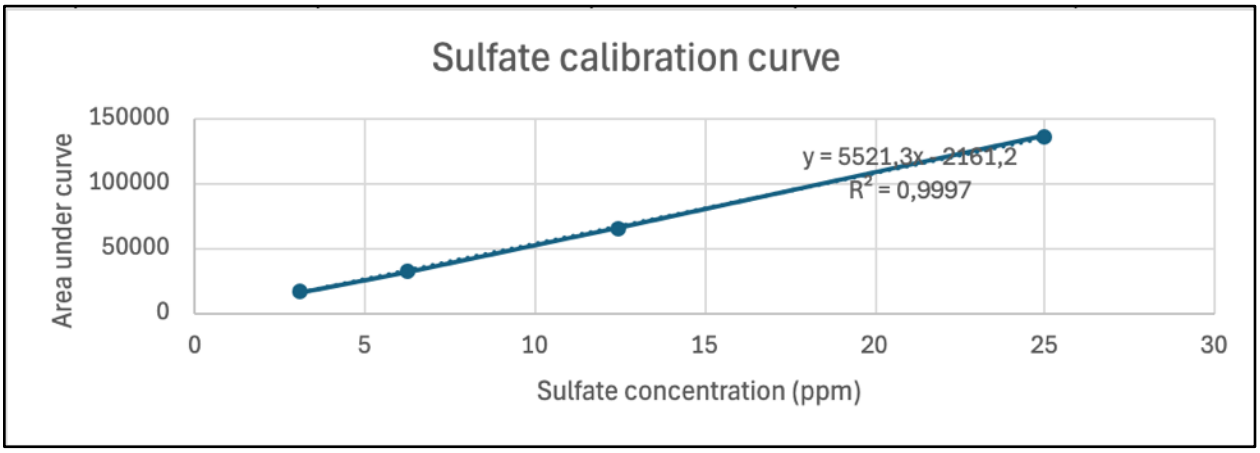


*Graph B2 – Sulfate calibration curve.*

**Table B2: Chloride : Sulfate ratio of each soil sample**

This table provides the relative mass abundance of chloride to sulfate in each soil sample at depth.

| Sample | Depth (m) | Chloride : Sulfate ratio |
|---|---|---|
| 1 | 29,78-30,53 | 1,263925676 |
| 2 | 30,53-31,35 | 2,192335356 |
| 3 | 31,35-32,32 | 1,905987644 |
| 4 | 32,32-32,89 | 2,395002834 |
| 5 | 32,89-33,89 | 2,004192831 |
| 6 | 34,44-35,29 | 2,043904419 |
| 7 | 35,29-36,19 | 1,189088602 |
| 8 | 36,19-37,13 | 1,6965774 |
| 9 | 37,15-38,02 | 0,96635855 |
| 10 | 38,02-38,98 | 1,820441995 |
| 11 | 38,98-39,85 | 0,568064479 |
| 12 | 39,85-40,68 | 2,025241115 |
| 13 | 40,68-41,40 | 1,984957659 |
| 14 | 41,40-42,13 | 1,360115111 |
| 15 | 42,13-42,56 | 1,746185147 |
| 16 | 43,04-43,90 | 1,764149643 |
| 17 | 43,9-44,68 | 1,526941057 |
| 18 | 44,68-45,19 | 0,673730707 |
| 19 | 45,19-46,05 | 1,914871747 |
| 20 | 46,05-47,02 | 0,624682698 |
| 21 | 47,05-47,93 | 1,883446107 |
| 22 | 47,95-48,91 | 0,526931226 |
| 23 | 48,91-49,90 | 0,281601035 |
| 24 | 49,90-50,89 | 0,240718331 |
| 25 | 50,89-51,87 | 0,52408547 |
| 26 | 51,91-52,87 | 0,640611865 |
| 27 | 52,87-53,89 | 0,53371541 |
| 28 | 5392-54,89 | 1,24908484 |
| 29 | 54,92-55,89 | 0,782430764 |
| 30 | 55,91-56,88 | 0,242640443 |
| 31 | 56,9-57,89 | 0,269611814 |
| 32 | 57,91-58,89 | 0,5961845 |
| 33 | 58,91-59,88 | 0,193146126 |
| 34 | 59,90-60,74 | 2,05521891 |
| 35 | 60,92-61,89 | 0,35736249 |
| 36 | 61,90-62,88 | 2,469789637 |
| 37 | 62,90-63,88 | 1,02868181 |

| | | |
|---|---|---|
| 38 | 63,90-64,90 | 0,241126652 |
| 39 | 64,91-65,90 | 0,556638044 |
| 40 | 65,91-66,90 | 0,836633646 |
| 41 | 66,91-67,88 | 0,434597225 |
| 42 | 67,90-68,88 | 0,492517257 |
| 43 | 68,89-69,89 | 0,187957111 |
| 44 | 70,42-71,42 | 0,562477231 |
| 45 | 71,45-72,45 | 0,353074536 |
| 46 | 72,45-73,44 | 0,311601297 |
| 47 | 73,47-74,45 | 0,508773725 |
| 48 | 74,47-75,42 | 0,333009235 |
| 49 | 75,47-76,34 | 0,122000029 |
| 50 | 76,46-77,46 | 0,56019525 |
| 51 | 77,97-78,65 | 0,345827448 |
| 52 | 78,67-79,59 | 0,259840391 |
| 53 | 79,63-80,31 | 0,628028275 |
| 54 | 80,32-81,17 | 0,465233794 |
| 55 | 81,20-82,04 | 0,579689075 |
| 56 | 82,05-82,97 | 0,385029399 |
| 57 | 82,99-83,60 | 1,586947819 |
| 58 | 83,60-84,53 | 1,352832887 |
| 59 | 84,82-85,96 | 0,738926364 |
| 60 | 85,99-86,99 | 0,65512501 |
| 61 | 86,99-87,81 | 1,769619377 |
| 62 | 87,81-88,81 | 2,87799874 |
| 63 | 88,87-89,80 | 5,726142293 |
| 64 | 89,84-90,84 | 5,257425241 |
| 65 | 90,87-91,80 | 1,650010464 |
| 66 | 91,87-92,80 | 1,721757452 |
| 67 | 92,86-93,78 | 1,594255064 |
| 68 | 93,80-94,70 | 1,436558257 |
| 69 | 94,72-95,72 | 0,175754849 |
| 70 | 96,72-97,29 | 0,103736853 |
| 71 | 97,29-98,27 | 0,254836062 |
| 72 | 98,30-99,18 | 0,507135124 |
| 73 | 99,77-100,23 | 0,156134155 |

**Table B3: Interpreted measurements**

This table provides the calculated chloride and sulfate concentrations in mg/kg and mg/L, the pH, and EC values (mS/cm). The values colored in orange indicate that they are average values.

| Sample | Depth (m) | Estimated Chloride (mg/kg) in dry soil | Estimated Sulfate (mg/kg) in dry soil | Estimated Chloride (mg/L) in porewater | pH | EC uS/cm |
|---|---|---|---|---|---|---|
| 1 | 29,78-30,53 | 1951,517657 | 1544,012986 | 17724,73 | 7,36 | 1293 |
| 2 | 30,53-31,35 | 2800,870481 | 1277,573923 | 14982,43 | 7,34 | 941,7 |
| 3 | 31,35-32,32 | 4059,978032 | 2130,117708 | 16496,87 | 6,60 | 1348 |
| 4 | 32,32-32,89 | 3027,784897 | 1264,209317 | 13338,62 | 7,20 | 1015 |
| 5 | 32,89-33,89 | 2407,397712 | 1201,180682 | 13913,94 | 8,21 | 813,4 |
| 6 | 34,44-35,29 | 3380,739588 | 1654,059533 | 17748,88 | 7,75 | 1130 |
| 7 | 35,29-36,19 | 2793,740961 | 2349,480901 | 11174,96 | 7,56 | 939,4 |
| 8 | 36,19-37,13 | 2969,328146 | 1750,187257 | 16050,26 | 8,10 | 1099 |
| 9 | 37,15-38,02 | 3277,653547 | 3391,757177 | 17174,12 | 7,53 | 1174 |
| 10 | 38,02-38,98 | 3655,628375 | 2008,099343 | 15584,52 | 7,53 | 1218 |
| 11 | 38,98-39,85 | 3034,04119 | 5341,015504 | 12328,19 | 6,65 | 1017 |
| 12 | 39,85-40,68 | 4166,128146 | 2057,102295 | 16156,45 | 7,44 | 1382 |
| 13 | 40,68-41,40 | 3844,521739 | 1936,828084 | 16127,02 | 7,35 | 1278 |
| 14 | 41,40-42,13 | 3166,698398 | 2328,257639 | 12666,79 | 7,60 | 1056 |
| 15 | 42,13-42,56 | 2895,837071 | 1658,379168 | 11766,63 | 8,05 | 973 |
| 16 | 43,04-43,90 | 2962,555606 | 1679,310833 | 12427,34 | 7,56 | 994,7 |
| 17 | 43,9-44,68 | 2650,963844 | 1736,127162 | 13917,56 | 7,59 | 893,2 |

| | | | | | | |
|---|---|---|---|---|---|---|
| 18 | 44,68-45,19 | 3703,166133 | 5496,50787 | 14584,07 | 7,62 | 1234 |
| 19 | 45,19-46,05 | 3322,036613 | 1734,861156 | 16511,02 | 7,82 | 1111 |
| 20 | 46,05-47,02 | 3132,126316 | 5013,947603 | 15025,13 | 7,49 | 1050 |
| 21 | 47,05-47,93 | 2908,143707 | 1544,054643 | 13709,82 | 7,41 | 976,3 |
| 22 | 47,95-48,91 | 4006,907551 | 7604,2325 | 19235,49 | 7,24 | 1332 |
| 23 | 48,91-49,90 | 3189,343707 | 11325,75279 | 15571,50 | 7,15 | 1067 |
| 24 | 49,90-50,89 | 3149,941419 | 13085,59015 | 17505,41 | 6,73 | 1056 |
| 25 | 50,89-51,87 | 3421,038444 | 6527,634597 | 16603,05 | 6,90 | 1176 |
| 26 | 51,91-52,87 | 2948,016476 | 4601,87617 | 19729,03 | 6,87 | 988,9 |
| 27 | 52,87-53,89 | 3758,422883 | 7041,998062 | 15644,88 | 6,93 | 1201 |
| 28 | 53,92-54,89 | 3664,156522 | 2933,472896 | 15753,40 | 7,69 | 1232 |
| 29 | 54,92-55,89 | 3599,794966 | 4600,784036 | 18552,79 | 6,71 | 1201 |
| 30 | 55,91-56,88 | 2863,383066 | 11800,93074 | 16884,09 | 6,66 | 961,3 |
| 31 | 56,9-57,89 | 2967,78032 | 11007,60489 | 14750,31 | 6,47 | 995,9 |
| 32 | 57,91-58,89 | 3622,172998 | 6075,590694 | 15696,08 | 6,92 | 1208 |
| 33 | 58,91-59,88 | 2886,672769 | 14945,53799 | 15737,02 | 7,15 | 969,4 |
| 34 | 59,90-60,74 | 3706,56659 | 1803,489921 | 16885,47 | 7,42 | 1235 |
| 35 | 60,92-61,89 | 4260,45492 | 11921,9421 | 18769,03 | 7,56 | 1412 |
| 36 | 61,90-62,88 | 3651,73913 | 1478,56282 | 16921,44 | 7,65 | 1217 |
| 37 | 62,90-63,88 | 2458,248055 | 2389,706935 | 13930,07 | 7,01 | 829,4 |
| 38 | 63,90-64,90 | 3691,961556 | 15311,29605 | 17710,71 | 7,66 | 1231 |

| | | | | | | |
|---|---|---|---|---|---|---|
| 39 | 64,91-65,90 | 3286,614188 | 5904,400938 | 16938,70 | 7,06 | 1099 |
| 40 | 65,91-66,90 | 4008,816476 | 4791,603227 | 17090,22 | 7,80 | 1331 |
| 41 | 66,91-67,88 | 3533,401373 | 8130,289769 | 19262,74 | 7,43 | 1179 |
| 42 | 67,90-68,88 | 4938,082838 | 10026,21283 | 17785,84 | 6,97 | 1676 |
| 43 | 68,89-69,89 | 3644,288787 | 19388,93809 | 13746,81 | 5,76 | 1165 |
| 44 | 70,42-71,42 | 3926,677346 | 6981,042309 | 13721,31 | 6,91 | 1306 |
| 45 | 71,45-72,45 | 3042,095195 | 8616,014145 | 11444,07 | 7,18 | 1020 |
| 46 | 72,45-73,44 | 3446,66087 | 11061,1249 | 13573,89 | 7,15 | 1151 |
| 47 | 73,47-74,45 | 3777,411442 | 7424,541123 | 13791,94 | 6,76 | 1257 |
| 48 | 74,47-75,42 | 3302,081465 | 9915,885552 | 12805,63 | 6,81 | 1105 |
| 49 | 75,47-76,34 | 1606,491533 | 13167,96024 | 10751,14 | 6,86 | 548,6 |
| 50 | 76,46-77,46 | 3586,081465 | 6401,484958 | 11355,92 | 6,9 | 1195 |
| 51 | 77,97-78,65 | 1527,14508 | 4415,916342 | 11469,83 | 6,96 | 522,6 |
| 52 | 78,67-79,59 | 2360,034783 | 9082,632514 | 12390,18 | 6,78 | 798 |
| 53 | 79,63-80,31 | 2181,469108 | 3473,52053 | 15270,28 | 7,03 | 739,8 |
| 54 | 80,32-81,17 | 2312,104348 | 4969,768696 | 11167,52 | 7,05 | 695,4 |
| 55 | 81,20-82,04 | 4296,117162 | 7411,071469 | 13604,37 | 7,9 | 1422 |
| 56 | 82,05-82,97 | 3330,622426 | 8650,306794 | 14432,70 | 7,13 | 1113 |
| 57 | 82,99-83,60 | 3887,727231 | 2449,814156 | 16574,00 | 7,11 | 1292 |
| 58 | 83,60-84,53 | 3414,272769 | 2523,794921 | 15041,26 | 6,84 | 1140 |
| 59 | 84,82-85,96 | 3009,418764 | 4072,691015 | 16724,47 | 7,04 | 1009 |

| | | | | | | |
|---|---|---|---|---|---|---|
| 60 | 85,99-86,99 | 3293,091991 | 5026,662 | 16972,09 | 7,22 | 1101 |
| 61 | 86,99-87,81 | 3323,873227 | 1878,29839 | 15286,23 | 6,78 | 1084 |
| 62 | 87,81-88,81 | 3587,226545 | 1246,430895 | 16622,50 | 6,87 | 1196 |
| 63 | 88,87-89,80 | 3784,720366 | 660,9546484 | 17241,50 | 6,95 | 1260 |
| 64 | 89,84-90,84 | 4202,901602 | 799,4220383 | 17350,44 | 7,22 | 1393 |
| 65 | 90,87-91,80 | 3963,549657 | 2402,136073 | 17155,10 | 6,95 | 1316 |
| 66 | 91,87-92,80 | 3630,792677 | 2108,771286 | 15230,47 | 7,06 | 1210 |
| 67 | 92,86-93,78 | 4191,187185 | 2628,931393 | 17302,08 | 7,02 | 1390 |
| 68 | 93,80-94,70 | 3835,583982 | 2669,981508 | 15588,48 | 6,97 | 1276 |
| 69 | 94,72-95,72 | 2976,873227 | 16937,64492 | 7848,12 | 6,9 | 998,2 |
| 70 | 96,72-97,29 | 1536,556522 | 14812,06037 | 7502,01 | 7,5 | 524,9 |
| 71 | 97,29-98,27 | 2178,631579 | 8549,149458 | 6120,92 | 7,31 | 738,6 |
| 72 | 98,30-99,18 | 3136,120824 | 6183,994512 | 11977,71 | 6,92 | 1051 |
| 73 | 99,77-100,23 | 2193,196339 | 14046,87101 | 5710,21 | 6,91 | 743,3 |

**Table B4: Bulk Resistivity measurements, Formation Factor and Effective Diffusion Coefficients with corresponding formation**

Values colored in red are the conservative literature-based formation factors (143) and corresponding upper-bound $D_{eff}$ coefficients which are not to be interpreted as direct measurements. The molecular diffusion coefficient ($D_0$) being 2.3 x $10^{-9}$.

| Samples | Avg. Depth (m) | Extract Resistivity (Ω·m) | Bulk Resistivity (Ω·m) | (Proxy) / Formation Factors (F*/lit. F) | Effective Diffusion Coefficients ($D_{eff}$) | Formation |
|---|---|---|---|---|---|---|
| 1 | 30,155 | 7,7 | | | | Oosterhout formation |
| 2 | 30,94 | 10,6 | | | | Oosterhout formation |
| 3 | 31,835 | 7,4 | | | | Oosterhout formation |
| 4 | 32,605 | 9,9 | | | | Oosterhout formation |
| 5 | 33,39 | 12,3 | | 143 | 1,6 x $10^{-11}$ | Breda formation |
| 6 | 34,865 | 8,8 | | 143 | 1,6 x $10^{-11}$ | Breda formation |
| 7 | 35,74 | 10,6 | | 143 | 1,6 x $10^{-11}$ | Breda formation |
| 8 | 36,66 | 9,1 | | 143 | 1,6 x $10^{-11}$ | Breda formation |
| 9 | 37,585 | 8,5 | | 143 | 1,6 x $10^{-11}$ | Breda formation |
| 10 | 38,5 | 8,2 | | 143 | 1,6 x $10^{-11}$ | Breda formation |
| 11 | 39,415 | 9,8 | 2080 | 211,54 | 1,1 x $10^{-11}$ | Breda formation |
| 12 | 40,265 | 7,2 | 1812 | 250,42 | 9,2 x $10^{-12}$ | Breda formation |
| 13 | 41,04 | 7,8 | 1843 | 235,54 | 9,8 x $10^{-12}$ | Breda formation |
| 14 | 41,765 | 9,5 | 2600 | 274,56 | 8,4 x $10^{-12}$ | Breda formation |
| 15 | 42,345 | 10,3 | 1231 | 119,78 | 1,9 x $10^{-11}$ | Breda formation |
| 16 | 43,47 | 10,1 | 1233 | 122,65 | 1,9X $10^{-11}$ | Breda formation |
| 17 | 44,29 | 11,2 | 1687 | 150,68 | 1,5 x $10^{-11}$ | Breda formation |
| 18 | 44,936 | 8,1 | 1675 | 206,70 | 1,1 x $10^{-11}$ | Breda formation |

| | | | | | | |
|---|---|---|---|---|---|---|
| 19 | 45,62 | 9,0 | 1285 | 142,76 | $1,6 \times 10^{-11}$ | Breda formation |
| 20 | 46,535 | 9,5 | 1614 | 169,47 | $1,4 \times 10^{-11}$ | Breda formation |
| 21 | 47,49 | 10,2 | 1730 | 168,90 | $1,4 \times 10^{-11}$ | Breda formation |
| 22 | 48,43 | 7,5 | 1646 | 219,25 | $1,0 \times 10^{-11}$ | Breda formation |
| 23 | 49,405 | 9,4 | 1732 | 184,80 | $1,2 \times 10^{-11}$ | Breda formation |
| 24 | 50,395 | 9,5 | 1264 | 133,48 | $1,7 \times 10^{-11}$ | Breda formation |
| 25 | 51,38 | 8,5 | 1858 | 218,50 | $1,1 \times 10^{-11}$ | Breda formation |
| 26 | 52,39 | 10,1 | 2400 | 237,34 | $9,7 \times 10^{-12}$ | Breda formation |
| 27 | 53,38 | 8,3 | 1178 | 141,48 | $1,6 \times 10^{-11}$ | Breda formation |
| 28 | 54,405 | 8,1 | 1799 | 221,64 | $1,0 \times 10^{-11}$ | Breda formation |
| 29 | 55,405 | 8,3 | 1736 | 208,49 | $1,1 \times 10^{-11}$ | Breda formation |
| 30 | 56,395 | 10,4 | 1278 | 122,85 | $1,9 \times 10^{-11}$ | Breda formation |
| 31 | 57,395 | 10,0 | 1390 | 138,43 | $1,7 \times 10^{-11}$ | Breda formation |
| 32 | 58,4 | 8,3 | 1182 | 142,79 | $1,6 \times 10^{-11}$ | Breda formation |
| 33 | 59,395 | 10,3 | 1172 | 113,61 | $2,0 \times 10^{-11}$ | Breda formation |
| 34 | 60,32 | 8,1 | 1171 | 144,62 | $1,6 \times 10^{-11}$ | Breda formation |
| 35 | 61,405 | 7,1 | 1216 | 171,70 | $1,3 \times 10^{-11}$ | Breda formation |
| 36 | 62,39 | 8,2 | 1329 | 161,74 | $1,4 \times 10^{-11}$ | Breda formation |
| 37 | 63,39 | 12,1 | 1196 | 99,20 | $2,3 \times 10^{-11}$ | Breda formation |
| 38 | 64,4 | 8,1 | 1177 | 144,89 | $1,6 \times 10^{-11}$ | Breda formation |
| 39 | 65,405 | 9,1 | 1349 | 148,26 | $1,6 \times 10^{-11}$ | Breda formation |
| 40 | 66,405 | 7,5 | 1168 | 155,46 | $1,5 \times 10^{-11}$ | Breda formation |
| 41 | 67,395 | 8,5 | 2360 | 278,24 | $8,3 \times 10^{-12}$ | Breda formation |
| 42 | 68,39 | 6,0 | | 143 | $1,6 \times 10^{-11}$ | Boom clay formation |

| | | | | | | |
|---|---|---|---|---|---|---|
| 43 | 69,39 | 8,6 | | 143 | 1,6 x $10^{-11}$ | Boom clay formation |
| 44 | 70,92 | 7,7 | | 143 | 1,6 x $10^{-11}$ | Boom clay formation |
| 45 | 71,95 | 9,8 | | 143 | 1,6 x $10^{-11}$ | Boom clay formation |
| 46 | 72,945 | 8,7 | | 143 | 1,6 x $10^{-11}$ | Boom clay formation |
| 47 | 73,96 | 8,0 | | 143 | 1,6 x $10^{-11}$ | Boom clay formation |
| 48 | 74,945 | 9,0 | | 143 | 1,6 x $10^{-11}$ | Boom clay formation |
| 49 | 75,905 | 18,2 | | 143 | 1,6 x $10^{-11}$ | Boom clay formation |
| 50 | 76,96 | 8,4 | | 143 | 1,6 x $10^{-11}$ | Boom clay formation |
| 51 | 78,31 | 19,1 | | 143 | 1,6 x $10^{-11}$ | Boom clay formation |
| 52 | 79,13 | 12,5 | | 143 | 1,6 x $10^{-11}$ | Boom clay formation |
| 53 | 79,97 | 13,5 | | 143 | 1,6 x $10^{-11}$ | Ruisbroek sand |
| 54 | 80,745 | 14,4 | | 143 | 1,6 x $10^{-11}$ | Ruisbroek sand |
| 55 | 81,62 | 7,0 | | 143 | 1,6 x $10^{-11}$ | Ruisbroek sand |
| 56 | 82,51 | 9,0 | | 143 | 1,6 x $10^{-11}$ | Ruisbroek sand |
| 57 | 83,295 | 7,7 | | 143 | 1,6 x $10^{-11}$ | Ruisbroek sand |
| 58 | 84,065 | 8,8 | | 143 | 1,6 x $10^{-11}$ | Ruisbroek sand |
| 59 | 85,39 | 9,9 | 1735 | 175,0615 | 1,3 x $10^{-11}$ | Ruisbroek sand |
| 60 | 86,49 | 9,1 | 1774 | 195,3174 | 1,2 x $10^{-11}$ | Ruisbroek sand |
| 61 | 87,4 | 9,2 | 1662 | 180,1608 | 1,3 x $10^{-11}$ | Ruisbroek sand |
| 62 | 88,31 | 8,4 | 1562 | 186,8152 | 1,2 x $10^{-11}$ | Ruisbroek sand |
| 63 | 89,335 | 7,9 | 1572 | 198,072 | 1,2 x $10^{-11}$ | Ruisbroek sand |
| 64 | 90,34 | 7,2 | 1589 | 221,3477 | 1,0 x 10-11 | Ruisbroek sand |
| 65 | 91,335 | 7,6 | 1750 | 230,3 | 1,0X 10-11 | Ruisbroek sand |
| 66 | 92,335 | 8,3 | 1716 | 207,636 | 1,1X 10-11 | Ruisbroek sand |

| | | | | | | |
|---|---|---|---|---|---|---|
| 67 | 93,32 | 7,2 | 2030 | 282,17 | 8,2 x $10^{-12}$ | Ruisbroek sand |
| 68 | 94,25 | 7,8 | 2090 | 266,684 | 8,6 x $10^{-12}$ | Ruisbroek sand |
| 69 | 95,22 | 10,0 | 1378 | 137,55196 | 1,7X 10-11 | Watervliet clay |
| 70 | 97,005 | 19,1 | 1450 | 76,1105 | 3,0X 10-11 | Watervliet clay |
| 71 | 97,78 | 13,5 | | 143 | 4,6X 10-11 | Watervliet clay |
| 72 | 98,74 | 9,5 | | 143 | 4,6X 10-11 | Watervliet clay |
| 73 | 100 | 13,5 | | 143 | 4,6X 10-11 | Watervliet clay |